

Centromeric Chromatin Assembly in Fission Yeast

Zrinka Vitkovic

181046741

Submitted in partial fulfilment of the requirements
of the Degree of Doctor of Philosophy

School of Biological and Behavioural Sciences
Queen Mary University of London

2023

Abstract

Centromeres are specialised chromosome loci which play an important role in cell division because they serve as the sites of kinetochore assembly, and this ultimately enables chromosome segregation. Interestingly, the DNA sequence at the centromere is not conserved – in fact, it varies significantly between organisms.

A centromere-specific histone H3 variant, CENP-A^{Cnp1} has been shown to be the epigenetic mark of functional centromeres and it is present across species[1, 2]. CENP-A^{Cnp1} deposition in each cell cycle is required to maintain the identity of the centromere.

Ccp1, a NAP (Nucleosome Assembly Protein) family member, has been found to play a role in the loading of Cnp1^{CENP-A} on fission yeast centromeres and to interact with Cnp1^{CENP-A} by physically associating with it[3]. The budding yeast ortholog of Ccp1, Vps75, functions as a regulatory subunit of a histone acetyltransferase Rtt109[3, 4], so this project sought to explore the role of fission yeast Rtt109 in centromere function.

Furthermore, the project investigated the role of Ccp1^{Vps75} in Cnp1^{CENP-A} deposition, as well as the interaction between Ccp1^{Vps75} and Cnp20^{CENP-T}, an inner kinetochore protein.

In this thesis Ccp1^{Vps75} has been identified as a Cnp1^{CENP-A} loading factor, and the data presented suggests that the *ccp1*Δ mutant has centromere clustering defects and that the centromeres may not cluster at the SPB in this mutant.

This study has also found Cnp20^{CENP-T} to interact with Ccp1^{Vps75} and that Ccp1^{Vps75} is involved in the maintenance of Cnp20^{CENP-T} levels at the centromere.

In this thesis it is also shown that *S. pombe* Ccp1 and *S. cerevisiae* Vps75 may

not be true functional orthologs. In budding yeast Rtt109 and Vps75^{Ccp1} work together to bring about correct acetylation of histone H3 at K9, K27 and K56[5, 6]. However, in fission yeast Rtt109 does not appear to be essential for the function of Ccp1^{Vps75} and they likely have separate functions. Furthermore, the results presented in this thesis suggest that Ccp1^{Vps75} does not support the function of Rtt109 in regulating the resistance to genotoxic agents.

Statement of originality

I, Zrinka Vitkovic, confirm that the research included within this thesis is my own work or that where it has been carried out in collaboration with, or supported by others, that this is duly acknowledged below and my contribution indicated. Previously published material is also acknowledged below.

I attest that I have exercised reasonable care to ensure that the work is original, and does not to the best of my knowledge break any UK law, infringe any third party's copyright or other Intellectual Property Right, or contain any confidential material.

I accept that Queen Mary University of London has the right to use plagiarism detection software to check the electronic version of the thesis. I confirm that this thesis has not been previously submitted for the award of a degree by this or any other university.

The copyright of this thesis rests with the author and no quotation from it or information derived from it may be published without the prior written consent of the author.

Signature: Zrinka Vitkovic

Date: 23rd June 2023

Details of collaboration and publications: Mass spectrometry experiments were carried out by Dr Steve Lynham at the Centre of Excellence for Mass Spectrometry Proteomics Facility, The James Black Centre, King's College London.

Acknowledgements

To my parents Zeljka and Andelko - I promise this is the last thesis. Thank you for going through three writing crises, always being there for me, always relentlessly believing in me, and for the unconditional support even when I was blatantly wrong. I am ridiculously lucky to have you.

To my sister Petra - it was significantly more difficult to write this time, with no sister dates(TM)(C) to look forward to. You have shared both my joy and misery, even though I'm sure I must have been pretty annoying at times. You have always been the best sister anyone could ask for.

To Phil - you could envisage this when it seemed utterly impossible to me, and believed in me when I didn't. I owe you an eternal debt of gratitude because without you, this would never have been finished. (Or started.) Thank you for the walks, the talks, the levelling, the belly laughs, the dancing, endless discoveries, always being there for me, being you, mountains of tacos and margaritas shared, and for getting me off the red run. And many, many more things that would require a another 300 pages just to list.

This has been an undertaking like no other - to all of you who have lent me your ears and shoulders through the birthing of this thesis, I can never say thank you enough. Dedicating a few lines to you here is a poor reflection of your importance and my gratitude, but I hope it starts to convey it.

Are we out of the woods yet?

T. A. S.

1

¹The majority of the work for this project was carried out during the COVID-19 pandemic, so the work and the scope of the project were greatly impacted by the pandemic.

Contents

1	Introduction	21
1.1	Motivation	21
1.2	<i>Schizosaccharomyces pombe</i>	23
1.2.1	Chromosome and gene organisation in fission yeast	23
1.3	Chromosomes, the centromere and the kinetochore	26
1.3.1	The centromere	27
1.3.2	The kinetochore	33
1.4	Constitutive centromere associated network of proteins (CCAN)	35
1.5	CENP-A function, deposition and maintenance	39
1.5.1	Establishment of CENP-A	40
1.5.2	The Mis18 complex	51
1.5.3	Maintenance of CENP-A	54
1.5.4	CENP-A localisation and distribution	57
1.5.5	Centromeric chromatin remodelling	63
1.6	Post-translational modifications and function of centromeric and pericentromeric chromatin	66
1.7	Ccp1 ^{Vps75}	70
1.8	Rtt109	73
1.9	Project aims	75
2	Materials and methods	76
2.1	Strains	76

2.1.1	<i>S. pombe</i> strains	76
2.2	Media	78
2.3	Oligonucleotides	80
2.4	Culturing <i>S. pombe</i> cells	81
2.5	Crossing <i>S. pombe</i> cells	82
2.5.1	Cell mating and growth	82
2.5.2	Cross selection	82
2.6	Spotting assays	84
2.6.1	Thiabendazole (TBZ) assays	85
2.6.2	Centromere silencing assays	86
2.6.3	DNA damage assays	87
2.6.4	Temperature sensitivity assays	87
2.7	Molecular techniques	88
2.7.1	Genomic DNA extraction	88
2.7.2	Polymerase chain reaction (PCR)	90
2.7.3	Agarose gel electrophoresis	90
2.7.4	Transformation of <i>S. pombe</i> cells using electroporation	92
2.7.5	Selection of transformants	92
2.8	Live imaging of <i>S. pombe</i> cells using fluorescence microscopy	93
2.8.1	Culture preparation	93
2.8.2	Image acquisition and analysis	93
2.9	Chromatin immunoprecipitation (ChIP)	94
2.9.1	Cell growth and harvesting	94
2.9.2	Chromatin immunoprecipitation	95
2.9.3	Analysis using quantitative Polymerase Chain Reaction (qPCR)	99
2.10	Immunoprecipitation followed by liquid chromatography coupled with tandem mass spectrometry (IP LC-MS/MS)	101
2.10.1	Cell growth and harvesting	101
2.10.2	Immunoprecipitation	102

2.10.3	LC-MS/MS	104
2.10.4	Data analysis	107
2.11	Co-immunoprecipitation (Co-IP)	108
2.11.1	Cell growth and harvesting	108
2.11.2	Co-immunoprecipitation	109
2.11.3	Sodium dodecyl-sulphate polyacrylamide gel electrophoresis (SDS-PAGE) and Western blotting	111
2.12	Bioinformatics	113
3	Investigation of the physical and genetic interaction between Ccp1^{Vps75} and Rtt109	114
3.1	Introduction	114
3.2	Results	116
3.2.1	Ccp1 ^{Vps75} and Rtt109 may have separate functions	116
3.2.2	Rtt109 may not be required for Ccp1 ^{Vps75} 's localisation at the centromere	118
3.3	Discussion	121
4	Investigation of the role of Ccp1^{Vps75} and Rtt109 in Cnp1^{CENP-A} loading at the centromere	125
4.1	Introduction	125
4.2	Results	127
4.2.1	<i>ccp1</i> Δ shows increased de-silencing at the centromere	127
4.2.2	In <i>ccp1</i> Δ mutant there is a decrease of GFP-Cnp1 ^{CENP-A} foci at the centromere	130
4.3	Discussion	136
5	Investigation of the interaction between Ccp1^{Vps75} and Cnp20^{CENP-T} in the context of Cnp1^{CENP-A} loading	141
5.1	Introduction	141
5.2	Results	143

5.2.1	Deleting <i>ccp1</i> affects Cnp20 ^{CENP-T} levels at the centromere . .	143
5.2.2	The physical interaction between Ccp1 ^{Vps75} and Cnp20 ^{CENP-T}	145
5.3	Discussion	151
6	Summary, conclusion and future perspectives	157
6.1	Summary of the results presented in the thesis	157
6.2	Conclusion	164
6.3	Future perspectives	166

List of Figures

1.1	Illustration of the mitotic chromosome and the organisation of centromere in fission yeast.	23
1.2	An illustration showing the position of the <i>arg3</i> gene in the centromeric core in cells used in experiments monitoring levels of (de)silencing at the centromere.	28
1.3	An illustration showing the proteins that make up the human CCAN, organised by the different functions they perform.	35
1.4	An illustration showing CENP-A propagation. Proteins such as CENP-C (CENP-A readers) recognise CENP-A and recruit the CENP-A chaperones, such as HJURP. The chaperone binds CENP-A in its pre-nucleosomal form.	40
1.5	The structure of the Ccp1 ^{Vps75} homodimer. (A) Top-down view of the dimer. (B) Alternative view. Adapted from the Protein Data Bank, entry 5GPL, as published by Dong et al.[3].	70
1.6	The structure of Rtt109. (A) Crystal structure of Rtt109 from <i>S. cerevisiae</i> . Adapted from the Protein Data Bank, entry 2RIM, as published by Lin et al.[276]. (B) The structure of the Rtt109-AcCoA/Vps75 complex from <i>S. cerevisiae</i> . Adapted from Protein Data Bank, entry 3Q35, as published by Tang et al.[277]. Vps75 ^{Ccp1} shown in red, Rtt109 shown in green.)	73

3.1	<i>ccp1</i> Δ <i>rtt109</i> Δ and <i>ccp1</i> Δ <i>rtt109</i> Δ cells are sensitive to TBZ. Serial dilutions of cells were plated on YES media containing several concentrations of TBZ. The plates were incubated at 25°C.	116
3.2	<i>rtt109</i> Δ cells are sensitive to both HU and MMS, while <i>ccp1</i> Δ cells are not. The sensitivity of <i>ccp1</i> Δ <i>rtt109</i> Δ mutant is attributable to the deletion of <i>rtt109</i> . Serial dilutions of cells were plated on YES media containing either HU or MMS at two different concentrations. The plates were incubated at 32°C.	117
3.3	Live images of wild type and <i>rtt109</i> Δ cells expressing Ccp1 ^{Vps75} -GFP. Scale bar = 5 μm.	118
3.4	A bar chart comparing the number of cells with Ccp1 ^{Vps75} -GFP foci in the imaged strains. N = 5. Error bars represent the standard deviation.	119
3.5	Rtt109 is not required for Ccp1 ^{Vps75} 's localisation at the centromere. ChIP comparing Ccp1 ^{Vps75} -GFP levels at <i>S. pombe</i> centromeres 1 and 3 in the wild type and <i>rtt109</i> Δ cells expressing Ccp1 ^{Vps75} -GFP. Error bars represent the standard error of the mean. N = 5.	120
4.1	Temperature sensitivity assay comparing the viability of <i>ccp1</i> Δ and <i>rtt109</i> Δ mutants in either the <i>cnp1-1 cnp1</i> Δ: <i>ura4</i> ⁺ or the wild type background. <i>ccp1</i> Δ and <i>rtt109</i> Δ cells survive at the restrictive temperature, however all cells containing the <i>cnp1-1</i> mutation do not survive at the restrictive temperature. Serial dilutions of cells of the indicated genotypes were plated on YES media supplemented with Phloxin B and incubated at indicated temperatures.	127

4.2 (A) *ccp1*Δ and *ccp1*Δ *rtt109*Δ show de-silencing, while *rtt109*Δ shows enhanced silencing at the centromere. Serial dilutions of cells of the indicated genotypes were plated on PMG media either supplemented with or without arginine and incubated at 32°C. (B) The position of the *arg3* gene in the central centromeric core. Imr = innermost repeats, otr = outermost repeats, cnt = central centromeric core. 128

4.3 (A) Live images of wild type, *rtt109*Δ, and *ccp1*Δ cells expressing GFP-Cnp1^{CENP-A}. Scale bar = 5μm. Red arrow points to declustered centromeres, the magnified image of which is shown in the insert. (B) A bar chart comparing the number of GFP-Cnp1^{CENP-A} foci in the imaged strains. N = 3. Error bars represent the standard deviation. (C) Live images of wild type and *ccp1*Δ cells expressing GFP-Cnp1^{CENP-A} and Sid4-Tomato. Scale bar = 5 μm. The distance between the two GFP-Cnp1^{CENP-A} foci was measured as 1.70 μm, and the magnified image of these foci is shown in the insert. (D) Live images of wild type and *ccp1*Δ cells expressing GFP-Cnp1^{CENP-A} and Sid4-mCherry. Scale bar = 5 μm. (E) A bar chart comparing the number of cells in which the GFP-Cnp1^{CENP-A} foci and the Sid4-mCherry foci overlap in the imaged strains. N = 3. Error bars represent the standard deviation. 130

4.4 ChIP comparing Cnp1^{CENP-A} levels at *S. pombe* centromeres in the wild type, *ccp1*Δ and *rtt109*Δ cells. Error bars represent the standard error of the mean. The drop in the Cnp1^{CENP-A} abundance in the *ccp1*Δ mutant was found to be significant at *p* values less than 0.001 using Student's t-test. 133

4.5	ChIP comparing histone H3 levels at <i>S. pombe</i> centromeres in the wild type, <i>ccp1</i> Δ and <i>rtt109</i> Δ cells. Error bars represent the standard error of the mean. The increase in the histone H3 levels in the <i>ccp1</i> Δ mutant was found to be significant at <i>p</i> values less than 0.05 using Student's t-test.	134
5.1	Live images of wild type and <i>ccp1</i> Δ cells expressing Cnp20 ^{CENP-T} -GFP. <i>ccp1</i> Δ show a decrease in the intensity of the Cnp20 ^{CENP-T} focus. Scale bar = 5 μ m. Some of the cells where this can be observed are noted with a red arrow.	143
5.2	Deletion of Ccp1 ^{Vps75} results in a decrease in Cnp20 ^{CENP-T} levels at centromeres. ChIP comparing Cnp20 ^{CENP-T} -GFP levels at <i>S. pombe</i> centromeres in the wild type and <i>ccp1</i> Δ cells expressing Cnp20 ^{CENP-T} -GFP. Error bars represent standard error of the mean. The decrease in the Cnp20 ^{CENP-T} -GFP levels in the <i>ccp1</i> Δ mutant was found to be significant at <i>p</i> values less than 0.01 using Student's t- test.	144
5.3	Co-IP of Ccp1 ^{Vps75} -GFP and Cnp20 ^{CENP-T} -FLAG. α -FLAG M2 antibody and Dynabeads were used for the immunoprecipitation, followed by a Western blot using the α -GFP antibody. The chemiluminescent signal was detected using BioRad Chemidocimaging system.	149
5.4	Co-IP of Ccp1 ^{Vps75} -GFP and Cnp20 ^{CENP-T} -FLAG. Invitrogen α -GFP antibody was crosslinked to Dynabeads and used for IP followed by a Western blot using α -FLAG M2 antibody and Abcam VeriBlot as the secondary antibody. The chemiluminescent signal was detected using Thermofisher iBright system.	149
5.5	Co-IP of Ccp1 ^{Vps75} -GFP and Cnp20 ^{CENP-T} -FLAG. α -FLAG M2 antibody was crosslinked to Dynabeads and used for IP, followed by a Western blot using the Invitrogen α -GFP antibody and Abcam VeriBlot as the secondary antibody. The chemiluminescent signal was detected using Thermofisher iBright system.	150

6.1	Multiple sequence alignment of NAP proteins from different organisms and the residues proposed for mutations. <i>S. pombe</i> Ccp1 sequence aligned with Nap1 from <i>S. japonicus</i> , <i>S. cryophilus</i> , <i>S. octosporus</i> , <i>S. cerevisiae</i> , <i>C. elegans</i> , Vps75 from <i>S. cerevisiae</i> , and SET from <i>H. sapiens</i> . The conserved residues within the NAP domain of <i>S. pombe</i> Ccp1 indicated with red arrows could be mutated to alanine to assess the impact of these mutations on the interaction between Ccp1 ^{Vps75} and Cnp20 ^{CENP-T}	168
-----	--	-----

List of Tables

2.1	<i>S. pombe</i> strains used in the project.	76
2.2	Yeast Extract with Supplements preparation.	78
2.3	Pombe Minimal Glutamate media preparation.	79
2.4	Malt Extract media preparation.	79
2.5	Oligonucleotides used in the project.	80
2.6	Supplementing YES agar with antibiotics.	82
2.7	DNA buffer preparation.	89
2.8	TE buffer preparation.	89
2.9	PCR conditions.	90
2.10	Buffer I preparation.	94
2.11	Lysis buffer preparation.	95
2.12	TES buffer preparation.	96
2.13	Wash buffer preparation.	97
2.14	qPCR master mix preparation.	99
2.15	qPCR conditions.	99
2.16	Lysis buffer preparation.	102
2.17	The preparation of lysis buffer supplemented with MgCl ₂	103
2.18	BD buffer preparation.	103
2.19	Reagents used for preparation of gel band samples for mass spectrometry.	104
2.20	Lysis buffer preparation.	109
2.21	5x SDS-PAGE running buffer preparation.	111

5.1	Results obtained in an IP-LC/MS-MS experiment using the wild type fission yeast and Ccp1 ^{Vps75} -GFP strains. Accession numbers given in the table below refer to the UniProt database.	145
5.2	Results obtained in an IP-LC/MS-MS experiment using the wild type fission yeast and Ccp1 ^{Vps75} -GFP strains. Accession numbers given in the table below refer to the UniProt database.	147
5.3	Results obtained in an IP-LC/MS-MS experiment using the wild type fission yeast and Ccp1 ^{Vps75} -GFP strains. Accession numbers given in the table below refer to the UniProt database.	148

List of abbreviations

Ago1	Argonaute, DNA binding protein
CATD	CENP-A targeting domain
CCAN	Constitutive centromere associated network
Ccp1	Counteractor of CENP-A loading protein
Cdc2	Cell division cycle protein 2
Cdc13	Cell division cycle protein 13 (G2/M B-type cyclin Cdc13)
CDK1	Cyclin-dependent kinase
CEN	Central core
CENP-A	Centromere protein A
CENP-B	Centromere protein B
CENP-C	Centromere protein C
CENP-N	Centromere protein N
CENP-T	Centromere protein T
Cig1	Cyclin involved in G1 (G1/S-specific B-type cyclin Cig1)
Cig2	G1/S-specific B-type cyclin Cig2
Clr4	Histone-lysine H3-K9 methyltransferase
Cnp1	Centromere protein 1
Cnp20	Centromere protein 20
cnt	Central core
Cse4	Chromosome segregation protein 4
COMA	Ctf19, Okp1, Mcm21, Ame1 complex
Dcr1	Dicer, Dcr1 RNase

Eic1	Eighteen-interacting centromere protein 1
Eic2	Eighteen-interacting centromere protein 2
FACT	Facilitates Chromatin Transcription
G1	Growth 1 phase
G2	Growth 2 phase
GFP	Green fluorescent protein
HAT/KAT	Histone (lysine) acetyltransferase
Hat2	Histone acetyltransferase type B subunit 2
HJURP	Holliday Junction Recognition Protein
HP1/Swi6	Heterochromatin (HP1) family chromodomain protein Swi6
HR	Homologous recombination pathway
imr	Innermost repeats
K	Lysine
KMN	KNL1/Mis12/Ndc80 complex
KNL2	Kinetochores null protein 2
MAP	Mitogen-activated protein
Mis16	Kinetochores protein mis16
Mis18	Kinetochores protein mis18
M18BP1	Mis18-binding protein 1
NAP	Nucleosome assembly protein
ncRNA	Non-coding RNA
Ndc80	NMS complex subunit ndc80
NHEJ	Non-homologous end-joining pathway
otr	Outermost repeats
Pol α	DNA polymerase alpha catalytic subunit
Pol δ	DNA polymerase delta catalytic subunit Cdc6
Pol ϵ	DNA polymerase epsilon catalytic subunit Pol2 (Cdc20)
Puc1	Pombe unidentified cyclin
RbAp46	Retinoblastoma-binding protein p46

RbAp48	Retinoblastoma-binding protein p48
RNAi	RNA interference
Rdp1	RNA-directed RNA polymerase
Rtt109	Regulator of Ty1 transposition protein 109
S	Synthesis phase
SAC	Spindle assembly checkpoint
Scm3	Suppressor of chromosome missegregation protein 3
siRNA	Small interfering RNA
SR protein/SR-like protein	Serine arginine-rich protein
SRRM1	Serine/arginine repetitive matrix protein 1
STE	Subtelomeric sequences
TOR	Target of rapamycin
tRNA	Transfer RNA
Vps75	Vacuolar protein sorting-associated protein 75
Wee1	M phase inhibitor protein kinase Wee1

Chapter 1

Introduction

1.1 Motivation

Centromeres are epigenetically inherited[7] and CENP-A, a centromere-specific histone H3 variant, has been shown to be the epigenetic mark of functional centromeres and it is present across species, with few exceptions, from yeast to humans[1].

CENP-A deposition in each cell cycle is required to maintain the identity of the centromere[8]. It has also been suggested that CENP-A plays a role in signalling, as it has been found that the spindle checkpoint is activated in cells which are deficient in CENP-A, leading to mitotic arrest[9].

Ccp1, a NAP (Nucleosome Assembly Protein) family member, has been found to function as a regulatory subunit of a histone acetyltransferase Rtt109 in budding yeast, *Saccharomyces cerevisiae*[6], however its role in fission yeast, *Schizosaccharomyces pombe*, remains to be explored.

Previous studies have found that CENP-T, a protein in the Constitutive Centromere Associated Network (CCAN), is important in promoting epigenetic stability of centromeres in fission yeast and that cooperation of Cnp20^{CENP-T} and Cnp1^{CENP-A} is important for stable centromere inheritance[10]. The authors of this paper suggest that the N-terminus of Cnp1^{CENP-A} recruits Cnp20^{CENP-T}, and through this, the CENP-T branch of CCAN. As the CENP-TWSX complex forms a nucleosome-like structure, it is possible that Ccp1 interacts, through its NAP domain, with

Cnp20^{CENP-T} to regulate CENP-A deposition at the centromere.

Due to the importance of CENP-A deposition and maintenance at the centromere for the correct progression of the cell cycle, and the crucial impact any errors in this process have on the cell, identifying all of the participating proteins and understanding each of their roles is crucial for our understanding of cell cycle.

This has further implications for translational research, and our understanding of diseases such as cancer, as errors in chromosome segregation can contribute to their development as well as their resistance to available treatments, as chromosomal instability can increase resistance to chemotherapeutic drugs in cancers[11].

1.2 *Schizosaccharomyces pombe*

1.2.1 Chromosome and gene organisation in fission yeast

The fission yeast has the genome size of 13.8 Mb[12, 13] and the *S. pombe* genome is organised into three relatively large chromosomes. The three *S. pombe* chromosomes are 5.7, 4.6 and 3.5 Mb in size[12].

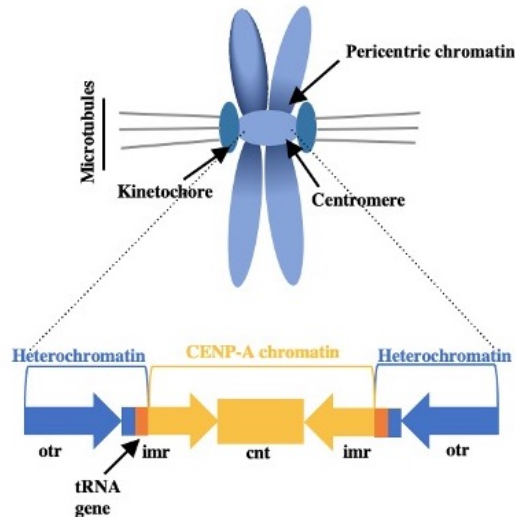


Figure 1.1: Illustration of the mitotic chromosome and the organisation of centromere in fission yeast.

S. pombe has regional centromeres, just like higher eukaryotes[14–16]. The three fission yeast centromeres are roughly 40, 69 and 110 kb in size[12, 14, 15].

Fission yeast has centromeres described as "regional"[16], whereas in budding yeast they are described as being "point" centromeres[14, 15]. *S. pombe* centromeres are more complex and significantly larger in size than the *S. cerevisiae* ones, and they contain numerous repetitive sequences, which is a feature they share with centromeres of higher eukaryotes[17]. The three centromeres of fission yeast measure approximately 35 kb (Chromosome I), 65 kb (Chromosome II) and 110 kb (Chromosome III) in length.

The centromeres consist of the central core (cnt, CEN) which are flanked by innermost repeats (*imr1R*, *imr1L*) and outermost repeats (*otr*), consisting of *dg* and *dh* sequences which vary in number. The central core measures approximately

4 kb in length, and a region of approximately 1.4 kb within it shares approximately 48% of its identity between all of the three centromeres[18, 19].

Other than in their complexity, fission yeast centromeres show the similarities with human centromeres also in the way the repetitive sequences are arranged. This is also true for the arrangement of the repetitive sequences in the centromere flanking regions. Meanwhile, budding yeast centromeres do not share such similarities with human and *S. pombe* centromeres[13, 18, 20–22].

RNAi machinery directs the assembly of heterochromatin at the centromere - most notably, RNAi pathway is required for recruiting of CENP-A, a centromere-specific histone H3 variant, to the central core of the centromere. This is crucial for kinetochore formation and chromosome segregation later in the cell cycle[23].

Dicer (Dcr1 RNase), Argonaute (Ago1 DNA binding protein) and Rdp1 (RNA-directed RNA polymerase) are necessary in the process of heterochromatin assembly in fission yeast[24]. All three components have also been found to be highly conserved components of the RNAi machinery. Dicer's role in the process is to mediate the conversion of the double stranded RNA, which is transcribed from repetitive regions, into siRNAs (small interfering RNAs). The resulting siRNAs are then multiplied by Rdp1. siRNAs then interact with Argonaute and guide the complexes which remodel chromatin to the genome sites whose sequence is complementary to the sequence of those siRNAs.

Two other processes take place in the same region of chromatin - one is the methylation of histone H3 on lysine 9 (H3K9), mediated by Clr4 (a methyltransferase), and, following the H3K9 methylation, which creates binding sites for the HP1 family of chromodomain proteins, recruitment and oligomerisation of the heterochromatin HP1/Swi6 protein. This results in formation and spreading of heterochromatin[25].

In summary, the chromosome and gene organisation in fission yeast has many shared

features with human, and in general metazoan, cells, from centromere and telomere structure, to gene structure, such as existence of several introns within a single gene, as well as gene expression modulation, making it a great model organism for epigenetics research.

1.3 Chromosomes, the centromere and the kinetochore

DNA molecules inside nuclei of eukaryotic cells are packed into highly condensed nucleoprotein structures called chromosomes, in which DNA is wrapped in a superhelical manner around histone octamers almost two times forming nucleosomes[26]. The octameric structure of canonical nucleosomes consists of two copies of each of the core histones: H2A, H2B, H3 and H4. Nucleosomes form chromatin fibres, which, in turn, form chromatin when various scaffolding proteins are incorporated into the structure.

This kind of packaging enables the large DNA molecules to fit into cell nuclei; however, this kind of efficient DNA packaging also hinders processes requiring access to the underlying DNA sequence - such as DNA repair, transcription, replication and recombination. Because of this during the cell cycle the structure of chromosomes varies and the factors that modify chromatin structure are crucial to the regulation of genetic processes in the cell.

Such processes include nucleosome assembly regulation by histone chaperones, the covalent modification (e.g. methylation, acetylation) of histone proteins and DNA, targeted incorporation of histone variants (e.g. CENP-A, a histone H3 variant) as well as mechanical remodelling of nucleosomes by ATP-dependent Snf2 family proteins[27–32].

During the S-phase the chromosomes are replicated and consist of two sister chromatids which are then separated during mitosis. The segregation of the sister chromatids and its accuracy depend on two structures - the centromere and the kinetochore.

1.3.1 The centromere

The centromere is a specialised chromosome locus where kinetochores assemble[1]. In the fission yeast *S. pombe*, it can be functionally divided into the centromere core (*cnt*) and the heterochromatic pericentromeric regions. The core region serves as the site of kinetochore complex assembly. It is characterised by CENP-A, a centromere-specific variant of the histone H3[1, 2]. It has been found that in *S. pombe* centromeres the majority of the histone H3 is replaced by an ortholog of CENP-A known as Cnp1[33].

In fact, based on the intensity of the Cnp1-GFP locus, it has been estimated that in a typical fission yeast cell there are 680 CENP-A molecules[34]. Further experiments, which used single molecule microscopy, have revealed that there are between 72 and 82 CENP-A molecules in a centromere cluster (i.e. in all three fission yeast centromeres together).

ChIP-Seq (chromatin immunoprecipitation coupled with DNA sequencing) has been employed to take these quantitation efforts further, and through these experiments it has been found that per centromere there are between 19 and 24 CENP-A nucleosomes, which would imply a total of 64 molecules of CENP-A in a haploid cell[35].

The centromeric core spans a region of the chromosome which is between 4 to 7 kb in length. Either side of the core are the repeat regions called the innermost repeats (*imr*). Cnp1^{CENP-A} is enriched in the *imr* regions as well as the core. Either side of the *imr* regions are the outermost repeat regions (*otr*) packaged in pericentromeric heterochromatin, which is characterised by nucleosomes containing histone H3 which has been methylated on lysine 9 (K9). tRNA genes provide a physical barrier which stops the pericentromeric heterochromatin from spreading into the central core[36].

Transcriptional silencing at the centromere

It has been shown that genes inserted in fission yeast centromeres are transcriptionally silenced[37]. This is due to specific packaging at the centromere, as functional centromeres have an optimal level of CENP-A. A reporter gene can be inserted at the centromere (commonly *arg3⁺*) and its expression monitored by using a selective medium.

In such an experiment, the endogenous copy of the gene must be deleted. This allows researchers to indirectly determine CENP-A levels at the centromere by monitoring whether the reporter gene within the centromere is silenced or expressed. This is commonly known as the centromere silencing assay. Figure 1.2 shows the position of the reporter gene (*arg3⁺*) in the central centromeric core in strains used in centromere silencing assays. Mutants of genes involved in CENP-A deposition at centromeres have been observed to de-silence *arg3* (i.e., grow on media lacking arginine) due to reduced CENP-A levels and correspondingly increased histone H3 levels at the centromere[38].

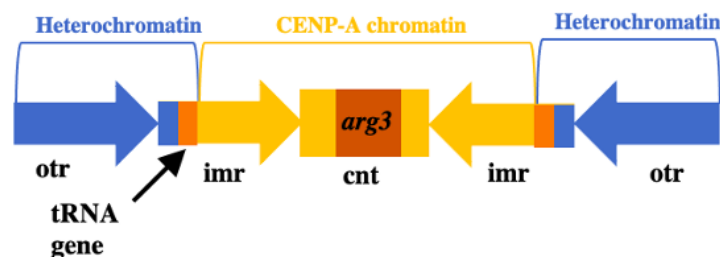


Figure 1.2: An illustration showing the position of the *arg3* gene in the centromeric core in cells used in experiments monitoring levels of (de-)silencing at the centromere.

In a variation of this experiment, *ura4⁺* can also be used as a reporter gene, and 5-fluoroorotic acid (5-FA) used in the selective medium. In addition, researchers have also used *ade6⁺* as the reporter gene, which gives in colony colour variation - the colonies are red when *ade6⁺* is repressed, and white when the *ade6⁺* reporter is expressed. It is important to note, however, that compared to silencing in the outer repeats, silencing of *ade6⁺* in the central domain is somewhat unstable, which results in variegated (i.e. sectored) colonies[20]. Interestingly, if moved only 1 kb

distal to the outer repeats, no silencing is observed - this has suggested that the transcriptional silencing happens only at the centromere[37, 39].

In fission yeast the first genetic screens using the position effect variegation (PEV) looked at mutants which allowed for expression of two normally silent cassettes - *mat2-P* and *mat3-M*. It was possible for researchers to identify these mutants because they exhibited an atypical mating pattern or because they could select for the expression of a *ura4+* transgene which has been previously inserted in the mating type region[40–42].

As a result of these screens a whole host of genes, named cryptic loci regulators (*clr*), were identified - namely, *clr1⁺*, *clr2⁺*, *clr3⁺*, *clr4⁺*. In addition to those genes, *rik1⁺* and *swi6⁺* were identified in these early screens. The products of these genes are the fission yeast counterparts of budding yeast silent information regulator (Sir) proteins[43].

Several of the Clr proteins identified in these screens were later shown to be required for centromere silencing and silencing at the mating type loci of fission yeast[39]. This brought into focus the connection between heterochromatin formation at centromeres and the mating type loci.

Interestingly, while both fission yeast and budding yeast have transcriptional silencing at the mating type loci, rDNA regions and telomeres, only fission yeast shows silencing at centromeres[20].

Such silencing requires histone modifications to be made - and histone H3K9 methylation in particular has been shown to be important in this process - as well as RNAi proteins, homologs of HP1 (heterochromatin protein 1) and the RNA polymerase II machinery. Such mechanisms are conserved in higher eukaryotes, however, unlike many other eukaryotes and *Neurospora crassa* with which *S. pombe* shares silencing mechanisms, in fission yeast there appears to be no DNA methylation at a detectable level[44]. DNA methylation has been found to be a common mechanism

used to transcriptionally silence chromatin, however in fission yeast this is achieved primarily by using the RNAi machinery and modifications of chromatin.

As highlighted by the findings discussed above, heterochromatin is important at centromeres to ensure normal chromosome segregation[39, 45].

Pericentromeric heterochromatin

The role of the pericentromeric heterochromatin is crucial in both mitotic and meiotic cell divisions, and it has been shown to provide elasticity and resistance to cohesin mediated tension. It is also necessary for tension sensing and signalling to the mitotic checkpoint[2, 46]. In addition, pericentromeric heterochromatin provides genome stability and sister-chromatin cohesion.

It is also important to note that this is not the only heterochromatin containing regions of *S. pombe* - in total, there are four of these regions: centromeres, mating type loci (*mat2-P* and *mat3-M*), the rDNA region, and telomeres[47]. Transcriptionally silenced chromatin found close to telomeres has been shown to have a role in meiotic chromosome segregation[48–50] - similarly to what has been found for centromeric chromatin.

While it has been identified, it still is not clear which function heterochromatin in the rDNA region of fission yeast plays[51, 52]. It has been suggested that it is involved in rDNA stability maintenance by preventing recombination from occurring between the rDNA repeats, similarly to budding yeast[43].

Centromeric and pericentromeric chromatin and post-translation modifications of histones are discussed in more detail in Section 1.6.

Regional and point centromeres

The centromeres of human cells are similar to those of *S. pombe*, and are characterised by α -satellites (chromosome-specific monomeric units of 171 bp). These are

arranged in head-to-tail tandem arrays[36].

While they are not related to those observed in humans, tandem repetitive sequences are also found in centromeres of other organisms, such as mice and plants[53]. Despite the evident importance of centromeres throughout evolution, the DNA sequence at the centromere is not highly conserved - it, in fact, varies significantly between organisms. Furthermore, the position of the centromere is not the same in different organisms either – they can be metacentric (in the middle of the chromosome), telocentric (close to the chromosome’s end) or acrocentric (centromeres which separate chromosome arms of different length)[1].

In the budding yeast *S. cerevisiae* the centromeres are described as “point” centromeres because they are occupied by a single Cse4 nucleosome and made up of a conserved 125 bp sequence for all 16 chromosomes in the genome. This sequence is both necessary and sufficient for the specification of centromere function[14, 15].

In contrast to the *S. cerevisiae* centromere, the centromeres of most organisms are far more complex and are referred to as “regional” centromeres because they span large regions of chromosomes[16], and such centromeres are found in *S. pombe*. In these centromeres it has not been possible to identify a connection between the DNA sequence of the centromere and the ability to form a kinetochore[53]. In fact, in *S. pombe* the conversion of a non-functional centromere to a functional one on mini-chromosomes can happen even if no changes in sequence or structure have been observed[54].

Furthermore, dicentric chromosomes show inactivation of one the two centromeres, which shows that the DNA sequence alone is insufficient for kinetochore formation[55]. There is also evidence to point to the fact that the repetitive sequences found in centromeres are also not necessary for a functional centromere – in *Drosophila melanogaster* acentric chromosomes acquire a neo-centromere at non-repetitive sequences[56].

All this points to the fact that centromeres are epigenetically inherited and it appears that CENP-A is crucial for the specification of centromeres as it is sufficient to promote kinetochore formation on ectopic loci[7]. The importance of CENP-A is emphasised by the fact that it is present at functional centromeres across species (with few exceptions), from yeast to humans[1].

1.3.2 The kinetochore

The kinetochore is a multi-protein complex which mediates attachments of sister chromatids to spindle microtubules during cell division[1]. The kinetochore assembles on the central domain of the centromere. This allows for the segregation of the chromatids into the daughter cells. As mentioned earlier in section 1.3.1, the centromere shows a distinct chromatin configuration which does not involve methylation of histone H3 on K9, which also reflects its role as the site of the kinetochore assembly.

Other than their role as sites of microtubule attachment, kinetochores act as mechanosensors and control the stability of microtubule attachment, thus preventing incomplete or incorrect attachment (e.g. mono-orientation)[57]. They are also known to regulate the spindle assembly checkpoint (SAC) as the SAC prevents premature mitotic exit in cells with unattached or incorrectly attached kinetochores[58]. In addition, they participate in maintaining cohesion between sister chromatids until anaphase[9].

It has been found that in kinetochore mutants, which have a disrupted CENP-A chromatin structure, show a pattern characteristic of bulk chromatin when digested with micrococcal nuclease, without any effect on the gene silencing in the *otr* region of the centromere or the adjacent chromatin[38, 59].

It has been suggested that the transcriptional silencing within the central domain of the centromere is in fact caused by the assembly of the kinetochore as this provides a steric obstacle to RNA Pol II so it becomes unable to access reporter genes inserted in the centromeric core. This is supported by the finding that in conditional temperature sensitive kinetochore mutants of fission yeast there is an increase in the transcription of the reporter gene at the centromere core, which could be explained by the fact that the kinetochore is only partially functional at the permissive temperature[38].

The kinetochore consists of the inner kinetochore and the outer kinetochore. The inner kinetochore consists of the constitutive centromere associated network of proteins, or CCAN (which are discussed in section 1.4 in greater detail), while the outer kinetochore comprises the KMN network (KNL1/Mis12/Ndc80 complex), which comprises a conserved network of proteins.

1.4 Constitutive centromere associated network of proteins (CCAN)

The constitutive centromere associated network is a network of 17 proteins which localise to the region of the kinetochore proximal to the centromere, acting as the interface between the centromere and the kinetochore. CCAN proteins also recruit components of the outer kinetochore, such as the KMN network (KNL1/Mis12/Ndc80 complex)[60]. These have been first discovered in patients with the autoimmune syndrome CREST and were named centromere proteins (CENP-). In yeasts, however, the nomenclature is less straightforward – for example, CENP-T is called Cnp20 in *S. pombe* and Cnn1 in *S. cerevisiae*.

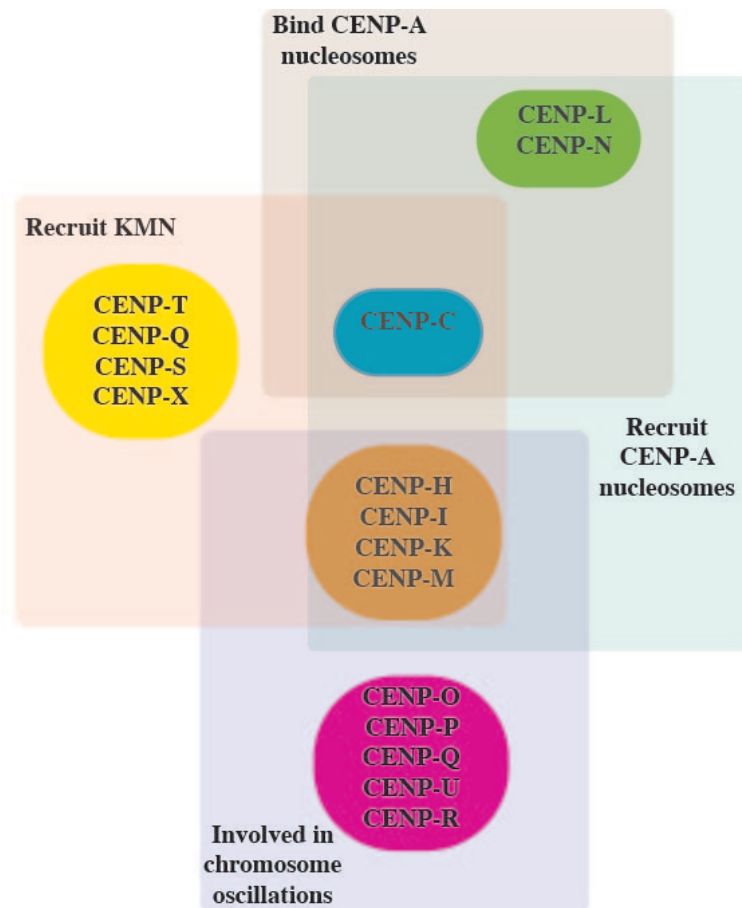


Figure 1.3: An illustration showing the proteins that make up the human CCAN, organised by the different functions they perform.

The CCAN proteins are divided in five groups according to their reported func-

tions (Fig. 1.3)[53]. These groups are: CENP-C, the CENP-LN complex, the CENP-HIKM complex, the CENP-OPQUR complex and CENP-TWSX complex.

So far, only CENP-C and CENP-N have been found to directly interact with CENP-A. Furthermore, these two CCAN proteins have also been found to show specificity for CENP-A when compared to H3 nucleosomes[61, 62].

Although both of these proteins interact directly with CENP-A, they don't use the same binding site to do so. CENP-N binds to CENP-A's centromere-targeting domain, while CENP-C interacts with the acidic patch of histones H2A and H2B, as well as CENP-A's C-terminus[62].

It appears that CENP-C uses two of its regions to bind to CENP-A: the central region and the CENP-C motif. Both of these regions consist of approximately 25 amino acid residues and have several conserved positively charged residues close to their N-terminus and two aromatic residues close to the C-terminus. It is thought that therefore the N-terminal positively charged residues interact with the acidic patches on histones H2A and H2B of the CENP-A nucleosome, while the aromatic residues interact with the C-terminal tail of CENP-A[62].

In fact, the C-terminal tail of CENP-A is known to be necessary for CENP-C binding[63]. It has been implied that the hydrophobicity of CENP-A's C-terminal tail is the key for specific recognition rather than the specific amino acid sequence – this is because while there is no significant conservation of the sequence of CENP-A C-terminus across species, CENP-A's C-terminal tail, across species, does show a higher hydrophobicity than that of the histone H3[62].

Interestingly, despite the central region of CENP-C and the CENP-C motif being related in sequence, only the central region is necessary and sufficient to promote CENP-A nucleosome binding *in vitro* and kinetochore targeting *in vivo*[62].

Despite CENP-C and CENP-N exhibiting a selectivity for CENP-A over histone H3 *in vitro*, this selectivity is described as modest and it is thought that other mechanisms are employed in cells to achieve the selectivity of kinetochore targeting of these proteins to the CENP-A nucleosome.

One such mechanism is the dimerisation of CENP-C through a cupin-like domain found on its C-terminus[62]. Furthermore, post-translational modifications are also thought to contribute to the selective recognition of CENP-A nucleosomes[64].

CENP-HIKM also contributes to the CENP-A binding affinity, however it does not show a preference for CENP-A over H3 nucleosomes, or, indeed, linear DNA[61].

CENP-TWSX complex forms when CENP-TW and CENP-SX subcomplexes associate to form a tetramer. All four subunits have histone fold domains, and CENP-T has additional sequences at its N-terminus which have a role in kinetochore assembly. It is thought that the CENP-TWSX tetramer forms a nucleosome-like structure which flanks the CENP-A nucleosome at centromeres, although both subcomplexes have distinct biological functions[65].

The *S. pombe* ortholog of CENP-T is Cnp20. Previous studies have found that Cnp20^{CENP-T} is important in promoting epigenetic stability of centromeres in fission yeast and that cooperation of Cnp20^{CENP-T} and Cnp1^{CENP-A} is important for stable centromere inheritance[10]. The authors of this paper suggest that the N-terminus of Cnp1^{CENP-A} recruits Cnp20^{CENP-T}, and through this, the CENP-T branch of CCAN.

CENP-T is an inner kinetochore protein. It has been found to be involved in Ndc80 complex assembly during mitosis, however there are still questions about temporal regulation of CENP-T throughout the cell cycle. A recent study has suggested that Mis16 plays a role in recruiting CENP-T to the centromere[66].

CENP-OPQRU forms when CENP-O, CENP-P, CENP-Q, CENP-R and CENP-

U associate to form a complex. The complex is recruited to the kinetochore and it is known that CENP-CHIKMLN is required for this process[1].

It is somewhat unclear what the importance of this complex is in vertebrates, as its role seems to vary in different systems. In budding yeast, however, in the CENP-OPQRU-related complex, known as the COMA complex (Ctf19, Okp1, Mcm21, Ame1), Ctf19 and Mcm21 are required for accurate chromosome segregation, even though they are non-essential[67]. Ame1 and Okp1 are, in contrast, essential for viability and Ame1 has been found to interact with the Mis12 complex of the KMN network[68].

CENP-B is the only specific DNA-binding protein at mammalian centromeres. It is not one of the CCAN proteins, however it interacts with some of the CCAN proteins, namely CENP-C. CENP-B binds to the CENP-B box, a conserved 17 bp box, and many copies of this box are found in the centromeric α -satellite repeats.

The role of CENP-B is uncertain as there is limited evidence for its conservation, the CENP-B boxes are not found in neocentromeres and chromosomes without the CENP-B boxes are known to exist[69]. However, CENP-B binds directly to CENP-C, so it may be required in an alternative CENP-C recruitment pathway. It is also thought to stabilise the structure of the centromere[70].

1.5 CENP-A function, deposition and maintenance

It is thought that the presence of nucleosomes containing CENP-A is the epigenetic mark indicating active centromeres. The CENP-A nucleosome is sufficient for the formation of the centromere and kinetochore assembly during mitosis[71]. Furthermore, CENP-A deposition in each cell cycle is required to maintain the identity of the centromere[8]. It has also been suggested that CENP-A plays a role in signalling, as it has been found that spindle checkpoint is activated in cells which are deficient in CENP-A, leading to mitotic arrest[9].

While there is a wealth of evidence suggesting that centromeres appear to be epigenetically specified, there is also evidence pointing to a contribution from the DNA sequence as well. Centromeric DNA as well as regions of the genome associated with neocentromere formation have been shown to promote centromere formation and CENP-A deposition[72–78].

In humans the sequence conservation between CENP-A and histone H3 is under 60% while between organisms this drops even further. Interestingly, while the sequence may be divergent it has been found that the conservation of function is extremely high - this has been demonstrated in experiments where the budding yeast Cse4 was able to complement a knockdown of human CENP-A[79].

1.5.1 Establishment of CENP-A

It has been shown that a region within the histone fold domain of CENP-A called CENP-A targeting domain (CATD) is both necessary and sufficient for centromere targeting[80–82]. The CATD in humans comprises of loop L1 and alpha helix $\alpha 2$ of CENP-A and it serves as a recognition area for several factors and chaperons, such as HJURP (Holliday Junction Recognition Protein, a CENP-A chaperone), CENP-C and CENP-N, which are both members of the CCAN[83–86]. As well as this, CENP-C has been shown to recognise the six terminal amino acids of CENP-A’s C-terminal tail.

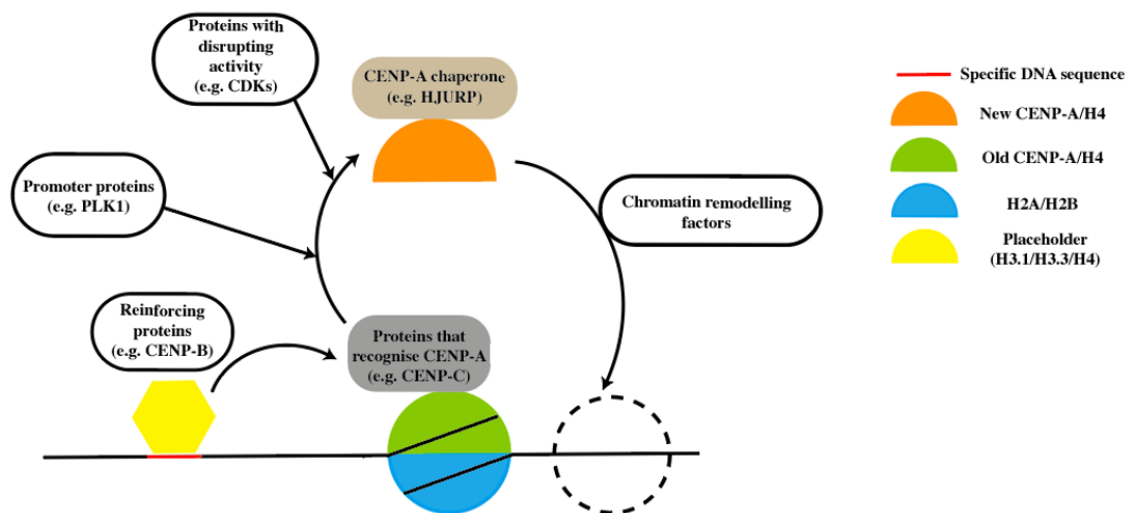


Figure 1.4: An illustration showing CENP-A propagation. Proteins such as CENP-C (CENP-A readers) recognise CENP-A and recruit the CENP-A chaperones, such as HJURP. The chaperone binds CENP-A in its pre-nucleosomal form.

During the S phase, when parental histones are inherited by one of the newly synthesised DNA strands, new histones are loaded to avoid dilution of histones. However, only canonical histones are loaded at this time and placeholder nucleosomes, which contain H3.3 or, in fission yeast, its close relative hht3 are employed to fill the gaps for CENP-A nucleosomes[76, 87]. CENP-A is loaded in subsequent stages of the cell cycle to maintain centromere identity, however exact timing of CENP-A loading is specific to each species - in humans this is from late telophase to G₁, in *Drosophila melanogaster* it is metaphase to G₁, and in *S. pombe* and *Ara-*

bidopsis thaliana this takes place in G₂[35, 76, 87–93].

A key player in CENP-A deposition is HJURP, which was found to specifically interact with CENP-A in its pre-nucleosomal form. Furthermore, it has been found to be both necessary and sufficient for deposition of newly synthesised CENP-A nucleosomes in human cells *in vivo*[94].

In yeast (both budding and fission), the CENP-A specific chaperone is Scm3. The sequence similarity between Scm3 and HJURP is limited, but they are functional orthologs[95]. Both of these chaperones interact with CENP-A through the N-terminal end of these proteins.

A multitude of experimental data show that the suppression of either of these chaperones results in a termination of CENP-A deposition, which in turn impacts kinetochore assembly, leading to mis-segregation of chromosomes[96]. Mutants of Scm3 are also defective for centromeric reporter gene silencing[97]. Scm3 has been found to disassociate from the centromeres during mitosis, similarly to Mis16 and Mis18[96, 97].

CENP-A chaperones HJURP, Scm3 and the *Drosophila* CAL1 have been shown to be essential for CENP-A targeting to the centromere[94, 96–99], and crystal structures of these chaperones have shown that they have considerable contact with CENP-A's CATD in its pre-nucleosomal form and the soluble CENP-A-H4 heterodimeric form[85, 95, 100].

Research has identified several CENP-A loading factors and chaperons, some of which have been mentioned above. Evidence suggests that the localisation of chaperones HJURP and CAL1 on chromatin is sufficient to incite the loading of CENP-A and therefore the formation of the centromere, other mechanisms must be in place in the cell to ensure that the loading of CENP-A takes place only on correct sites.

Mis16 and Mis18 have been identified as conserved centromeric proteins with a role in CENP-A deposition and deacetylation of histones in the centromeric core[59]. The first known step of CENP-A deposition is the localisation of the Mis18 complex to the centromere. In *S. pombe* temperature sensitive mutants of Mis18, the mis-segregation of chromosomes was observed because of a decrease in centromeric Cnp1^{CENP-A} levels[59]. In *S. pombe* Mis18 dissociates from the centromere in metaphase and re-associates in telophase, whereas in human cells it is only present in the G₁ phase[101].

The Mis18 complex is (in vertebrates) composed of Mis18 α Mis18 β and Mis18BP1. The complex interacts with CENP-C as well as the CENP-A nucleosome at the centromere and HJURP-CENP-A-H4[102–105]. To ensure that CENP-A is loaded onto the centromere only once in every cell cycle, cyclin-dependent kinases 1 and 2 (CDK1 and CDK2) are employed to phosphorylate HJURP as well as Mis18BP1 during the S and G₁ phases to prevent their localisation at the centromere.

This mechanism ensures CENP-A loading is limited to late telophase and G₁ when CDK activity drops[106–108]. The CDK phosphorylation of Mis18BP1 has an additional function - it disrupts its interaction with not only the centromere, but also Mis18 α and Mis18 β which in turn causes a further inhibition of CENP-A deposition[108]. The Mis18 complex will be discussed in more detail in section 1.5.2.

CDK activity in this context is antagonised by PLK1 (Polo-like kinase 1) as it phosphorylates Mis18BP1 at other residues, and promotes CENP-A loading as well as the localisation of Mis18BP1 at the centromere[109].

Studies have also identified a human SUMO peptidase SENP6 as a factor in regulating the localisation of CENP-A because it acts to antagonise the activity of PIAS4, a SUMO ligase, which sumoylates Mis18BP1.

This leads to the degradation of Mis18BP1 through a SUMOylation-dependent ubiquitin ligase RNF4. By antagonising the activity of PIAS4 SENP6 acts as a

protector of Mis18BP1[110]. Similarly to this finding, a deubiquitinase USP11 has been shown to protect HJURP and promote its interaction with CENP-A[111].

Chaperones RbAp46 and RbAp48 have also been implicated in CENP-A loading. As they form a part of several chromatin associated complexes, such as NURF and NURD, they are also thought to work together with HAT1 to promote acetylation of histone H4 at K5 and K12 in the prenucleosomal complex of CENP-A and histone H4[59].

Sim3 is a NASP-like protein, which has also been found to interact with CENP-A and act as a chaperone[112].

While chaperones have an important role in the targeting and loading of CENP-A at the centromere, post-translational modifications of CENP-A have also been hypothesised to be involved in this process.

In particular, phosphorylation of serines S68 and S18 by Cdk1 have been proposed to regulate CENP-A targeting and loading. The phosphorylation of S68 has been suggested to disrupt the binding of CENP-A to HJURP as well as to play a role in the degradation of CENP-A[113–116]. Meanwhile, phosphorylation of S18, which was identified through high resolution mass spectrometry, has been found to have an effect on the stability of CENP-A at the centromere[117, 118].

In an experiment where mCherry-LacI-HJURP was tethered to LacO repeats it has been found that a mutant of CENP-A carrying a point mutation S18D can still be recruited by HJURP, however most of the protein ended up mislocaling, leading to a hypothesis that S18D is a mutation which causes the weakening of CENP-A's interaction with HJURP[118].

In addition to this mechanism, CENP-B has been shown to bind short DNA motifs in α satellite repeats, and, through this, stabilise CENP-C at centromeres[69, 119]. Experiments with cells lacking CENP-B have shown that CENP-B is not es-

essential for CENP-A loading or the formation of centromeres, however cells lacking CENP-B have also been observed to have reduced levels of CENP-A[70, 120–122]. This could point to the fact that there is a CENP-A establishment mechanism which is DNA-dependent.

HJURP and the Mis18 complex are not conserved across all organisms - for example, *Drosophila* has the protein CAL1 which is believed to be both a CENP-A chaperone as well as a CENP-A targeting factor, thus combining the activity of HJURP and the Mis18 complex.

Drosophila studies support this hypothesis as CAL1 has been found to recruit dCENP-A (or CID, centromere identifier) and establish functional centromeres, as well as to be sufficient (with dCENP-C) for dCENP-A propagation in a heterologous system[98, 123, 124]. Interestingly, while CAL1 seems to be unrelated to HJURP crystal structure data has revealed that CAL1 binds to dCENP-A using its N-terminus in a manner similar to the specialised contacts that HJURP employs to bind CENP-A. Additionally, though its C-terminus CAL1 also interacts with the conserved cupin dimerisation domain of dCENP-C[98, 100, 123–125].

In addition to CAL1, there are other factors which have been shown to regulate the loading of *Drosophila* CENP-A. One such factor is the FACT (Facilitates Chromatin Transcription) complex which has been shown to interact with CAL1 and be required for the loading of dCENP-A[126]. As well as the FACT complex, there is evidence to suggest that the histone chaperone p55^{RbAp48} is involved in the process of dCENP-A loading and that its role is to chaperone dCENP-A-H4 complex and to assemble it on chromatin[127, 128].

Unlike the above mentioned monocentric organisms, *Caenorhabditis elegans* is holocentric, so there are several centromeres assembled throughout its chromosome[129, 130]. In the nematode *C. elegans* the key CENP-A loading factor is KNL2^{Mis18BP1} as

a number of CENP-A loading factors, such as Mis18 α and Mis18 β of the Mis18 complex, are not conserved[131]. Interestingly, in the absence of a specific CENP-A chaperone in *C. elegans* it may be CENP-A itself that performs the function of a chaperone - it has been found that the N-terminus of *C. elegans* CENP-A *Cnp1* in fact partially resembles HJURP and mediates the interaction with KNL2^{Mis18BP18}[132, 133]. In addition to the above, the histone chaperone LIN-53^{RbAp46/48} has been found to be necessary for the loading of CENP-A. However, while necessary in humans, in *C. elegans* the acetylase activity of HAT1 is not necessary for CENP-A loading[134]. In contrast to this, in order to establish centromeres *de novo* on an artificial chromosome, HAT1 is required as well as the condensin I/II subunit Smc-4[135].

In fission yeast the Cnp1^{CENP-A} deposition factors are largely conserved. Its Mis18 complex consists of Mis18^{Mis18 α /Mis18 β} , Mis16^{RbAp46/48}, and Eic1^{Mis18BP1}[59, 136]. Cnp1^{CENP-A} is targeted to the centromere by the combined action of Scm3^{HJURP}, the Cnp1^{CENP-A} chaperone, and the Mis18 complex[59, 96, 97]. In contrast to what has been found in human cells, Cnp1^{CENP-A} in fission yeast takes place in the G₂ phase of the cell cycle and the CCAN/Mis6/Ctf9 complex, which interacts with the Mis18 complex and is a part of the kinetochore, is thought to be in charge of the timing of the loading of Cnp1^{CENP-A}[76, 136–138].

While all of the organisms discussed above rely on epigenetics to define and regulate centromeres, the budding yeast's point centromeres are defined genetically - the presence of a specific DNA sequence approximately 125 bp in length, containing three centromeric DNA elements (CDEI, CDEII, CDEIII) is what defines the *S. cerevisiae* centromere.

The budding yeast centromeres also contain Cse4, which is a CENP-A homolog, and which is assembled as a single nucleosome. The proteins mediating this assembly are the Cse4^{CENP-A} chaperone Scm3^{HJURP}, Cbf1 which recognises the CDEI sequence, and the CBF3 complex, which binds the CDEIII sequence and is required

to assemble the kinetochore[99, 139]. The localisation of Scm3^{HJURP} in budding yeast is dependent on the interaction with the CBF3 complex in contrast to how Scm3^{HJURP} is localised in organisms with regional centromeres. Cse4^{CENP-A} is loaded in the S phase of the cell cycle[139, 140].

Across eukaryotic organisms, distant or more closely related, there are conserved mechanisms and factors which orchestrate the loading of CENP-A at the centromere and the three main ingredients of this process across species are:

- The CENP-A chaperone - such as HJURP or CAL1;
- The protein (or protein complex) that recruits the chaperone. This protein (complex) localises to the centromere - such as the Mis18 complex or CENP-C;
- Regulation to enhance and antagonise the recruitment or interaction of those factors - such as phosphorylation of HJURP by CDK1 (inhibitory regulation) or phosphorylation of Mis18BP1 by PLK1 (enhancing regulation).

In some organisms there are additional layers of regulation, however these are not universally present (such as CENP-B). Temporal regulation of CENP-A deposition is related to the cell cycle – *S. pombe* Scm3 dissociates from centromeres in early mitosis and re-associates in late mitosis, while HJURP associates with human centromeres in telophase[112].

It has also been shown that HJURP requires Mis18 to be targeted to the centromere, while the Mis18 complex can remain at the centromere even in the presence of dysfunctional HJURP. All of this shows that it is the Mis18 complex that initiates the HJURP targeting to the centromere, which then facilitates CENP-A deposition[97, 141]. There is also evidence pointing to inhibition of CENP-A deposition through HJURP and CENP-A phosphorylation[1]. It is currently not known why or how the CENP-A deposition in fission yeast is restricted to the G₂ phase of the cell cycle.

In general, organisms with regional centromeres tend to load CENP-A outside of the S phase - potentially due to the promiscuity of histone chaperones combined to the high levels of histone H3 during replication, so the restriction of the CENP-A loading to outside of the S phase could serve to prevent nonspecific interactions between the histones and chaperones as a result of the competition between histones H3/H3.3 and CENP-A for binding to the chaperones[142].

Furthermore, it can be imagined that such regulation ensures that ectopic kinetochores do not get created and that the centromere identity is preserved. Naturally, if the CENP-A loading is genetically regulated, such as in *S. cerevisiae*, the dependence on the cell cycle is less important because the centromere is defined by a DNA sequence.

In human cells, CENP-A deposition is uncoupled from replication and occurs in the G₁ phase, following the exit from mitosis[8]. CDK phosphorylation of CENP-A, HJURP and Mis18BP1 is employed to restrict the CENP-A deposition to the G₁ phase[143]. While in fission yeast this happens mainly during G₂ phase, there is, however, some evidence to suggest that there is some deposition of CENP-A happening in the S phase too[35, 138]. Once it is deposited on the centromere, CENP-A doesn't dissociate from it[1].

Centromeric transcription has also been implied to have a role in functional centromere inheritance as it has been found that loss of some subunits of the Mediator complex, which directs transcription of ncRNAs and regulates assembly of centromeric heterochromatin, causes a loss of CENP-A from the centromeric core and therefore defective kinetochore function and chromosome segregation. In such mutants this effect can be alleviated by using inhibitors of RNA Pol II, further supporting the idea that correct levels of transcription at the centromere are needed to ensure correct CENP-A levels and centromere inheritance[144].

When centromeric transcription is inhibited, the centromeric levels of CENP-A

have been found to decrease[73, 142, 145–148]. In order for CENP-A to transition from being chromatin-associated to stably incorporated, RNA Pol II transcription and the accompanying chromatin remodelling are required[149].

This is thought to happen due to the fact that chromatin remodelling associated with transcription can evict nucleosomes[150–153], so the centromeric transcription could result in the eviction of placeholder H3.3 nucleosomes (in fission yeast these are H3 nucleosomes), which leads to the incorporation of CENP-A into chromatin[126, 147, 149, 154–157].

On the other hand, it is important to note that unchecked transcription can directly lead to centromeric instability by destabilising the CENP-A that has already been incorporated[158, 159].

Interestingly, centromeric RNA transcripts have themselves been suggested to make direct contact with various proteins, such as CENP-A, CENP-A^{Cnp3} and HJURP as well as kinetochore proteins[160–169]. While it is still unclear whether the transcription-mediated chromatin remodelling or the centromeric transcripts themselves have the key role in regulation of CENP-A loading, it can be argued that centromeric transcription is an important part of CENP-A deposition because centromeric transcription is present across distant organisms.

Apart from the mentioned chaperons and various loading factors, SNF2 family members have also been found to be required for CENP-A deposition. SNF2 family proteins are chromatin-remodelling factors, and a member of this protein family, Hrp1, has been found to be localise to centromeric chromatin. Its role is to maintain high CENP-A levels[170] by evicting histone H3 and maintaining CENP-A at centromeres during transcription coupled remodelling of chromatin as the nucleosome must be disassembled and reassembled during transcription of the centromeric central core[146].

In agreement with this finding, it has been shown that in fission yeast cells which have mutations in factors which safeguard stable histone H3 chromatin levels during transcription exhibit promiscuous CENP-A deposition in place of histone H3 outside of the centromere. It has been found that mutations in the FACT complex have a pronounced effect on maintenance of H3 chromatin and increased incorporation of CENP-A outside of the centromeric chromatin.

Clr6 complex II (which has a histone deacetylation function) has been found to have a more subdued effect, however a loss of Clr6 complex II allows for CENP-A to be deposited on centromeric DNA *de novo*, without the need for heterochromatin[171].

In plasmids having only partial *otr* regions and most of the central centromeric domain, functional centromeres can still be assembled (although the assembly is inefficient) suggesting that these elements are sufficient for centromere assembly. Interestingly, once the functional centromeres have been established, however inefficiently, the functional centromeric state can then be propagated through mitosis and meiosis[54, 172]. It is possible that *otr* regions make the environment favourable for kinetochore assembly and once it is assembled, the CENP-A chromatin is propagated through a possibly replication coupled mechanism[173].

Heterochromatin could possibly have a role to play in CENP-A deposition by inducing or assisting the CENP-A deposition on the central core - this could perhaps happen in a way that allows only one block of heterochromatin to be sufficient for kinetochore assembly. In fact, heterochromatin and RNAi machinery have been found to be required for *de novo* CENP-A deposition when naked (naïve) DNA is introduced into cells[174].

By studying neocentromeres it has been found that they can form in subtelomeric regions in absence of any centromeric DNA sequences if centromere deletion is

induced. Therefore, it could be the proximity of subtelomeric heterochromatin which supports centromere formation, which supports the hypothesis that heterochromatin is important for centromere establishment[175, 176].

In dicentric chromosomes it has been observed that one of the centromeres can become inactivated through the disassembly of CENP-A chromatin at the kinetochore, leading to the assembly of heterochromatin over the centromeric central core[177]. However, when there is no heterochromatin, centromeres can still be inactivated through hypoacetylation of chromatin. After the CENP-A chromatin has been established, heterochromatin is not required for its propagation.

In summary, it has been found that while *establishment* of CENP-A requires heterochromatin, *maintenance* of CENP-A does not - it relies on chaperones, loading factors as well as chromatin-remodelling factors.

1.5.2 The Mis18 complex

Mis18 was originally discovered in fission yeast and is one of the key players in the Cnp1^{CENP-A} deposition pathway. In fact, defective Mis18 will cause an arrest in Cnp1^{CENP-A} deposition and is lethal[101, 141, 178]. Furthermore, it has been shown in mice that Mis18 deficiency leads to reduced DNA methylation, changes in histone modifications and uncontrolled noncoding transcripts in the centromere region[178]. In both humans and *S. pombe*, Mis18 forms oligomers[179, 180].

In humans, the Mis18 complex consists of Mis18 α , Mis18 β and Mis18BP1^{KNL2}, while in fission yeast it consists of Mis18, Mis16, Eic1/Mis19 and Eic2/Mis20[131, 179]. Mis18 α and Mis18 β show high sequence similarity with *S. pombe* Mis18. Mis18BP1^{KNL2} and Eic1 are functional homologs, however it seems that Mis18BP1^{KNL2} serves a more complex function and is differently regulated[101]. It has been shown that human Mis18 α and Mis18 β form a heterotetramer.

The Mis18 α -Mis18 β heterotetramer is required to bind Mis18BP1^{KNL2} and centromeres. Upon HJURP binding the Mis18 heterotetramer is disrupted and converted into two heterodimers, which eliminates Mis18 from the centromere. This allows for CENP-A deposition regulation[181].

The localisation of Mis18 to the centromere is cell cycle-dependent and requires the complex to interact with CENP-C. Specifically, Mis18BP1^{KNL2} associates with centromeres via the C-terminus of CENP-C and recruits Mis18 to the centromere[136]. *In vitro* pull downs have shown that the M18BP1^{KNL2} dimer recognises the Mis18 α -Mis18 β hexamer[143].

It has been also shown that chicken M18BP1^{KNL2} localises to centromeres throughout the cell cycle, and that its localisation is dependent on CENP-A, but not CENP-C. However, chicken M18BP1^{KNL2} has a CENP-C-like motif (found to be missing in human M18BP1^{KNL2}) which is important for centromere localisation, and it uses this motif to directly bind to CENP-A nucleosomes[182].

In fission yeast, Mis18 initiates the assembly of the Mis18 complex by undergoing homotetramerisation. However, the role of Mis18 has not yet been pinpointed, although a Yippee-like domain in its N-terminus has been described and this domain is important for the homodimer interface both *in vitro* and *in vivo*. Furthermore, it has a cradle-shaped binding pocket which is important for the localisation and function of Mis18[179].

Human Mis18 α and Mis18 β have also been shown to form a heterodimer through their Yippee-like domains[179, 181], which implies that this may have a role in Mis18 regulation as it is a conserved feature. Mis16 (orthologous to *S. cerevisiae* Hat2 and human RbAp46/48) is a known ubiquitous histone H4 chaperone which interacts with Eic1 through its C-terminal domain. This is interesting because this is the binding site of histone H4, which indicates that Eic1 and histone H4 have to compete for the same binding site on Mis16[183]. Mis16 is known to bind to the C-terminal region of Scm3^{HJURP}, which leads to the recognition of the Cnp1^{CENP-A}/Scm3^{HJURP} complex[184].

There is also evidence, obtained from yeast two hybrid screens and the study of temperature sensitive mutants, that Mis16 interacts with Ccp1^{Vps75}, a NAP (Nucleosome Assembly Protein) family protein that may regulate Cnp1^{CENP-A} loading on centromeres (described in Section 1.7).

Eic1 has several functions – first of all, it is needed for other components of the Mis18 complex, namely Mis18 and Mis16, and Scm3^{HJURP} to associate to centromeres. In addition to this role, Eic1 also serves the same function as Mis18BP^{KNL2} in humans, and associates with CCAN proteins, namely Mal2^{CENP-O}, Fta7^{CENP-Q} and Cnl2^{Nkp2}[136, 184].

Eic1, as well as Mis16 and Mis18, has been shown to be essential for the maintenance of normal Cnp1^{CENP-A} levels at the centromere, while Eic2 is non-essential[59,

95, 101, 136]. Eic2 is not necessary for maintenance of Scm3^{HJURP} and Cnp1^{CENP-A} as *eic2*Δ mutants show no loss of Cnp1^{CENP-A} from centromeres[136, 185]. It is possible that, while non-essential for Cnp1^{CENP-A} maintenance, Eic2 has a role in establishment of Cnp1^{CENP-A} on naïve DNA.

1.5.3 Maintenance of CENP-A

Interestingly, centromere transcription occurs in mitosis - the phase of the cell cycle when the rest of chromatin is transcriptionally silent. As mentioned previously, centromeric transcription seems to have a role to play in the maintenance of centromeric identity, however it is not required in order for cells to progress through mitosis[156, 186, 187].

When transcription is inhibited, there is defective incorporation of CENP-A into nucleosomes[149]. To enable transcription, nucleosomes must be disassembled and reassembled once the RNA polymerase is gone. During this process the existing CENP-A are retained, which enables the conservation of the epigenetic information, while the placeholder nucleosomes are removed.

The exact intricacies of how this happens remain unclear, however two histone chaperones have been proposed to play a role in this process. The first of these is the FACT complex, and the other is Spt6, which is the transcription elongation factor, both of which play a role in general histone recycling throughout the genome[188, 189].

Spt6 has been shown to travel with Rna Pol II and to have an N-terminus that can bind directly both histones H3/H4 as well as dCENP-A/H4 *in vitro*[156, 190–192]. Spt6 preferentially binds dCENP-A over histone H3 in co-immunoprecipitation (co-IP) experiments using S2 cell extracts from *Drosophila melanogaster*. The interaction has been shown to depend both on the tail of dCENP-A as well as the nucleosome core.

When the N-terminus of dCENP-A is phosphorylated at S77 the maintenance of dCENP-A at the centromere is defective, which may be due to the negative effect of phosphorylation on the interaction of dCENP-A and Spt6[128, 156].

In mammals the S77 phosphorylation site is not conserved, however phosphorylation of S30 on the N-terminus of CENP-A in murine cells has been shown to lead

to the removal of CENP-A from the centromere under stress and in human CENP-A phosphorylation has been found to occur on S31[193, 194].

Additionally, in HeLa cells it has been shown that the depletion of Spt6 leads to defective maintenance of CENP-A[156], so there may be a phosphorylation-regulated pathway which regulates the interaction between CENP-A and Spt6.

Much like the process of DNA transcription, DNA replication requires chromatin disassembly to allow for DNA polymerases to access and replicate DNA. This means that during the S phase of the cell cycle parental histones will be allocated to one of the new DNA strands, leaving gaps on the other strand which then need to be populated by *de novo* assembly of nucleosomes. HJURP, the CENP-A chaperone, has been shown to interact with DNA helicase MCM2-7 complex through its MCM2 subunit, which has been shown to facilitate the reincorporation of parental CENP-A at the replication fork[195]. The interaction of HJURP and MCM2 has been likened to the interaction of MCM2 with Asf1 α which has a role in histone H3 maintenance[196, 197].

It is hypothesised that the interaction of CENP-A, MCM2, and HJURP happens simultaneously - HJURP binds the CATD of CENP-A while MCM2 binds the R63-K64 motif, the conserved motif in all variants of histone H3, including CENP-A[195, 198].

However, it is also possible that there is an alternative way for this interaction to occur as HJURP and MCM2 can compete for the binding of the α 1 helix of CENP-A. Based on the fact that HJURP binds CENP-A-H4 as a dimer, while MCM2 can bind the variants of histone H3-H4 as both heterotetramers and heterodimers, it has been proposed that MCM2 binds the CENP-A-H4 heterotetramer.

Following this, the heterotetramer is split and HJURP binds the newly formed dimers. As HJURP is known to dimerise, it is possible that two CENP-A-H4 heterodimers are re-assembled into a heterotetramer in this way and recycled as a

heterotetramer[197, 199].

In addition to this model, there is also evidence of other proteins being required for the maintenance of CENP-A during DNA replication. Due to the fact that almost 60% of all CENP-A nucleosomes in the cell is in fact outside of centromeres[200, 201]. It is known that the presence of CENP-A outside of the centromere can result in ectopic centromere formation, so it is important for cells to employ mechanisms to prevent this.

One such process uses the DNA replication machinery to remove any CENP-A accumulated on ectopic sites, while not removing the centromeric CENP-A[201]. The authors of this study also found that when CENP-C is removed during the S phase the centromeric levels of CENP-A drop significantly, which could indicate that the CCAN also plays a direct role in the maintenance of CENP-A at the centromere.

1.5.4 CENP-A localisation and distribution

As mentioned in the previous section, CENP-A is commonly found outside of centromeric sites, suggesting that the mechanisms governing CENP-A deposition are not sufficient to prevent ectopic deposition of CENP-A[200]. While the CENP-A nucleosomes are massively outnumbered by the H3 nucleosomes at the centromere (the ratio of CENP-A to H3 nucleosomes at the centromeres being 1:25), there is an approximately 50 fold CENP-A enrichment at the centromere compared to the rest of the genome.

This could suggest that it is such enrichment of CENP-A that is needed for kinetochore assembly[200], therefore the ectopically deposited CENP-A under normal physiological levels of expression does not lead to assembly of functional ectopic kinetochores.

In contrast to what occurs under normal levels of CENP-A expression, when overexpressed, CENP-A has been shown to mislocalise and promote the assembly of ectopic kinetochores[7, 175, 202–210]. For this reason it is very important for cells to ensure regulation of CENP-A levels and both transcriptional and post-transcriptional control is employed to avoid ectopic CENP-A localisation and promote correct loading at centromeres.

CENP-A transcription is tied to when CENP-A is loaded in some organisms and it seems to be uncoupled from the transcription of the canonical histones. As discussed previously, the transcription of the CENP-A gene in humans happens during the G₂/M phase, whereas in *S. pombe* this occurs in the G₁ phase[33, 211, 212]. This indicates that the transcription of the CENP-A happens before the cell cycle phase when it is loaded on to the centromere. There are several factors known to be involved in the process of CENP-A transcription. In humans a protein called Cdk5rap2 has been found to interact with CENP-A through its promoter region and upregulate the transcription of the CENP-A gene[213]. Meanwhile in *S. pombe* the MBF (*MluI* box-binding factors) complex has been shown to bind the MCB

(*MluI* cell cycle) box and repress the transcription of CENP-A and restrict it to the G₁ phase[212].

It has also been found in fission yeast that when CENP-A transcription is regulated by different promoters and CENP-A is assembled outside of the G₁ phase, CENP-A can still be loaded at the centromere, however the levels of CENP-A are in this case correlated to ectopic incorporation[212].

Findings from other organisms also support the notion that cells which have CENP-A levels above or below normal can be functional, however there is a limit for this as once the CENP-A levels pass the threshold up to which the cells can compensate the additional or missing CENP-A before it results in non-centromeric CENP-A accumulation leading to ectopic kinetochore assembly and ultimately defective chromosome segregation[202, 203, 205–208, 210].

Evidence from *Drosophila* suggests that post-translational regulation also plays a role in CENP-A distribution regulation. The levels of dCENP-A are restricted during G₁ and S phases by two proteins - SCF^{Ppa} and APC/C^{Cdh1}, which are both E3 ubiquitin ligases[203].

Another ubiquitin ligase, CUL3/RDX, has been found to stabilise CENP-A by monoubiquitinating it when it is bound to CAL1[214]. The interaction of dCENP-A and CAL1 has another function in this context as well, as it has been found to prevent the degradation of dCENP-A mediated by SCF^{Ppa}[203]. This could suggest that binding to CAL1 limits binding of dCENP-A to other chaperones, which ultimately leads to non-ectopic dCENP-A loading[214].

CKII (casein kinase II) has also been found to regulate enrichment of dCENP-A at the centromere by phosphorylating it at S20. This phosphorylation has been shown to be upstream of SCF^{Ppa} and is required for dCENP-A to be degraded in its pre-nucleosomal form.

The phosphorylation of S20 has also been implied to promote the deposition of dCENP-A on chromatin and to increase the turnover of dCENP-A and its elimination from non-centromeric sites. However, it is also important to note that phosphorylated dCENP-A has been shown to be stably incorporated at centromeres, so it may be possible that at the centromere there are additional factors, such as dCENP-C, which prevent dCENP-A degradation on centromeric sites specifically[215].

While evidence from human cells is more limited, there is indication that similar mechanisms are employed by human cells too to regulate the dynamics of CENP-A levels. For example, studies in senescent cells have found that ubiquitination is used to regulate the degradation of CENP-A[216]. In herpes simplex type 1 virus the protein ICP0 has been found to promote the degradation of CENP-A in infected cells[217].

Post-translational modifications are known to influence the stability of CENP-A and regulate its function. One such modification, (de)phosphorylation of S68 by PP1 α and Cdk1 respectively, is widely observed, however its function still remains somewhat unclear. It has been found that its presence leads to polyubiquitination of CENP-A on K49 and K124 by DCAF11 (E3 ubiquitin ligase) in mitosis[113–116].

It has been proposed that S68 is phosphorylated by Cyclin B-Cdk1 after the translation of CENP-A in G₂ and early M phase, which results in the degradation of CENP-A in mitosis. In this theory the S68 phosphorylation by CyclinB-Cdk1 plays a similar role to the *Drosophila* SCF^{Ppa} preventing the mislocalisation of CENP-A on non-centromeric sites.

Cells with S68A and K49R/K124R mutations have, surprisingly, not been found to exhibit a phenotype. However, when aphidicolin or thymidine treatment is used on these cells to arrest them in the S phase, it has been shown that they have an enrichment of CENP-A on non-centromeric sites. This further supports the findings suggesting that the DNA replication machinery has a role to play in the removal of

ectopic CENP-A[201, 213].

When researchers followed the process of CENP-A loading throughout the cell cycle, it has been observed that in the G₁ phase CENP-A is deposited promiscuously throughout the genome. However, in the subsequent G₂ phase all of the ectopically deposited CENP-A is removed.

In addition to this, researchers observed that the non-centromeric CENP-A sites were replicated early in the S phase, while for centromeric CENP-A sites this occurred in the late stages of the S phase[201].

Ectopic CENP-A is removed by the replication fork, however the centromeric CENP-A reloads on the same site. Interestingly, it has been found that the CCAN (especially CENP-C) plays an essential role in preventing CENP-A eviction from centromeres by the replication fork as the CCAN stays associated with the centromere during replication[201]. This supports previous findings that CENP-C and CENP-N^{Mis15} protect the CENP-A nucleosomes[218, 219].

In *S. cerevisiae* ubiquitination is employed to regulate the levels of Cse4^{CENP-A} and stop it from accumulating on non-centromeric sites. Doa1 ubiquitinates the N-terminus of Cse4^{CENP-A} and Psh1 (an E3 ubiquitin ligase) ubiquitinates the CATD of Cse4^{CENP-A}, which leads to the degradation of Cse4^{CENP-A}[220–223].

To prevent excessive degradation of Cse4^{CENP-A} as well as its mislocalisation, budding yeast uses a deubiquitinase Ubp8, which is a part of the SAGA complex[224]. Similarly to what is observed in *Drosophila* with the binding of CAL1 to dCENP-A, Cse4^{CENP-A} can be protected from degradation when bound to Scm3^{HJURP} and Pat1, a kinetochore protein[223]. The deletion of Psh1 leads to Cse4^{CENP-A} accumulating close to nucleosome depleted sites at intergenic regions. The localisation of Cse4^{CENP-A} in these regions uses the Ino80 complex, which is known to have remodelling activity[225].

In addition to this, there are other ubiquitin ligase factors that have been shown

to play a role in the mislocalisation of Cse4^{CENP-A}[226, 227]. It has also been found that Sx15, a SUMO targeted ubiquitin ligase (STUbL), sumoylates Cse4^{CENP-A} on K65, which is needed for the prevention of mislocalisation of Cse4^{CENP-A} and its proteolysis[228].

As well as the factors already discussed, histone H2A.Z, chromatin remodelling factors CHRAC and SWI/SNF and two chaperones FACT and Spt6 have also been shown to play a role in preventing the ectopic deposition of CENP-A[171, 229–232].

However, the overarching mechanism used to regulate expression and prevent the mislocalisation of CENP-A appears to be degradation mediated by ubiquitination. Any ectopically deposited CENP-A seems to be removed through a replication-coupled mechanism. CENP-A chaperones play a role in protecting CENP-A from proteolysis and in CENP-A loading at the centromere. CCAN components have also been shown to contribute to the protection of CENP-A from degradation and eviction. However, as CCAN proteins are not present across all species, it is at present unclear whether this mechanism is conserved.

Interestingly, CENP-A has been found to be commonly ectopically deposited at DNA double strand breaks, along with CENP-N, CENP-T and CENP-U. The CENP-A deposition at these sites has been suggested to be related with the non-homologous-end-joining pathway (NHEJ)[233–235]. It has been suggested that the ectopic CENP-A deposition occurs during the early stages of the NHEJ pathway because it has been shown not to be dependent on Ligase IV, DNA-dependent protein kinases (DNA-PKc) and the histone H2A.X[235].

In addition to the NHEJ, CENP-A has also been implicated in the homologous recombination (HR) pathway as it has been found to be able to recruit proteins of the HR pathway when DNA double strand breaks are induced[111] so CENP-A may be connected to the DNA damage repair mechanisms. This potentially links CENP-A to transcription as well through DNA repair as it has been found that transcription

recruits proteins involved in the DNA damage repair pathway[234].

There is evidence to suggest that the chaperone complex ATRX-DAXX mediates the deposition of CENP-A to the sites of DNA double strand breaks as the complex has been shown to both bind CENP-A and to be involved in both the HR and the NHEJ pathway[236–238]. However, while there may be a correlation between ectopically deposited CENP-A and transcription further research is needed to understand whether there is causation in this case.

1.5.5 Centromeric chromatin remodelling

When DNA needs to be replicated and transcribed, the machinery requires DNA access which means that the centromeric chromatin needs to be remodelled to allow for this as the nucleosomes form a physical obstacle to the replication and transcription machinery.

One of the mechanisms the cells employ to overcome this is post-translational modifications of histones, which regulate the interactions between nucleosomes and can lead to chromatin being either open or closed to the transcription and replication machinery as different proteins can recognise the post-translational modifications of histones.

Additionally, ATP-dependent remodellers of chromatin are employed. The chromatin remodelling complexes are divided into four groups based on the core ATPase:

- Chromatin-Helicase-DNA-binding(CHD);
- Switch/Sucrose Non-Fermentable (SWI/SNF);
- Imitation Switch (ISWI);
- Inositol Auxotrophy 80 (INO80);

These complexes have different types of activity. The CHD and INO80 complexes have the nucleosome editing activity, which causes a change in the composition of histones in a nucleosome. CHD, as well as SWI/SNF, also acts to open the chromatin by changing the space between nucleosomes, which can happen in several ways: nucleosomes can be partially disassembled, evicted or slid. Finally ISWI and CHD act to ensure that the nucleosomes are correctly assembled and then relocated to create an array with regular gaps between the nucleosomes[239].

As discussed in previous sections, centromeres have placeholder nucleosomes containing histones H3 or H3.3 due to the fact that CENP-A is loaded outside of the S phase[76, 87].

As these placeholder nucleosomes have to be evicted to allow for the new CENP-A to be loaded, chromatin remodelling factors have an important role at the centromere. However, it is yet not fully understood how this process occurs.

Recent evidence from RNAi experiments has identified that several components of the transcriptional machinery, chromatin remodellers and a histone chaperone (SMARCAD1, SMARCD3, ASF1B) have a role in CENP-A deposition as the knock-down of these proteins causes a decrease in the deposition of CENP-A. In addition to the deposition of CENP-A, it has also been found that when chromatin remodellers SMARCAD1, ACT68, CHD8 and HLTF are knocked down the cells have defects in CENP-A maintenance[240].

In *S. pombe* the ortholog of SMARCAD1 is Fft3, which has been found to have role in histone turnover regulation at heterochromatic regions[241, 242]. There is evidence that Fft3^{SMARCAD1} collaborates with the FACT complex to disassemble nucleosomes as RNA Pol II approaches[243].

Additionally, Fft3^{SMARCAD1} has been found to be enriched both at heterochromatic sites as well as at the centromere. When Fft3^{SMARCAD1} is deleted, the levels of H2A.Z and H4K12ac at these regions rise, suggesting that Fft3^{SMARCAD1} acts to prevent euchromatisation[244].

In *S. cerevisiae* the homologue of SMARCAD1, Fun30, has a role in promoting establishment of correct chromatin structure at the point centromeres[245].

A member of the ISWI remodeller family, the RSF complex consisting of SNF2h (ATPase) and RSF1, has been identified to have a role in the maintenance of centromeric chromatin as well as DNA repair. RSC was found to be enriched at centromeres during the G₁ phase and a reduction in the levels of RSF complex has been shown to cause a reduction in CENP-A loading and mitotic defects[246, 247].

There is also evidence to suggest that the RSF complex is involved in recruiting CENP-A to the sites of DNA double strand breaks. It is unclear whether this happens through a physical interaction[233, 248].

Meanwhile in *S. pombe* the Ino80 complex has been shown to support removal of histone H3 during transcription to ensure correct centromere establishment[155, 249, 250]. In *S. pombe* as well as vertebrates there is some evidence that CHD1 and Hrp1, both CHD remodellers, are also involved in this process, whereas the same appears not to be conserved in *Drosophila*[170, 251, 252].

1.6 Post-translational modifications and function of centromeric and pericentromeric chromatin

Heterochromatin has an important role to play at centromeres and its formation is a complex process - as discussed previously in Section 1.3, its formation is mediated by several factors, such as noncoding RNA, chromatin factors, RNA polymerase II as well as a host of proteins associated with them.

As mentioned in Section 1.3, centromeres appear to be epigenetically specified and regulated. It is thought that post-translational modifications of histones regulate epigenetic switching between different states of chromatin because post-translational modifications define functional chromatin domains[253].

The main sites for post-translational modifications of the four core histones (H2A, H2B, H3, H4) are their N-termini. Most commonly, these undergo acetylation, methylation, ubiquitination or phosphorylation[254]. These post-translational modifications indicate the state of chromatin, i.e., whether it is active or repressed, and some researchers have suggested that this “histone code” is necessary to create a complex hierarchy of chromatin regulation through specific combinations of histone modifications[255].

Indeed, a correlation between the chromatin state and the acetylation or methylation of histones H3 and H4 has been shown. Specifically, methylation of histone H3 at lysine 4 (K4) has been linked to transcriptionally active chromatin. In contrast, methylation of histone H3 at lysine 9 (K9) has been linked to transcriptionally silent chromatin[254, 255]. In fact, in fission yeast centromeric heterochromatin at outer repeats has been found to have both di- and trimethylated histone H3 at K9 which are, again, characteristic of silent heterochromatin in most eukaryotes[256, 257].

Interestingly, different levels of regulation have been observed depending on how

many modifications there are on the same amino acid – dimethylation of histone H3 at K4 is associated with chromatin that is either active or potentially active, whereas trimethylation of the same amino acid is associated with active chromatin[258].

The process of heterochromatinisation is thought to occur by joint action of various histone deacetylases (HDACs), the histone lysine methyltransferase Clr4 (KMT/HMTase) and the heterochromatin protein 1 (HP1) homolog Swi6. The role of HDACs (e.g. Clr3, Clr6, Sir2) is to, as the name suggests, deacetylate histone H3 at various lysine residues[259–261].

Clr3 has been shown to operate within a multienzyme complex named SHREC, which is an effector complex for heterochromatic transcriptional gene silencing in fission yeast. SHREC comprises a core of four proteins: Clr1, Clr2, Clr3, and Mit1 which are distributed throughout heterochromatin domains and affect transcriptional silencing via Clr3 and Mit1, an Snf2 chromatin remodelling factor homolog.

In addition to this role, SHREC has been shown to be recruited to the telomeres and to euchromatic sites - the mechanism of euchromatic SHREC localisation has been shown to be different from its heterochromatin localisation mechanism, which is mediated by Swi6^{HP1}[262].

Clr4 forms a part of a complex called CLRC which mediated the methylation of H3K9 and, through that, creates a specific binding site for proteins which contain a chromodomain motif. Clr4 itself also contains a chromodomain, meaning that its role is not solely to methylate H3K9 but also to bind H3K9me2/H3K9me3. This is thought to bring about adjacent H3K9 methylation through its catalytic domain[263].

Another chromodomain-containing factor is Swi6^{HP1}, which has been shown to bind methylated H3K9 and contribute to heterochromatin formation over the outer repeats. Swi6^{HP1} has also been shown to have a chromoshadow domain, which causes

it to self-dimerise[264]. It has been suggested that this allows Swi6^{HP1} to bridge nucleosomes during heterochromatin assembly[265] to change the length of nucleosome repeats in heterochromatin compared to the length found in euchromatin[266].

When reporter genes are inserted at the outer repeats, they are found to be enriched in H3K9me2 and Swi6 proteins, further highlighting how important the role of Clr4 and Swi6 is in heterochromatin establishment within in the outer repeats as well as the adjacent sequences[257, 264].

In fission yeast there are four chromodomain proteins - Chp1, Chp2, Swi6 and Clr4. The affinity of Chp1 and Clr4 for methylated H3K9 changes depending on the acetylation state of H3K4. When H3K4 is acetylated by a histone lysine acetyltransferase (HAT/KAT) called Mst1.

H3K4 therefore acts like a switch for heterochromatin reassembly: once DNA is replicated the occupancy of Chp1 and Clr4 at H3K9me2 and H3K9me3 is promoted on histones which have been newly deposited as their H3K4 is unacetylated. Once Mst1 acetylates H3K4, Chp2 and Swi6 become the favoured occupants, which leads to heterochromatin reassembly[267].

Another interesting function of Swi6 is in destroying the transcripts which originate from heterochromatic regions, and this is mediated by a strong RNA binding activity of its hinge region.

When the hinge domain is mutated, reduced silencing of heterochromatic transcripts is observed, however the integrity of the heterochromatin itself remains unaffected. This suggests that Swi6 acts downstream from methylated H3K9[268].

H3 histones proximal to CENP-A are found to exhibit a complex set of post-translational modifications rather than a uniform modification pattern[117]. When it comes to CENP-A itself, the post-translational modifications are not conserved, which is due to the fact that various orthologs in CENP-A across different species show significant levels of variation, especially in the N-terminal region, which is also

the site of most post-translational modifications.

Some site-specific modifications are shared with histone H3, however most of the modifications are specific to nucleosomes containing CENP-A[269]. Most commonly, CENP-A is modified by acetylation, phosphorylation or ubiquitination[9].

Phosphorylation of serine 7 (S7) is important for correct mitotic progression, acetylation of arginine 37 (R37) is important for regulation of kinetochore recruitment, while ubiquitylation has been found to stabilise CENP-A in flies[270, 271].

Lysine acetylation of histones has been recognised to have a role in transcriptional regulation, and there is evidence for it being important for DNA damage repair as well[5]. An increase in histone acetylation in *S. pombe* Mis18 and Mis16 mutants has been previously observed, which is believed to be due to Cnp1^{CENP-A} being replaced with acetylated histone H3. They also report an increase in histone H4 acetylation, and argue that this implies a role for Mis16 and Mis18 in maintaining histones in a deacetylated state[59].

1.7 Ccp1^{Vps75}

Ccp1 is the fission yeast homolog of Vps75 in budding yeast and SET in humans[3, 4]. In *S. cerevisiae* Vps75 was first identified in a screen for mutants with defective vacuolar sorting.

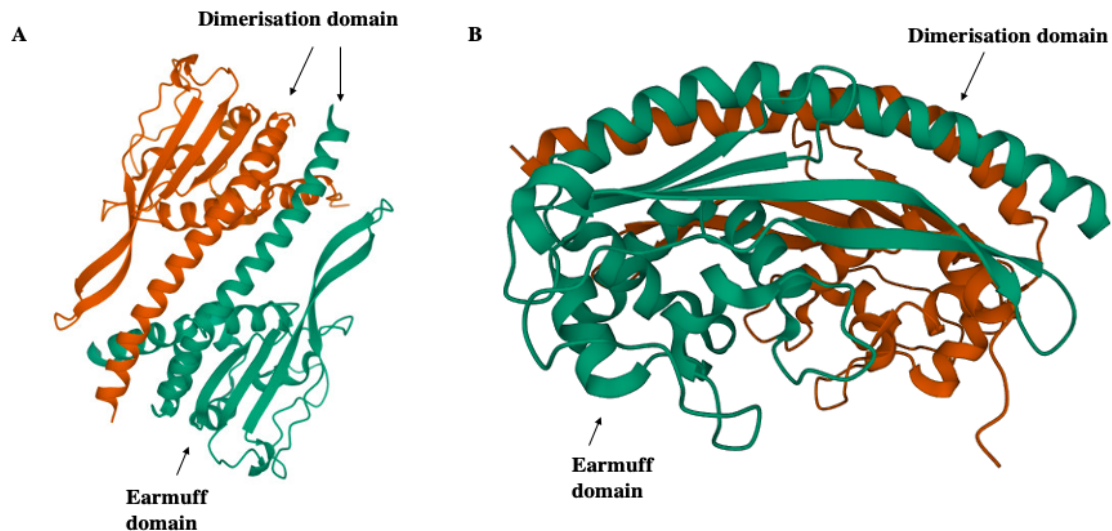


Figure 1.5: The structure of the Ccp1^{Vps75} homodimer. (A) Top-down view of the dimer. (B) Alternative view. Adapted from the Protein Data Bank, entry 5GPL, as published by Dong et al.[3].

Ccp1^{Vps75} is a NAP (Nucleosome Assembly Protein) family protein. A study by Dong et al. proposes that Ccp1^{Vps75} antagonises Cnp1^{CENP-A} loading not only at the centromere, but also at noncentromeric regions, thus maintaining the Cnp1^{CENP-A} levels at the centromere as well as preventing ectopic centromere assembly[3].

Ccp1^{Vps75} directly interacts with Cnp1^{CENP-A} by physically associating to it, and its recruitment to the centromere is Mis16^{RbAp48/46}-dependent. Some structural analyses of Ccp1^{Vps75} suggest that it forms a homodimer and that the homodimer is required for the anti-Cnp1^{CENP-A} loading activity[3]. Researchers reported two characteristic domains for Ccp1^{Vps75} - the earmuff domain and the dimerisation domain[3]. However, other researchers report a tetrameric structure for Vps75 in *S. cerevisiae*[272, 273].

Overexpression of Ccp1^{Vps75} in fission yeast wild type cells has been found to evict Cnp1^{CENP-A} from native centromeres. In fact, in this study the single Cnp1^{CENP-A}-GFP focus was lost from 76% of centromeres, and cells overexpressing Ccp1^{Vps75} were also shown to be highly sensitive to thiabendazole (TBZ, a microtubule destabilising drug)[3].

So far it has been suggested that in *S.cerevisiae* Vps75^{Ccp1} (which has a nuclear localisation signal) imports a histone acetyltransferase Rtt109 into the nucleus and stabilises it, and positions histone H3 for acetylation by Rtt109[6, 274].

A recent study has suggested that Ccp1^{Vps75}'s localisation to the centromere needs Cnp20^{CENP-T} and that Ccp1^{Vps75} may bind to the N terminus of Cnp20^{CENP-T} through what the authors have called the Ccp1 interaction motif (CIM), which they found to be proximal to the motif binding Ndc80.

Furthermore, the authors find that deleting the CIM domain of Cnp20^{CENP-T} produces the same effect as deleting Ccp1^{Vps75} itself and that phosphorylation of the CIM domain by CDK1 leads to a weaker interaction with Cnp20^{CENP-T}. Interestingly, the authors also suggest a competition between Ccp1^{Vps75} and Ndc80 for binding of the N terminus of Cnp20^{CENP-T}[66].

Ccp1^{Vps75} was also found to be dependent on the inner kinetochore components Mis6^{CENP-I} and Sim4^{CENP-K} for correct localisation at the centromere[4]. In addition, there is evidence to suggest that Ccp1^{Vps75} is involved in the distribution of heterochromatin across the genome, including both the pericentromeric and subtelomeric sites[4].

In an affinity purification experiment it has been found that Ccp1^{Vps75}-TAP interacts with a nucleolar protein Gar2, in addition to histones[4]. The authors also found Gar2 and Ccp1^{Vps75} to have a genetic interaction[4]. It is therefore possible that Ccp1^{Vps75} and Gar2 work together to regulate the centromeric epigenetic stability.

While many roles of Vps75^{Ccp1} in *S. cerevisiae* have been already investigated, at the moment it is not known if *S. cerevisiae* Vps75 and *S. pombe* Ccp1 are true functional orthologs and the full scope of the role of Ccp1 in fission yeast remains to be investigated.

1.8 Rtt109

Rtt109 is a member of the HAT (histone acetyltransferase) family and is required for the acetylation of histone H3 on lysines 9, 27 and 56 (K9, K27, K56)[274, 275].

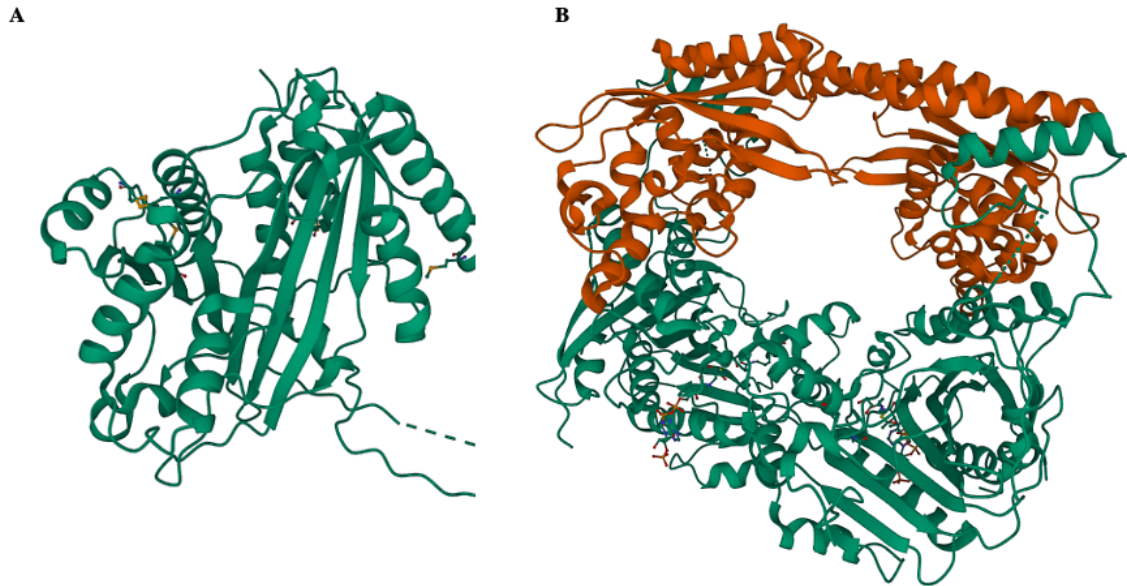


Figure 1.6: The structure of Rtt109. (A) Crystal structure of Rtt109 from *S. cerevisiae*. Adapted from the Protein Data Bank, entry 2RIM, as published by Lin et al.[276]. (B) The structure of the Rtt109-AcCoA/Vps75 complex from *S. cerevisiae*. Adapted from Protein Data Bank, entry 3Q35, as published by Tang et al.[277]. Vps75^{Ccp1} shown in red, Rtt109 shown in green.)

In *S. cerevisiae* Rtt109 was found to associate with two histone chaperones *in vivo*: Vps75^{Ccp1} and Asf1. Vps75^{Ccp1} and Asf1 are unrelated chaperones, however, they both interact with the H3-H4 dimer and (H3-H4)₂ tetramer. In budding yeast it has been shown that *in vitro* acetylation of histone H3 increases after the addition of either Asf1 or Vps75^{Ccp1}.

However *in vivo* Asf1 and Rtt109 have been shown to be essential for histone H3 acetylation at K56, while Vps75^{Ccp1} was not.

Interestingly, acetylation of the histone H3 at K9 and K27 by Rtt109 are both Vps75^{Ccp1}-dependent[6]. In *S. pombe* it has been found that Rtt109 acetylates histone H3 (particularly on K56) *in vitro* and *in vivo*, and in *rtt109*Δ single mutants acute sensitivity to genotoxic agents has been observed[5].

The authors of this paper therefore suggested that the acetylation of histone H3 by Rtt109 is involved in DNA damage response in cells. *rtt109* Δ mutant cells have been found to be viable, however they do exhibit genomic instability[278, 279].

A recent study has implicated Rtt109 in nucleosome eviction and replacement of H3 nucleosomes ahead of the replication fork in *S. cerevisiae* cells. In contrast, Rtt109 has been found to stabilise the nucleosomes *behind* the replication fork[280].

Interestingly, the authors found the H3 nucleosome replacement activity was not related to acetylation of H3K56, which is the primary target of Rtt109 acetyltransferase activity, but rather depended on the Vps75^{Ccp1}-dependent activity of Rtt109 on the N terminal tail of histone H3[280].

As new findings about Rtt109 emerge, it is yet unclear whether it has a similar role in fission yeast too.

1.9 Project aims

The aim of the PhD project was to investigate the mechanisms, specifically those relating to the incorporation of Cnp1^{CENP-A} within centromeric chromatin, which regulate chromosome segregation in *S. pombe*.

The project has aimed to explore the interaction between Rtt109, Ccp1^{Vps75} and Cnp20^{CENP-T} in the context of Cnp1^{CENP-A} deposition regulation.

Chapter 2

Materials and methods

2.1 Strains

2.1.1 *S. pombe* strains

The fission yeast strains used in experiments are given below in Table 2.1.1.

Table 2.1: *S. pombe* strains used in the project.

Strain name	Genotype
FY1645	<i>h⁺ ade6-210 arg3-D4 his3-D1 leu1-32 ura4-D18</i>
TGS55	<i>h⁻ leu1-32 ura4-D18 ade6-M210/D1 ccp1Δ::kanMX arg3Δ::ura4⁺ TM1:arg3</i>
LS747	<i>h⁺ ade6-210 arg3-D4 his3-D1 leu1-32 ura4-D18 rtt109Δ::hphMX</i>
LS758	<i>h⁺ leu1-32 ura4-D18 ade6-M210/216 ccp1Δ::kanMX</i>
LS851	<i>h⁺ leu1-32 ura4-D18 ade6-M210/216 ccp1Δ::kanMX</i>
LS848	<i>h⁻ leu1-32 ura4⁻ cnp1::ura4⁺ lys1⁺::cnp1-1</i>
LS948	<i>h⁻ leu1-32 ura4-D18 lys1 GFP-cnp1-NAT</i>
LS931	<i>h[?] cnp20-GFP-kanMX6 leu1-32 ura4-D18 his3-D1 ade6-210 arg3-D4</i>
LS1007	<i>h⁺ ccp1-GFP-kanMX6 ade6-210 arg3-D4 his3-D1 leu1-32 ura4-D18</i>
MF24	<i>h[?] ade6-210 arg3-D4 his3-D1 leu1-32 ura4-D18 cnp20-3FLAG-natMx Ccp1-GFP-kanMX</i>
MF28	<i>h[?] ade6-210/M216 arg3[?] his3[?] leu1-32 ura4[?] Cnp20-?FLAG-KanMX Ccp1-GFP-kanMX</i>
MF29	<i>h[?] ade6-210/M216 arg3[?] his3[?] leu1-32 ura4[?] Cnp20-?FLAG-KanMX Ccp1-GFP-KanMX</i>
MF35	<i>h[?] ade6-210/M216 arg3[?] his3[?] leu1-32 ura4[?] Cnp20-ts3-?FLAG-kanMX Ccp1-GFP-kanMX</i>

Strain name	Genotype
MF37	<i>h?</i> <i>ade6-210/M216</i> <i>arg3?</i> <i>his3?</i> <i>leu1-32</i> <i>ura4?</i> <i>cnp20-ts3-?FLAG-kanMX</i> <i>Ccp1-GFP-kanMX</i>
ZR1177	<i>h?</i> <i>leu1-32</i> <i>ura4-D18</i> <i>ade6?</i> <i>his3?</i> <i>arg3?</i> <i>rtt109Δ::hphMX</i> <i>cnp1Δ::ura4⁺ lys1⁺:cnp1-1</i>
ZR1178	<i>h?</i> <i>leu1-32</i> <i>ura4-D18</i> <i>ade6?</i> <i>his3?</i> <i>arg3?</i> <i>rtt109Δ::hphMX</i> <i>cnp1Δ::ura4⁺ lys1⁺:cnp1-1</i>
ZR1179	<i>h?</i> <i>leu1-32</i> <i>ura4-D18</i> <i>ade6-M210</i> <i>his3?</i> <i>arg3?</i> <i>rtt109Δ::hphMX</i> <i>arg3D::ura4⁺ TM1:arg3</i>
ZV1264	<i>h⁺</i> <i>leu1-32</i> <i>ura4-D18</i> <i>ade6-M210/216?</i> <i>his3-D1?</i> <i>arg3-D4?</i> <i>rtt109Δ::hphMX</i> <i>ccp1Δ::kanMX</i>
ZV1265	<i>h⁺</i> <i>leu1-32</i> <i>ura4-D18</i> <i>ade6-M210/216?</i> <i>his3-D1?</i> <i>arg3-D4?</i> <i>rtt109Δ::hphMX</i> <i>ccp1Δ::kanMX</i>
ZV1266	<i>h⁺</i> <i>leu1-32</i> <i>ura4-D18</i> <i>ade6-M210/216?</i> <i>his3-D1?</i> <i>arg3-D4?</i> <i>rtt109Δ::hphMX</i> <i>ccp1Δ::kanMX</i>
ZV1267	<i>h⁺</i> <i>leu1-32</i> <i>ura4-D18</i> <i>ade6-M210/216?</i> <i>his3-D1?</i> <i>arg3-D4?</i> <i>rtt109Δ::hphMX</i> <i>ccp1Δ::kanMX</i>
ZV1270	<i>h?</i> <i>leu1-32</i> <i>ura4-D18</i> <i>ade6-M210/D1?</i> <i>his3?</i> <i>ccp1Δ::kanMX</i> <i>rtt109Δ::hphMX</i> <i>arg3Δ::ura4⁺ TM1:arg3</i>
ZV1290	<i>h?</i> <i>leu1-32</i> <i>ura4-D18</i> <i>ade6-M210/216?</i> <i>lys1?</i> <i>his3-D1?</i> <i>arg3-D4?</i> <i>GFP-cnp1-NAT</i> <i>rtt109Δ::hphMX</i> <i>ccp1Δ::kanMX</i>
ZV1291	<i>h?</i> <i>leu1-32</i> <i>ura4-D18</i> <i>ade6-M210/216?</i> <i>lys1?</i> <i>His3-D1?</i> <i>arg3-D4?</i> <i>GFP-cnp1-NAT</i> <i>rtt109Δ::hphMX</i> <i>ccp1Δ::kanMX</i>
ZV1294	<i>h?</i> <i>leu1-32</i> <i>ura4-D18</i> <i>lys1?</i> <i>ade6-M210/M216?</i> <i>ccp1Δ::kanMX</i> <i>GFP-cnp1-NAT</i>
ZV1297	<i>h?</i> <i>leu1-32</i> <i>ura4-D18</i> <i>arg3?</i> <i>his3?</i> <i>ade6?</i> <i>lys1?</i> <i>rtt109Δ::hphMX</i> <i>GFP-cnp1-NAT</i>
ZV1299	<i>h?</i> <i>leu1-32</i> <i>ura4-D18</i> <i>arg3?</i> <i>his3?</i> <i>ade6?</i> <i>lys1?</i> <i>rtt109Δ::hphMX</i> <i>GFP-cnp1-NAT</i>
ZV1311	<i>h?</i> <i>ccp1-GFP-kanMX</i> <i>leu1-32</i> <i>ura4-D18</i> <i>ade6-210</i> <i>arg3-D4</i> <i>his3-D1</i> <i>rtt109Δ::hphMX</i>
ZV1412	<i>h?</i> <i>leu1-32</i> <i>ura4-D18</i> <i>ade6-M21/216?</i> <i>arg3-D4?</i> <i>his3-D18</i> <i>ccp1Δ::natMX</i> <i>cnp20-GFP-kanMX6</i>

2.2 Media

Standard fission yeast media was used, Yeast Extract with Supplements (YES) as well as minimal medium (Pombe Minimal Glutamate, PMG) and Malt Extact (ME).

Yeast Extract with Supplements

Yeast Extract with Supplements was prepared by dissolving the powders listed in the Table 2.2 below in MilliQ-water. Once all the ingredients have been added, the solution is sterilised by autoclaving.

Table 2.2: Yeast Extract with Supplements preparation.

Ingredient	γ Γ^1
Yeast Extract	5.0
Glucose	30.0
L-Histidine	0.1
Uracil	0.1
L-Leucine	0.1
Adenine sulphate	0.1
Bacteriological grade agar (if used)	20.0

Pombe Minimal Glutamate Media

Minimal media was prepared by dissolving the EMM Glutamate broth powder in Milli-Q water, and adding supplements as needed right before use. All ingredients are listed in the Table 2.3 below. The dissolved EMM glutamate solution is sterilised by autoclaving, and once cool, filter sterilised supplements can be added to the solution. All supplement solutions are kept at 4° C, apart from the adenine solution, which is stored at room temperature.

Table 2.3: Pombe Minimal Glutamate media preparation.

Ingredient	$\gamma/\text{mg l}^{-1}$
EMM Glutamate broth	31.0×10^3
L-Arginine	75.0
L-Leucine	75.0
L-Histidine	75.0
Adenine sulphate	375.0
Urcail	375.0
L-Lysine	75.0
Bacteriological grade agar (if used)	20.0×10^3

Malt Extract

Malt extract powder is dissolved in MilliQ-water, supplemented as described in Table 2.4 and sterilised by autoclaving.

Table 2.4: Malt Extract media preparation.

Ingredient	$\gamma/\text{g l}^{-1}$
Malt extract powder	3.0
L-Leucine	0.05
L-Histidine	0.05
Adenine sulphate	0.05
Urcail	0.05
Bacteriological grade agar	20.0

2.3 Oligonucleotides

A list of oligonucleotides used in the project is given in the Table 2.5 below.

Table 2.5: Oligonucleotides used in the project.

Oligonucleotide name	Description	Sequence
qCnt1F	Forward primer for centromeres 1 and 3	5' CAGACAATCGCATG-GTACTATC
qCnt1R	Reverse primer for centromeres 1 and 3	5' AGGTGAAGCG-TAAGTGAGTG
q293	Forward primer for centromere 2	5' AAACAAACAACG-GCACACTG
q295d	Reverse primer for centromere 2	5' AAGCCAGCAAATTC-CTTGAGT
qAct1-for	Forward primer for actin	5' GGTTTCGCTGGA-GATGATG
qAct1-rev	Reverse primer for actin	5' ATAC-CACGCTTGCTTTGAG
qFbp1-fwd	Forward primer for Fbp1	5' AAGGCGATATTAGC-GATGTC
qFbp1-rev	Reverse primer for Fbp1	5' CAGTGTCCAAGGT-GAAGC

2.4 Culturing *S. pombe* cells

Wild type strains were grown at 32°C, while the temperature sensitive strains were grown at 25°C and the restrictive temperature for these cells was 36°C.

When growing liquid cultures the cultures were maintained in the exponential growth phase with between 2×10^6 and 1×10^7 cells ml⁻¹.

To get cultures in the exponential growth phase, a fresh colony of a strain was grown from frozen stock on YES agar at the appropriate temperature overnight. A small sample of the colony was diluted in 10 ml of YES liquid medium and incubated overnight at the appropriate temperature with shaking to ensure that the cells do not settle on the bottom of the flask.

The optical density at 595 nm of the resulting pre-culture was measured and the equation given below was used to calculate the required volume of pre-culture to generate a larger culture:

$$V_{\text{pre-culture}} = \frac{V_{\text{culture}} \times \text{OD}_{\text{required}}}{2^n}$$

where V_{culture} is the desired volume of culture, $\text{OD}_{\text{required}}$ is the required OD at 595 nm, and n is the expected number of generations (assuming that at 32°C the doubling time of fission yeast is 2.5 hours).

When growing liquid cultures, flasks used were chosen based on the volume of culture that needed to be grown - the volume of the flask used was double the volume of the required culture (i.e. a 200 ml flask was used for a 100 ml culture, and so on).

2.5 Crossing *S. pombe* cells

2.5.1 Cell mating and growth

To induce mating the desired freshly growing strains of opposite mating types are mixed in a sterile microtube in 1 ml of sterile water and spread on an ME agar plate as this medium is lacking in nitrogen. The plates are incubated at 25°C for 2 days. To check if zygotic asci were produced, a small sample of the growing cells can be taken and diluted in some water to be observed under the light microscope.

Once zygotic asci have been produced, cytohelicase (an enzyme from *Helix pomatia*) is added at the concentration of 2 mg ml⁻¹ to 500 µl of cells suspended in sterile water. The cells are incubated with the enzyme overnight at room temperature, which leads to the breakdown of the cell wall and releases the spores.

The next day the spores are washed with sterile water three times by centrifuging gently, removing the supernatant and resuspending the spores in fresh 500 µl of water. The spores are counted using a haemocytometer and plated on YES agar plates at various dilutions (e.g. 10², 10³, 10⁴ spores) and incubated at 32°C.

2.5.2 Cross selection

The strains used in this project used resistance to antibiotics as a way of selecting the cells with the desired mutation(s), so the selection of crosses was performed using YES agar plates supplemented with hygromycin B, G418 disulphate or nourseothrecin. The antibiotics were added to the YES agar at concentrations listed in Table 2.6. Antibiotics are added to liquid YES agar just before the plates are poured.

Table 2.6: Supplementing YES agar with antibiotics.

Antibiotic	γ/mg ml ⁻¹
G418 disulphate	0.1
Hygromycin B	0.3
Nourseothrecin	0.1

The single cell colonies that grew on antibiotic selection plates after incubation at 32°C were then either streaked onto YES plates to create a stock of the strain or replica plated onto another selection plate if there were multiple markers to be checked.

2.6 Spotting assays

To set up a spotting assay, one sterile Petri dish is filled with ethanol and a 8 x 6 metal pin is soaked in the dish containing ethanol. The pin is then flamed in a Bunsen burner flame to sterilise it. Once sterilised, the pin can be set aside in another sterile Petri dish.

Sterile water is poured into another Petri dish and a multichannel pipette is used to fill the first six columns of a sterile 96 well plate with 200 μl of sterile water. A pipette tip or a sterile toothpick is used to pick up the same amount of freshly growing cells from an agar plate. Every strain is resuspended in the first well of the first column of the 96 well plate.

A five fold serial dilution of each of the strains is prepared by pipetting 50 μl resuspended cells from the first column of the plate with a multichannel pipette into the second column, resuspending the cells, taking a fresh 50 μl aliquot of the diluted solution from the second column, resuspending it in the third column and so on, until the final 50 μl aliquot of cells has been dispensed into the sixth column.

The metal pin is used to transfer the cells from the 96 well plate to agar plates. Once all cells have been transferred, the agar plates are incubated as needed.

If more strains need to be used, the metal pins need to be rinsed with water, sterilised by soaking in ethanol and flaming. The pin needs to cool down before used again.

2.6.1 Thiabendazole (TBZ) assays

Thiabendazole (TBZ) is a microtubule destabilising drug, so sensitivity to TBZ indicates chromosome segregation defects. Wild type cells survive even at high concentrations of the drug, while cells that do not have the normal chromosome segregation machinery do not grow as well as the wild type cells when the drug is added to the media.

TBZ was added to YES agar plates just before the plates were going to be poured at either $15.0 \mu\text{g ml}^{-1}$ or $17.5 \mu\text{g ml}^{-1}$. Plates with no added TBZ were used as a control.

Once the cells were transferred onto plates prepared as described, the plates were incubated at 25°C until full growth.

2.6.2 Centromere silencing assays

It has been shown that genes inserted in fission yeast centromeres are transcriptionally silenced[37] as discussed in section 1.

This happens because functional centromeres have an optimal level of Cnp1^{CENP-A}. A reporter gene can be inserted at the centromere (commonly *arg3*) and its expression monitored by using a selective medium. In such an experiment, the endogenous copy of the reporter gene must be deleted. This allows for indirect determination of Cnp1^{CENP-A} levels at the centromere by monitoring whether the reporter gene within the centromere is silenced or expressed. If Cnp1^{CENP-A} levels drop, the corresponding levels of histone H3 increase allowing for derepression of the reporter gene. This is commonly known as the centromere silencing assay. The position of the reporter gene (*arg3*) in the central centromeric core, in strains used in centromere silencing assays, is shown in Figure 1.2. Mutants of genes involved in Cnp1^{CENP-A} deposition at centromeres have been shown to de-silence *arg3* (i.e., grow on media lacking arginine) due to reduced Cnp1^{CENP-A} levels and correspondingly increased histone H3 levels at the centromere[38].

The cells were prepared as described in Section 2.6, and the selective medium used was PMG agar not supplemented with arginine as described in Table 2.3. PMG agar plates with arginine were used as a control. The PMG agar plates with cells were incubated at 32°C until full growth.

2.6.3 DNA damage assays

In DNA damage assays hydroxyurea (HU) and methyl methanesulfonate (MMS) were added to YES agar just before the plates were about to be poured. HU was added at the concentration of 5 mM, while MMS was added at either 0.00125% or 0.0025%. Plates with no added genotoxic agents were used as a control. Once cells have been transferred to the plates as described in Section 2.6, the plates were incubated at 32°C until full growth.

2.6.4 Temperature sensitivity assays

To determine temperature sensitivity of a strain, plates with YES agar and Phloxin B were used. Phloxin B stains the dead cells, which makes the cells easier to see. Phloxin B was added to the medium just before the plates were poured at the concentration of 2.5 $\mu\text{g ml}^{-1}$.

Once the cells have been transferred to the plates as described in Section 2.6, the plates were incubated at the restrictive temperature and non-restrictive temperature as a control.

2.7 Molecular techniques

2.7.1 Genomic DNA extraction

10 ml of a liquid culture in the exponential growth phase is centrifuged at 1,500 rpm for 5 minutes, which ensures that all *S. pombe* cells settle at the bottom of the tube.

The cell pellet is resuspended in 250 μ l of DNA buffer, the recipe for which is given in Table 2.7 below. Glass beads are added to the microtube containing the resuspended cells.

The microtube was shaken using the FastPrep-24 homogeniser at speed 5.0 for 15 seconds, with a pause of 1 minute before the second cycle of homogenisation using the same speed and time settings.

Following homogenisation, the microtubes are quickly inverted to ensure that the glass beads accumulate near the lid. The bottom of the microtube is punctured using a sterile needle which has been heated in a Bunsen burner flame.

Once punctured, the microtubes are inserted into clean microtubes and centrifuged at 2,000 rpm for 30 seconds. The upper microtube is discarded after centrifugation and 250 μ l of phenol-chloroform-isoamyl alcohol solution is added to the cell lysate in a fume hood.

250 μ l of TE buffer (the recipe for which is given in the Table 2.8 below) is added to the lysate and inverted to mix. The microtubes are centrifuged at 13,200 rpm for 5 minutes. Following centrifugation the aqueous phase containing the DNA is transferred to a fresh microtube in a fume hood. This step is repeated to purify the DNA.

40 μ l of 3M Sodium Acetate (pH 5.2) and 800 μ l of 100% ethanol (stored at -20°C) is added to concentrate and purify the DNA. The DNA is left to precipitate for approximately 30 minutes at -20°C .

Once DNA has precipitated, the microtubes are centrifuged at 13,200 rpm for 10 min in a centrifuge chilled to 4°C to pellet the DNA. The pellet was washed with 70% ethanol (stored at -20°C) and centrifuged at 13,200 rpm for 5 minutes.

Supernatant is removed with a pipette and the microtubes centrifuged on a short spin to remove any residual ethanol. The DNA pellet is left to air dry for approximately 10 minutes. The dry pellet is resuspended in 50 µl of the TE buffer containing 20 µg mL⁻¹ of RNase A. The RNase is allowed to work at room temperature for approximately one hour and the resulting DNA can be stored at -20°C or used immediately.

Table 2.7: DNA buffer preparation.

Ingredient	<i>c</i>/mol l⁻¹
Tris-HCl, pH 8.0	0.1
NaCl	0.1
EDTA pH 8.0	1 x 10 ⁻³

SDS needs to be added to the resulting solution at the concentration of 1%.

Table 2.8: TE buffer preparation.

Ingredient	<i>c</i>/mmol l⁻¹
Tris-HCl, pH 8.0	10.0
EDTA pH 8.0	1.0

2.7.2 Polymerase chain reaction (PCR)

The basic cycling conditions used for PCR reactions using Taq polymerase are given in the Table 2.9 below. NEB T_m calculator was used to ensure the correct annealing temperature for a given set of primers. The extension length is 30 - 35 cycles.

Table 2.9: PCR conditions.

Temperature/°C	Time/s
98.0	30.0
98.0	10.0
55.0	30.0
72.0	30.0 per kb of product
72.0	600.0
10.0 - 15.0	as desired

2.7.3 Agarose gel electrophoresis

Agarose gels were prepared by dissolving agarose powder in a suitable volume of TAE buffer. A microwave oven is used to heat the buffer and the agarose powder. When the agarose powder is dissolved, and the solution has cooled down, SafeView stain is added to the gel to facilitate visualisation of the DNA bands and the gel is poured into a gel casting tray and a comb inserted to create wells.

To ensure good resolution of the bands, the following agarose concentrations were used:

- For bands under 300bp, 2% agarose;
- For bands between 300 and 600bp, 1.5% agarose;
- For bands between 600 - 1,200bp, 1% agarose;
- For bands over 1,200bp, 0.8% agarose.

When the gel is ready, samples are diluted with DNA loading dye and loaded onto the gel, and the electrophoresis started.

To visualise the bands, BioRad Chemidoc MP Imaging System was used with a UV filter.

2.7.4 Transformation of *S. pombe* cells using electroporation

A 50 ml liquid culture that is in the exponential growth phase is centrifuged at 1,500 rpm for 5 minutes and the supernatant decanted. The tube containing the cells is placed on ice and washed with 10 ml of 1.2 M ice-cold sorbitol by gently inverting the closed tube. The tube is centrifuged and supernatant decanted as described. There are a total of three sorbitol washes.

After the final wash, the cell pellet is resuspended in 600 μ l of sorbitol and 250 μ l of the resulting cell solution is mixed with a sample of DNA (up to 10 μ l of DNA is used) in a chilled 2 mm electroporation cuvette. The electroporation was performed using BioRad Genepulser Xcell using the *S. pombe* pre-set protocol.

Following electroporation, 1 ml of the ice-cold sorbitol was added to the electroporated cells and the cells were transferred to a microtube and then plated as required and incubated.

2.7.5 Selection of transformants

Randomly selected single cell colonies were selected and patched onto a fresh YES agar plate and incubated at the appropriate temperature until full growth.

The colonies were replica plated using a sterile velvet cloth onto YES agar and YES agar plates with selective antibiotics. Only strains that were shown to be resistant to the required antibiotic(s) were patched onto YES agar to create a stock that can be used in experiments.

2.8 Live imaging of *S. pombe* cells using fluorescence microscopy

2.8.1 Culture preparation

A small pre-culture is prepared from freshly growing cells. Once the OD₅₉₅ of the pre-culture indicates that the pre-culture is in the exponential growth phase, a larger culture is prepared as described in Section 2.4.

When the cultures are ready, the tubes containing the cultures are centrifuged at 1,500 rpm for 5 minutes, supernatant is removed and the cells are washed with PMG medium and centrifuged again.

After the second centrifugation and removal of the supernatant, the cells are resuspended in a small amount of PMG (approximately 1 ml). 10 μ l of the cell suspension is pipetted on a fresh microscope slide and covered with a cover slip. Bubbles are removed by very gently pressing the cover slip.

2.8.2 Image acquisition and analysis

The prepared cells were imaged using the DeltaVision Elite system. Images were taken as 27 z-stacks with an oil immersion objective (x60). Deconvolution was performed using SoftWoRX software.

2.9 Chromatin immunoprecipitation (ChIP)

2.9.1 Cell growth and harvesting

The density of the cell culture is checked by measuring OD₅₉₅. The density of the culture should be approximately 5×10^6 cells ml⁻¹. 50 ml of culture is needed for each ChIP, and the culture should be prepared in YES wherever possible.

Each culture is poured into a 50 ml centrifuge tube and centrifuged at 1,500 rpm for 5 minutes. The supernatant is removed and the cell pellet is resuspended in 36 ml of ice-cold PBS.

In a fume hood, 1 ml of 37% solution is added to the cell suspension and the tubes are placed on a nutator to mix for 15 minutes. The crosslinking is quenched by adding 3 ml of 2.5 M glycine solution to the tubes and mixed on the nutator for 5 minutes.

The tubes are centrifuged in a centrifuge chilled to 4°C at 1,500 rpm for 5 minutes. The supernatant is removed in a fume hood, and the tubes containing cell pellets are placed on ice. The cell pellets are resuspended in 0.8 ml of ice-cold Buffer I, the recipe for which is given below in Table 2.10.

Table 2.10: Buffer I preparation.

Ingredient	Effective concentration
1 M HEPES-KOH, pH 7.5	50.0 mmol l ⁻¹
5 M NaCl	140.0 mmol l ⁻¹
0.5 M EDTA pH 8.0	1.0 mmol l ⁻¹
10% Triton X-100	1%
10% Sodium deoxycholate	0.1%

The cell solution is transferred into pre-cooled microtubes and the microtubes are centrifuged in a centrifuge chilled to 4°C at 13,200 rpm for 1 minute. The supernatant is removed.

If not proceeding with ChIP immediately, the tubes with cell pellets can be snap frozen in liquid nitrogen and stored at -80°C until ready to proceed.

2.9.2 Chromatin immunoprecipitation

If using frozen cell pellets, the pellets are thawed on ice. Once the pellets are thawed, 400 μ l of lysis buffer (the recipe is given below in Table 2.11 - it is important to note that the buffer must be freshly supplemented with PMSF and protease inhibitors just before use).

Table 2.11: Lysis buffer preparation.

Ingredient	Effective concentration
1 M HEPES-KOH, pH 7.5	50.0 mmol l ⁻¹
5 M NaCl	140.0 mmol l ⁻¹
0.5 M EDTA pH 8.0	1.0 mmol l ⁻¹
10% Triton X-100	1%
10% Sodium deoxycholate	0.1%
100 mM PMSF	1.0 mmol l ⁻¹
Protease inhibitors	1x

Glass beads are added to the microtubes and the cells are lysed in the MP Biomedical FastPrep 24 homogeniser with dry ice added to the tube holder. 6 cycles of lysis of 20 seconds at speed 6.5 with a 30 second pause between the cycles should achieve 70-80% lysis, which can be checked under a light microscope.

Microtubes are taken out, inverted and the bottom punctured using a needle heated in a Bunsen burner flame. The microtubes are placed into fresh microtubes and the tubes are centrifuged at 1,000 rpm for 15 seconds.

The upper microtubes are discarded and 250 μ l of the lysate is transferred into fresh, pre-cooled microtubes. Pellets can be gently vortexed only if required.

The lysates are placed in a sonicator water bath cooled to 4°C and sonicated for 40 cycles of 30 seconds of sonication in each cycle. The lysates are centrifuged in a centrifuge cooled to 4°C at 13,200 rpm for 15 minutes to pellet cell debris. The supernatant is transferred to fresh pre-cooled microtubes following centrifugation.

The protein concentration is estimated using the Bradford's assay. 1:20 dilutions of lysates in lysis buffer are used. Inputs for each ChIP should be standardised to 4

mg of whole cell extract in 210 - 260 μ l of lysis buffer. 5 μ l of the dilution is set aside to be used as input control and the rest used for the experiment,

To ensure the samples have been sufficiently sonicated, a shearing check can be performed by using 25 - 100 μ l of lysate. The lysate is diluted 1:4 with TES buffer, which is prepared as described in Table 2.12.

A maximum of 100 μ l of the lysate should be used for shearing check. The protocol is given for 25 μ l of lysate, but if using more, this can be scaled up accordingly. The given volume of proteinase K should be used even if more than 25 μ l of the lysate is used.

Table 2.12: TES buffer preparation.

Ingredient	Effective concentration
1M Tris, pH 8.0	50.0 mmol l ⁻¹
0.5M EDTA, pH 8.0	25.0 mmol l ⁻¹
10% SDS	1.0%

0.01 mg of proteinase K is added to the microtubes and the tubes are inserted into the thermoblock set to 65°C. The tubes are left in the thermoblock with shaking at 750 rpm overnight.

Proteinase K is inactivated by heating the tubes to 80°C for 10 minutes. Once the microtubes have cooled down, RNase A is added to the concentration of 20 μ g ml⁻¹. The lysates are incubated with RNase A for 1 hour at 37°C.

The lysates are treated again with 0.15 μ g of proteinase K at 55°C for 2-3 hours.

DNA is extracted and purified using the phenol-chloroform extraction and 1 μ l of glycogen is added when precipitating the DNA. The DNA pellet is resuspended in TE buffer with no RNase A.

The DNA samples are loaded onto a 1.8% agarose gel to which ethidium bromide has been added. The electrophoresis should run for 40 minutes at 120V.

The input control samples are frozen at -20°C. Antibody is added to the ChIP sam-

ples and the tubes are put on a nutator at 4°C. The samples need to be incubated with the antibody for at least 2 hrs.

Magnetic beads need to be pre-washed with the lysis buffer 2-4 times, and 30 µl of the beads per sample is used. The washed beads are added to the samples and incubated on a nutator at 4°C for at least 3 - 4 hrs or overnight.

The supernatant is removed, leaving the beads behind. The beads are washed with 1 ml of each of the following buffers.

- Lysis Buffer - two brief washes;
- Buffer I with 0.5 M NaCl - two 10 minute washes;
- Wash Buffer - two 10 minute washes;
- TE Buffer pH 8.0 - one 10 minute wash.

Wash buffer is prepared as described in Table 2.13 below.

Table 2.13: Wash buffer preparation.

Ingredient	Effective concentration
1M Tris-HCl, pH 8.0	10.0 mmol l ⁻¹
1M LiCl	250.0 mmol l ⁻¹
0.5M EDTA pH 8.0	1.0 mmol l ⁻¹
10% NP-40	0.5%
10% Sodium deoxycholate	0.5%

For longer washes, the tubes should be left on a nutator at 4°C. On the last wash supernatant is removed with a 5 ml syringe and a small needle.

A fresh 10% slurry of Chelex-100 resin is prepared in sterile water. 100 µl of 10% Chelex resin is added to each sample and input control sample. The samples are boiled samples at 100°C for 12 minutes.

The tubes are cooled down at room temperature and centrifuged quickly before adding 2.5 µl of 10 mg ml⁻¹ proteinase K to each sample. The samples are incubated

with proteinase K at 55°C for 30 minutes on the thermoblock while shaking at 1,000 rpm.

To inactivate proteinase K the samples are boiled at 100° for 10 minutes and the tubes are centrifuged quickly. 70 µl of supernatant is transferred to fresh tube containing 100 µl of water and 20 µl of 10x TE buffer. The resin must be excluded while pipetting as it will prevent qPCR from working. The DNA is stored at -20C.

2.9.3 Analysis using quantitative Polymerase Chain Reaction (qPCR)

The immunoprecipitate and input control samples are thawed at room temperature. To ensure that all Chelex resin is settled on the bottom of the microtubes, the tubes are quickly centrifuged using a high speed at room temperature.

1:10 dilutions of immunoprecipitate and 1:500 dilutions of input control samples are prepared in water. If the dilutions are not going to be used immediately, the dilutions can be kept at 4°C to avoid repeat freeze - thaw cycles, which make qPCRs unreliable.

The mix for the qPCR for each primer pair is prepared as described in Table 2.14 below. The volumes given below are per 10 µl reaction.

Table 2.14: qPCR master mix preparation.

Component	V / µl
NEB Luna Universal qPCR Master Mix	5.0
Forward primer	0.25
Reverse primer	0.25
Template DNA	4.0
Sterile Milli-Q water	to 10.0

Once all mixtures have been pipetted, the multiwell plate can be gently tapped to ensure the qPCR mixture sinks to the bottom of the well. The plate is sealed using optically clear film - it is important to ensure that all of the edges are sealed to avoid sample evaporation. Once sealed, the plate can be quickly centrifuged in a plate centrifuge.

To run the qPCR reaction, the settings given in Table 2.15 below were used. The program was ran for 45 cycles. All qPCRs were carried out on the BioRad CFX384 Touch machine. All samples had three technical replicates.

Table 2.15: qPCR conditions.

Temperature/°C	Time/s
95.0	60.0
95.0	15.0
60.0	180.0

The data obtained by the qPCR was analysed using BioRad CFX Maestro software and MS Office Excel.

First of all, the raw data from the experiment, which is given as a .zpcr file, was converted into a .pcrd file using the CFX Maestro software. Once all the wells have been labelled, the data is exported as an Excel spreadsheet for analysis.

When examining data in the spreadsheet, it is important to note the standard deviations for the mean C_q (C_t) values. Where the standard deviation of the C_q value was below 0.5, the mean C_q value was used in the calculations. Where the standard deviation value was larger than 0.5, the individual C_q values were examined to determine which of the three value is an outlier, and the mean of the remaining two values was taken for subsequent calculations.

The first step is to calculate the difference in the mean C_q value of the input control and the immunoprecipitation samples (ΔC_q) for a given strain. Following this, $2^{\Delta C_q}$ is calculated and multiplied by 100 as the results are given in percentages. The resulting number is divided by the dilution factor. Finally, this is multiplied by the ratio of volumes of the input controls and the immunoprecipitates used for the ChIP.

2.10 Immunoprecipitation followed by liquid chromatography coupled with tandem mass spectrometry (IP LC-MS/MS)

2.10.1 Cell growth and harvesting

1 l of *S. pombe* culture is grown in 4xYES media to approximately $1 - 2 \times 10^8$ cells/ml. The cultures are collected and centrifuged for 30 minutes at 3,500 rpm. The cell pellets are washed with PBS twice and resuspended in the volume of water that is approximately the fifth of the volume of the cell pellets.

A syringe is filled with the viscous cell suspension and small spheres of the suspension are slowly dropped into liquid nitrogen. The frozen spheres of the cell suspension can be stored at -80°C or used immediately.

The frozen cell suspension needs to be ground into a fine powder before being used for immunoprecipitation. The pestle and mortar used for this experiment need to be thoroughly cleaned with ethanol before being cooled down. To cool down the mortar a small water bucket is filled with dry ice and the mortar placed on top. Liquid nitrogen is poured into the mortar to cool it down further.

Once the mortar has cooled down, a small amount of liquid nitrogen is poured into it and the frozen cell suspension is added. The suspension is ground into a fine powder. While grinding liquid nitrogen needs to be re-added throughout to ensure that the cell suspension doesn't thaw. Once ground, the powder is collected in 5 g portions in centrifuge tubes that have been pre-cooled in liquid nitrogen.

2.10.2 Immunoprecipitation

10 ml of cold lysis buffer, which has been prepared as described in Table 2.16 below, to the cell powder. The powder is rotated with the buffer for approximately 30 minutes at 4°C to solubilise.

Table 2.16: Lysis buffer preparation.

Ingredient	Effective concentration
HEPES-NaOH, pH 7.5	50.0 mmol l ⁻¹
KCl	150.0 mmol l ⁻¹
10% NP-40	0.1%
To be added fresh just before use:	
Dithiothreitol, DTT	5.0 mmol l ⁻¹
Roche EDTA-free protease inhibitors cocktail	1x
Sigma protease inhibitors cocktail	1x
PMSF	0.2 mmol l ⁻¹
Benzamide	0.2 mmol l ⁻¹

Affinity beads are prepared by washing protein G magnetic beads (25 µl is required per sample) and washing them three times with 1 ml of PBS. Once the beads are washed, they are coupled with 8 µl of antibody in 0.5 ml of PBS. The microtube is rotated for 30 minutes at 4°C. Once the affinity beads have been prepared, they are washed twice with PBS, once with the lysis buffer and finally resuspended in lysis buffer (using 10 µl of the buffer per sample.)

The solubilised cell extract is centrifuged at 4,000 rpm for 10 minutes. The supernatant is collected and centrifuged for 45 minutes at 14,000 rpm at 4°.

10 µl of the prepared affinity beads are added to the supernatant and the microtubes are rotated for 1 hour at 4°C.

Following the rotation, the supernatant is discarded and the beads are transferred into a fresh Eppendorf Protein Lo-Bind tube using 1 ml of the lysis buffer.

The beads are washed with the lysis buffer, collected and the supernatant is discarded. The beads are resuspended in 0.5 ml of lysis buffer with 2 mM MgCl₂ which has been prepared as described in Table 2.17. 500 units of benzonase are

added and the microtubes are rotated at 4°C for 15 minutes.

Table 2.17: The preparation of lysis buffer supplemented with MgCl₂.

Ingredient	Effective concentration
HEPES-NaOH, pH 7.5	50.0 mmol l ⁻¹
KCl	150.0 mmol l ⁻¹
10% NP-40	0.1%
MgCl ₂	2.0 mmol l ⁻¹

The beads are collected and the supernatant discarded. The beads are resuspended in 1 ml of lysis buffer and transferred into a new Protein Lo-Bind tube, washed and the supernatant discarded.

The beads are resuspended in 0.5 ml of BD buffer, which has been prepared as described in the Table 2.18 below, washed, collected and the supernatant discarded.

Table 2.18: BD buffer preparation.

Ingredient	Effective concentration
Tris-HCl, pH 8.0	20.0 mmol l ⁻¹
NaCl	150.0 mmol l ⁻¹
CaCl ₂	2.0 mmol l ⁻¹

The washed beads are resuspended in 10 µl of 20 mmol l⁻¹ Tris-HCl (pH 8.0). 5 µl of the NEB 3x Blue Loading Dye for protein gels and 0.5 µl of NEB 30x DTT. The samples are boiled at 99°C for 5 minutes. Following this the samples can be either frozen if not used immediately.

When ready, the samples are loaded onto an SDS page gel. 150 V was used to start the electrophoresis. The electrophoresis only needs to be performed for several minutes to ensure that the samples enter the stacking gel. After this the gel is stained using Invitrogen SilverQuest Silver Staining kit to visualise the protein bands. The bands are excised and put into Protein Lo-Bind tubes containing 500 µl of Milli-Q water.

2.10.3 LC-MS/MS

The gel bands samples were subjected to in-gel reduction, alkylation and digestion with trypsin.

To ensure the reduction of cysteine residues, DTT was used and iodoacetamide was used to create stable carbamidomethyl derivatives. Trypsin digestion was performed at 37°C for two hours and after that overnight at room temperature. The reagents used to prepare the samples are given in the Table 2.19 below.

Table 2.19: Reagents used for preparation of gel band samples for mass spectrometry.

Reagent	Effective concentration
Tetraethylammonium bromide, TEAB	100.0 mmol l ⁻¹
Tetraethylammonium bromide, TEAB	50.0 mmol l ⁻¹
DTT	10.0 mmol l ⁻¹
Iodoacetamide	55.0 mmol l ⁻¹
Trypsin	13.0 ng µl ⁻¹

The gel bands are cut into 2 mm² pieces and transferred into fresh microfuge tubes. The gel pieces are washed with 100 mmol l⁻¹ TEAB for 5 minutes. The supernatant is removed and acetonitrile added to wash the gel pieces. Once the gel pieces are washed, acetonitrile is decanted and fresh acetonitrile added to ensure full dehydration of the gel pieces. The acetonitrile is removed and the gel pieces dried in a SpeedVac vacuum concentrator for 5 minutes.

The gel pieces are rehydrated with 10 mmol l⁻¹ DTT and heated at 56°C for 30 minutes. DTT is removed and acetonitrile added. The gel pieces are dehydrated and dried in SpeedVac for 5 minutes.

Iodoacetamide is added and the gel pieces are incubated with it for 20 minutes in the dark. The supernatant is then discarded, the gel pieces briefly washed with the TEAB buffer. The buffer is discarded and the gel pieces washed for another 5 minutes with a fresh aliquot of the TEAB buffer.

Following the wash the liquid is decanted, gel pieces dehydrated with acetonitrile and dried in SpeedVac for 5 minutes. Finally, the gel pieces are rehydrated in 50 µl

of the trypsin solution at 40°C for 20 minutes. Unabsorbed trypsin is removed, 50 µl of 50 mmol l⁻¹ TEAB buffer is added to cover the gel pieces and the pieces are incubated with trypsin at 37°C for 2 hours and then overnight at room temperature.

After the trypsin incubation the supernatant is removed from the gel pieces and collected into a fresh microfuge tube. The gel pieces are washed in 50 µl of 50 mmol l⁻¹ TEAB buffer for 5 minutes at 37°C and the supernatant is pooled with the supernatant removed in the previous step.

The gel pieces are dehydrated with 50 µl of acetonitrile at 37°C for 5 minutes, and the supernatant then pooled with the previously collected supernatant. Finally, the TEAB washing and acetonitrile dehydration steps are repeated and the supernatant acquired is pooled with the previously collected one.

The resulting peptide extract is frozen and the pooled supernatants are dried in a SpeedVac. The samples can be stored at -80°C until needed.

The peptide samples are resuspended in 40 µl of resuspension buffer (which consists of 2% acetonitrile in 0.05% formic acid). The liquid chromatography is performed on a ThermoFisher Scientific U3000 UHPLC NanoLC system. Peptide resolution was achieved by using reverse phase chromatography on a 75 µm C18 Pepmap 50 cm column. A three step linear gradient of 80% acetonitrile in 0.1% of formic acid.

The peptides were eluted at the flow rate of 250 nl min⁻¹ over one hour. The initial elution (0 - 5 minutes) used 5% of solvent B, which was increased to 40% for further 35 minutes, then 99% for the 5 minute wash step and the equilibration step used 5% of solvent B. The peptide eluate was ionised using electrospray ionisation in a ThermoFisher Scientific Orbitrap Fusion Lumos using Xcalibur v4.1.5.

The instrument was programmed to acquire using an Orbitrap-Ion Trap method by defining a 3 second cycle time between a full MS scan and MS/MS fragmentation. Orbitrap spectra were collected at a resolution of 120,000 over a scan range

of m/z 375-1500 with an automatic gain control (AGC) setting of 4.0×10^5 with a maximum injection time of 35 ms.

Monoisotopic precursor ions were filtered using charge state (+2 to +7) with an intensity threshold set between 5.0×10^3 to 1.0×10^{20} and a dynamic exclusion window of 35 seconds \pm 10 ppm. MS2 precursor ions were isolated in the quadrupole set to a mass width filter of 1.6 m/z . Ion trap fragmentation spectra were collected with an AGC target setting of 1.0×10^4 with a maximum injection time of 35 ms with CID collision energy set at 35%.

2.10.4 Data analysis

The raw data was processed into peak list files using Proteome Discoverer (ThermoScientific; v2.2). The raw data file was processed and searched using the Mascot search algorithm (v2.6.0; www.matrixscience.com) and the Sequest search algorithm[281] against the Uniprot All Taxonomy database (561,911 entries) and the Uniprot *Schizosaccharomyces pombe* database (5,303 entries).

The database output file was uploaded in to Scaffold software (v 4.11.0; www.proteomesoftware.com) for visualisation and manual verification.

2.11 Co-immunoprecipitation (Co-IP)

2.11.1 Cell growth and harvesting

100 ml of exponentially growing culture in YES medium is needed per sample. To ensure that the cultures are in the exponential growth phase the density of the cell culture is checked by measuring OD₅₉₅. The density of the culture should be approximately 5×10^6 cells ml⁻¹.

Each culture is poured into a 50 ml centrifuge tube and centrifuged at 1,500 rpm for 5 minutes. The supernatant is removed and the cell pellet is resuspended in 36 ml of ice-cold PBS.

In a fume hood, 1 ml of 37% solution of formaldehyde is added to the cell suspension and the tubes are placed on a nutator to mix for 15 minutes. The crosslinking is quenched by adding 3 ml of 2.5M glycine solution to the tubes and mixed on the nutator for 5 minutes.

The tubes are centrifuged in a centrifuge chilled to 4°C at 1,500 rpm for 5 minutes. The supernatant is removed in a fume hood, and the tubes containing cell pellets are placed on ice.

The cell pellets are resuspended in 0.8 ml of ice-cold Buffer I, the recipe for which is given in Table 2.10.

The cell solution is transferred into pre-cooled microtubes and the microtubes are centrifuged in a centrifuge chilled to 4°C at 13,200 rpm for 1 minute. The supernatant is removed.

If not using the cell pellets immediately, the tubes with cell pellets can be snap frozen in liquid nitrogen and stored at -80°C until ready to proceed.

2.11.2 Co-immunoprecipitation

The cell pellets are thawed on ice and resuspended in 400 μl of lysis buffer, which is prepared as described in Table 2.20 below.

Table 2.20: Lysis buffer preparation.

Ingredient	Effective concentration
1 M HEPES-KOH, pH 7.5	50.0 mmol l^{-1}
5 M NaCl	150.0 mmol l^{-1}
60% Glycerol	10%
0.5 M EDTA pH 8.0	5.0 mmol l^{-1}
10% NP40	0.5%
50 mM Sodium flouride, NaF	5.0 mmol l^{-1}
100 mM PMSF	1.0 mmol l^{-1}
DTT	1.0 mmol l^{-1}
Sodium orthovanadate, Na_3VO_4	1.0 mmol l^{-1}
Protease inhibitors	1x

Glass beads are added to the cell suspension and the cells are lysed in the MP Biomedical FastPrep 24 homogeniser with dry ice added to the tube holder. 6 cycles of lysis of 20 seconds at speed 6.5 with a 30 second pause between the cycles is used to lyse the cells.

Microtubes are taken out, inverted and the bottom punctured using a needle heated in a Bunsen burner flame. The microtubes are placed into fresh microtubes and the tubes are centrifuged at 1,000 rpm for 15 seconds.

The upper microtubes are discarded and the lysate is transferred into fresh, pre-cooled microtubes. The lysates are centrifuged at 13,000 rpm for 15 minutes at 4°C.

After the centrifugation the supernatants are transferred into fresh pre-cooled microtubes and placed on ice.

All whole cell extracts (WCEs) need to be diluted to the same concentration in 250 μl of lysis buffer, so Bradford's assay is used to estimate the protein concentration in WCEs. 45 μl of the WCE is taken into fresh microtubes as input control,

and the rest of the sample is used to prepare the dilutions to be used in immunoprecipitation.

Input control samples are supplemented with NEB 4x SDS sample loading buffer and boiled at 100°C for 5 minutes. The samples are then quickly centrifuged and frozen at -20°C until ready to proceed with SDS-PAGE electrophoresis.

30 µl of protein G magnetic beads per sample is pipetted into a fresh microtube. The storage buffer is removed and the beads are resuspended in 800 µl of ice-cold lysis buffer. The buffer is removed and the washing process is repeated two more times.

On the final wash, the supernatant is removed and the beads are resuspended in lysis buffer to the original volume of beads that was taken out. 8 µl of the antibody is added to the beads and the microtubes with the beads is left on a nutator at 4°C for 2 hours to allow for the beads to bind the antibody.

Following the incubation of the beads with the antibody, 30 µl of prepared magnetic beads is added and the tubes are placed on a nutator for a further two hours at 4°C.

Once the incubation has finished, the beads are washed with 800 µl of the lysis buffer as described before and on the final wash all supernatant is removed. 4x SDS sample loading buffer is added to the beads and the tubes are boiled at 100°C for 5 minutes.

If not using the samples immediately, they can be stored at -20°C and boiled at 100°C for two minutes when ready to be used.

2.11.3 Sodium dodecyl-sulphate polyacrylamide gel electrophoresis (SDS-PAGE) and Western blotting

BioRad Mini-PROTEAN TGX polyacrylamide gel was placed in the BioRad Mini-PROTEAN Tetra cell. The inner and outer chambers of the cell were filled with SDS-PAGE running buffer, prepared as described in Table 2.21 below and diluted to 1x prior to use. The comb from the gel was removed and 20 μl of samples and 5 μl of protein ladder was loaded on the gel.

Table 2.21: 5x SDS-PAGE running buffer preparation.

Ingredient	Effective concentration
Tris base	15.1 g l ⁻¹
Glycine	94.0 g l ⁻¹
SDS	10%

100 V was used to start electrophoresis and ensure that samples stack well in the stacking gel after which the voltage was increased to 150 V to ensure good separation of proteins. The electrophoresis ran for approximately 60 minutes.

To transfer the separated proteins on a nitrocellulose membrane BioRad Trans-Blot Turbo Transfer System was used according to the manufacturer's instructions. The blotting sandwich was assembled by placing the ion reservoir stack, nitrocellulose membrane, gel, and the top ion reservoir stack on the cassette anode and covering the sandwich with the cassette cathode.

The cassette was inserted in the instrument and the transfer started using the Mixed MW program, which allows for transfer of proteins with molecular weights between 5 and 150 kDa and uses a constant 1.3 A current.

Following the transfer the membrane was stained using the Ponceau S stain for 1 minute with gentle shaking. The Ponceau S solution was then removed and the membrane rinsed in water several times.

The membrane was blocked in 5% milk solution in TBST, which is prepared

by dissolving a tablet of Sigma Tris BUffered Saline, TBS in 500 ml of water and supplementing the solution with Tween 20 to a concentration of 0.2%. The blocking should be at least 30 minutes long, with shaking.

Once blocked, a membrane is placed in a black box for incubation with the antibodies. α -GFP antibody was used at a 1:2,000 dilution which was prepared in 5% milk in TBST. The antibody incubation was performed overnight on a nutator at 4°C.

The membrane is washed three times in TBST for 10 minutes each time. The secondary antibody solution (α -rabbit HRP) is prepared at 1:10,000 dilution in 5% milk in TBST. The membrane is incubated with the secondary antibody for two hours at room temperature on a nutator.

Amersham ECL Western Blotting Detecting Agent was used as per manufacturer's instructions. The chemiluminescent signal was detected using either the BioRad Chemidoc or ThermoFisher iBright system.

2.12 Bioinformatics

Multiple sequence alignment was performed using EMBL-EMBI Clustal Omega (<https://www.ebi.ac.uk/Tools/msa/clustalo/>)[282, 283]. Sequences were obtained in a FASTA format from PomBase(<https://www.pombase.org>)[284] and NCBI Gene database (<https://www.ncbi.nlm.nih.gov/gene/>)[285].

Chapter 3

Investigation of the physical and genetic interaction between Ccp1^{Vps75} and Rtt109

3.1 Introduction

Rtt109 is a member of the HAT (histone acetyltransferase) family and is required for the acetylation of histone H3 on K9, K27 and K56[274, 275]. *S. cerevisiae* Rtt109 associates with two histone chaperones *in vivo*: Vps75^{Ccp1} and Asf1. Vps75 is the *S. cerevisiae* ortholog of Ccp1.

Vps75^{Ccp1} and Asf1, while being unrelated chaperones, both interact with the H3-H4 dimer and (H3-H4)₂ tetramer. In *S. cerevisiae* it has been shown that *in vitro* acetylation of H3 increases after the addition of either Asf1 or Vps75^{Ccp1}, however *in vivo* Asf1 and Rtt109 have been shown to be essential for H3 acetylation at K56, while Vps75^{Ccp1} notably was not. Interestingly, acetylation of the histone H3 at K9 and K27 by Rtt109 are both Vps75^{Ccp1}-dependent[6].

Meanwhile, research in *S. pombe* has found that Rtt109 acetylates histone H3 (par-

ticularly on K56) both *in vitro* and *in vivo*, and *rtt109* Δ single mutants exhibit acute sensitivity to genotoxic agents[5]. The authors of this paper hypothesise that this effect is due to the the acetylation of histone H3 by Rtt109 being involved in DNA damage response in cells.

Ccp1 is the fission yeast homolog of the budding yeast Vps75 and SET in humans[3, 4]. In *S. cerevisiae* Vps75 was identified through a screen for mutants with defective vacuolar sorting, and has been found to be a NAP (Nucleosome Assembly Protein) family protein.

Some structural analyses of Ccp1 suggest that it forms a homodimer and that the homodimer is required for the anti-CENP-A loading activity[3]. However, other researchers report a tetrameric structure for *S. cerevisiae* Vps75[272, 273]. Cells overexpressing Ccp1^{Vps75} were also shown to be highly sensitive to TBZ[3].

So far it has been suggested that in *S. cerevisiae* Vps75^{Ccp1}, which has a nuclear localisation signal, imports Rtt109 into the nucleus and stabilises it, and additionally positions H3 for acetylation by Rtt109[6, 274]. It is also possible that acetylation mediated by Ccp1-Rtt109 aids in flagging centromeres for Mis18 recruitment in *S. pombe*.

While many roles of Vps75 in *S. cerevisiae* have been already investigated, at the moment it is not known if *S. cerevisiae* Vps75 and *S. pombe* Ccp1 are true functional orthologs. For this reason, the role of Ccp1 in fission yeast remains to be explored and the question of whether Ccp1 and Vps75 are true functional orthologs is yet to be answered.

3.2 Results

3.2.1 Ccp1^{Vps75} and Rtt109 may have separate functions

When subjected to TBZ, both the *rtt109*Δ and *ccp1*Δ single mutants are hypersensitive to TBZ, while the *ccp1*Δ *rtt109*Δ double mutants have been shown to be even more sensitive to TBZ than either of the single mutants, as shown in Figure 3.1. *csi1*Δ cells are used as a control for the assay as these cells are extremely sensitive to TBZ[286].

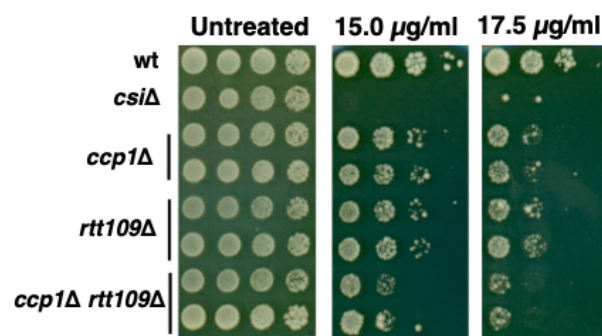


Figure 3.1: *ccp1*Δ *rtt109*Δ and *ccp1*Δ *rtt109*Δ cells are sensitive to TBZ. Serial dilutions of cells were plated on YES media containing several concentrations of TBZ. The plates were incubated at 25°C.

These results are in agreement with what has previously been observed in TBZ sensitivity assays of *ccp1*Δ mutants[3]. However, if Ccp1^{Vps75} and Rtt109 form a complex to maintain functional centromeres, the *ccp1*Δ *rtt109*Δ double mutant should not show increased sensitivity to TBZ compared to the single mutants. It is, however, possible that Ccp1^{Vps75} and Rtt109 work together, but it may be that Rtt109, as already shown in *S. cerevisiae*, has other interactions (e.g. with Asf1 as well as Ccp1 to bring about acetylation of histone H3); this would also result in increased sensitivity of the double mutant to TBZ.

This result therefore suggests that Rtt109 and Ccp1^{Vps75} may not work together or, perhaps, that they are a part of a larger pathway regulating chromosome segregation and/or resistance to genotoxic agents, in line with suggested roles of *S. cerevisiae* Rtt109 and Vps75^{Ccp1} and *S. pombe* Ccp1^{Vps75}.

Rtt109 is known to be involved in cells' response to DNA damaging agents[5]. To investigate whether Ccp1^{Vps75} and Rtt109 were both involved in a pathway regulating resistance to genotoxic agents, hydroxyurea (HU) and methyl methanesulfonate (MMS) were used to induce DNA damage and the viability of the single and double deletion mutants of Ccp1^{Vps75} and Rtt109 compared to the wild type was assessed.

In agreement with previous studies, *rtt109*Δ cells show increased sensitivity to both of the genotoxic agents. In contrast, *ccp1*Δ cells do not exhibit sensitivity to the genotoxic drugs, while the sensitivity of the *ccp1*Δ *rtt109*Δ double mutants may be attributable to the deletion of *rtt109*, as shown in Figure 3.2.

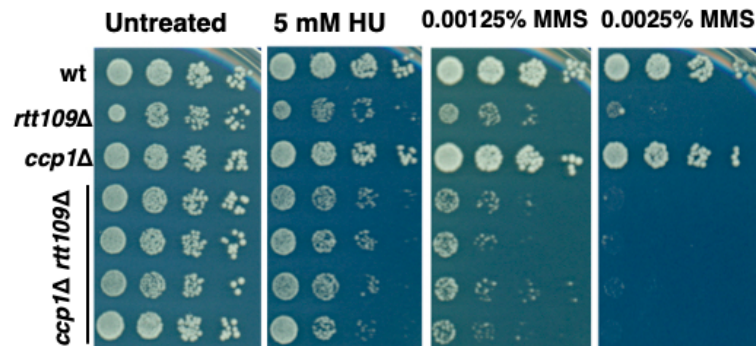


Figure 3.2: *rtt109*Δ cells are sensitive to both HU and MMS, while *ccp1*Δ cells are not. The sensitivity of *ccp1*Δ *rtt109*Δ mutant is attributable to the deletion of *rtt109*. Serial dilutions of cells were plated on YES media containing either HU or MMS at two different concentrations. The plates were incubated at 32°C.

This suggests that in fission yeast Rtt109 may not be essential for Ccp1^{Vps75}'s function at centromeres. At the same time, Ccp1^{Vps75} appears not to be essential for Rtt109's function in the DNA damage response.

3.2.2 Rtt109 may not be required for Ccp1^{Vps75}'s localisation at the centromere

To further investigate whether fission yeast Rtt109 is required for the function of Ccp1^{Vps75}, cells expressing Ccp1^{Vps75} C-terminally fused to GFP (Ccp1^{Vps75}-GFP) in either the wild type or the *rtt109*Δ background were imaged.

The deletion of *rtt109* appears to cause a very small decrease in the number of cells with Ccp1^{Vps75}-GFP foci, and the Ccp1^{Vps75}-GFP signal in general, however this is not a significant decrease, as shown in Figure 3.3.

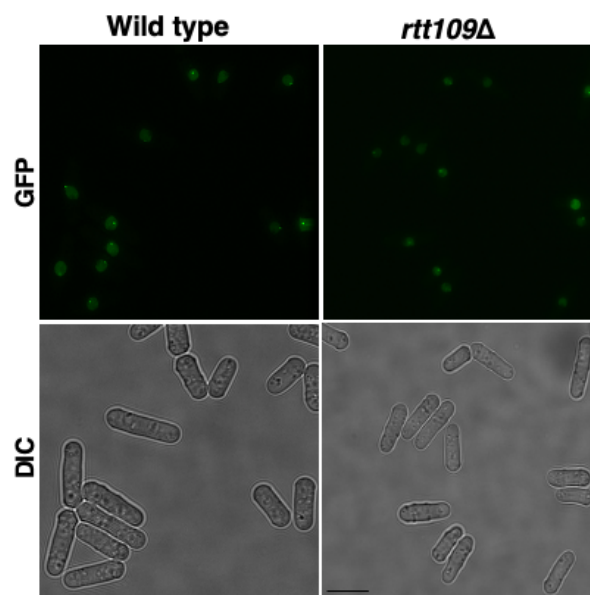


Figure 3.3: Live images of wild type and *rtt109*Δ cells expressing Ccp1^{Vps75}-GFP. Scale bar = 5 μm.

There is a proportion of wild type and *rtt109*Δ cells which do not have a single Ccp1^{Vps75}-GFP focus, as evident in Figure 3.3. This is likely due to the fact that the association of Ccp1^{Vps75} is cell cycle-dependent, as previously reported[3]. In contrast to the cell cycle-dependent association of Ccp1^{Vps75} to the centromere, the localisation of Rtt109 is not cell cycle-dependent[287].

Microscopy results were also quantified by counting the number of cells showing a Ccp1^{Vps75}-GFP focus in both wild type and *rtt109*Δ cells expressing Ccp1^{Vps75}-GFP. As shown in Figure 3.4 the small drop in the number of cells with a Ccp1^{Vps75}-GFP foci in the *rtt109*Δ mutant is not significant.

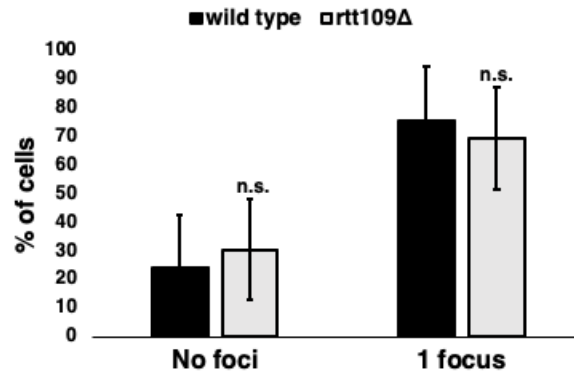


Figure 3.4: A bar chart comparing the number of cells with Ccp1^{Vps75}-GFP foci in the imaged strains. N = 5. Error bars represent the standard deviation.

Finally, chromatin immunoprecipitation (ChIP) was employed to test the association of Ccp1^{Vps75} with centromeres in strains expressing Ccp1^{Vps75}-GFP in wild type cells and *rtt109*Δ mutants to explore whether Rtt109^{Vps75} plays a role in the maintenance of Cnp1^{CENP-A} levels at the centromere. The same strains which were used for fluorescence microscopy were also used in the ChIP experiments.

The results from ChIP experiments are in accordance with what was observed in the imaging experiment as there is a very small decrease in the Ccp1^{Vps75}-GFP levels at centromeres in the *rtt109*Δ mutant, as shown in Figure 3.5. However, the observed decrease is not statistically significant. Therefore, all of the results suggest that in fission yeast Rtt109 and Ccp1^{Vps75} do have independent functions, in contrast to what has been reported in budding yeast.

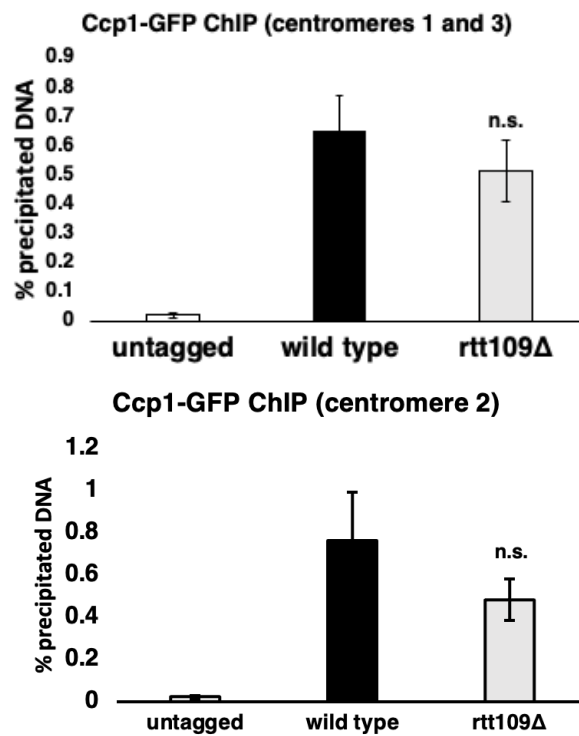


Figure 3.5: Rtt109 is not required for Ccp1^{Vps75}'s localisation at the centromere. ChIP comparing Ccp1^{Vps75}-GFP levels at *S. pombe* centromeres 1 and 3 in the wild type and *rtt109*Δ cells expressing Ccp1^{Vps75}-GFP. Error bars represent the standard error of the mean. N = 5.

3.3 Discussion

The evidence from budding yeast has shown that the histone acetyltransferase Rtt109 is involved in the acetylation of histone H3 at lysines 9, 27 and 56. The K56 acetylation is of particular interest because of its location in the globular domain of the histone H3 where the DNA entry and exit point is located on the nucleosome[279, 288–291].

The K56 acetylation on histone H3 has also been found to play a role in the resistance to DNA damage[5]. If there are DNA breaks during the DNA replication, budding yeast histone H3 maintains acetylation on K56 in a DNA damage checkpoint-dependent fashion.

Therefore in budding yeast the acetylation of histone H3 on K56 is crucial in DNA damage response as the cells that do not have the ability to acetylate histone H3 on K56 have been shown to be hypersensitive to genotoxic agents[292–294].

Budding yeast Rtt109 was found to interact with two H3/H4 histone chaperones *in vivo*, Asf1 and Vps75^{Ccp1}, and *in vitro* that the acetylation of histone H3 in *S. cerevisiae* was increased when either Asf1 or Vps75^{Ccp1} were added[279, 288], while *in vivo* both Rtt109 and Asf1 have been found to be essential for acetylation of histone H3 at K56, and Vps75^{Ccp1} was not[6].

Assays comparing the sensitivity to genotoxic agents have also found budding yeast cells lacking Rtt109, Asf1 or H3K56 to be hypersensitive to the genotoxic drugs, however cells lacking Vps75^{Ccp1} were not found to be sensitive[279, 288].

Furthermore, when the levels of Rtt109 in budding yeast cells harbouring the *vps75*Δ mutation were examined, it was found that the levels of Rtt109 have dropped in absence of Vps75^{Ccp1}[295]. This could suggest that Vps75^{Ccp1} acts as a chaperone for Rtt109 and plays a role in stabilising it, as well as protecting it from degradation.

When acetylation of *S. cerevisiae* histone H3 was examined, it was found that while acetylation of K9 and K27 was primarily performed by Gcn5, another histone acetyltransferase, in *gcn5* Δ cells Rtt109 has also been shown to acetylate K9 and K27 of histone H3[295].

What is particularly interesting is that in contrast to Rtt109 acetylation of K56, the acetylation of K9 and K27 in budding yeast by Rtt109 is dependent on Vps75^{Ccp1}. Furthermore, when combined a deletion of Gcn5, the deletion of either Rtt109 or Vps75^{Ccp1} results in a complete loss acetylation of K9 and K27 on histone H3, causing a severe growth defect[295, 296].

With the above findings in mind, it is possible to envision two feasible explanations for the fact that, in budding yeast, Vps75^{Ccp1} is crucial for one aspect of the histone acetyltransferase activity of Rtt109 (namely the acetylation of K9 and K27 of histone H3) and not for another (namely the acetylation of Rtt109's primary target - K56 of histone H3).

First of all, it is possible that Vps75^{Ccp1} acts as an Rtt109 chaperone and stabilises it. Therefore, when Vps75^{Ccp1} is deleted the degradation rate of Rtt109 increases and the levels of Rtt109 drop to levels that are sufficient only to sustain the acetylation activity of Rtt109's primary target, K56.

On the other hand, it is also possible to envision a role for Vps75^{Ccp1} which promotes, or perhaps regulates, the acetylation of K9 and K27 on histone H3 by Rtt109. As the ortholog of Vps75^{Ccp1} Nap1 is known to promote nuclear import of other proteins, it is possible that Vps75^{Ccp1} also has a nuclear localisation sequence which could aid the import of Rtt109 into the nucleus when the two proteins bind.

In this thesis it has been shown that in *S. pombe* Rtt109 may not be essential for the function of Ccp1^{Vps75}, in contrast to what has been previously reported in *S. cerevisiae*[6]. As demonstrated in TBZ assays of *ccp1* Δ , *rtt109* Δ and *ccp1* Δ *rtt109* Δ mutants, while both single mutants are sensitive to the drug, the double

mutants have been found to be hypersensitive to TBZ (shown in Figure 3.1).

If Ccp1^{Vps75} and Rtt109 form a complex that maintains functional centromeres deletion of either of the genes would disrupt the complex and would have the same effect as deleting both genes. However, the increased sensitivity to TBZ of the double mutant could be due to Rtt109 having other interactions in addition to the one with Ccp1^{Vps75}.

Therefore, Ccp1^{Vps75} and Rtt109 likely do not work together in fission yeast as they do in budding yeast. However, it is possible that they are a part of a larger pathway regulating chromosome segregation as suggested by the hypersensitivity of *ccp1*Δ *rtt109*Δ cells to TBZ.

In agreement with previous studies in both fission and budding yeast, this study has also found *rtt109*Δ cells to be hypersensitive to genotoxic agents hydroxyurea and methyl methanesulphonate (see Figure 3.2).

Moreover, this study has found *S. pombe* cells harbouring *ccp1*Δ mutation, which agrees with findings from *S. cerevisiae*. This confirms one similarity between the *S. cerevisiae* Vps75 and *S. pombe* Ccp1 in two distantly related yeasts.

Previous fission yeast studies have also found that Ccp1^{Vps75}'s activity in regulating the nucleosomal epigenetic stability does not depend on Rtt109[4].

However, the data presented also suggests that, while it is not essential, Rtt109 may promote the function of Ccp1^{Vps75} in *S. pombe* as a small drop in Ccp1^{Vps75} levels is observed in *rtt109*Δ mutants (as shown in Figures 3.3, 3.4, 3.5).

It is important to note that the observed decrease in Ccp1^{Vps75}-GFP levels in *rtt109*Δ cells is not statistically significant and that, in contrast to what has been reported in budding yeast, fission yeast Rtt109 and Ccp1^{Vps75} have separate functions and may not be true functional orthologs.

Many roles of Rtt109 in budding yeast have already been established and its im-

portance for the acetylation of histone H3 at K9, K27 and K56 and, subsequently, resistance to genotoxic agents is well known.

However, in fission yeast the interplay of Ccp1^{Vps75} and Rtt109 is not as clear cut and well researched as in budding yeast and remains an exciting area of exploration for researchers.

Chapter 4

Investigation of the role of Ccp1^{Vps75} and Rtt109 in Cnp1^{CENP-A} loading at the centromere

4.1 Introduction

Ccp1^{Vps75} is a NAP (Nucleosome Assembly Protein) family protein. A recent study proposes that Ccp1^{Vpa75} antagonises Cnp1^{CENP-A} loading not only at the centromere, but also at non-centromeric regions, thus maintaining the Cnp1^{CENP-A} levels at the centromere as well as preventing ectopic centromere assembly[3]. It directly interacts with Cnp1^{CENP-A} by physically associating to it, and its recruitment to the centromere is Mis16-dependent.

Some structural analyses of Ccp1 suggest that it forms a homodimer and that the homodimer is required for the anti-Cnp1^{CENP-A} loading activity[3]. However, other researchers report a tetrameric structure for *S. cerevisiae* Vps75[272, 273].

Overexpression of Ccp1^{Vps75} in fission yeast wild type cells has been found to

evict CENP-A from native centromeres. In fact, in this study the single CENP-A-GFP focus was lost from 76% of centromeres, and cells overexpressing Ccp1^{Vps75} were also shown to be highly sensitive to TBZ[3].

Ccp1 was identified in a genome-wide screen for non-essential genes that act through the central Cnp1^{CENP-A} chromatin domain of centromeres (cnt). Dr Subramanian has found that Ccp1 is required to maintain Cnp1^{CENP-A} levels at the centromere, and that there is a synthetic interaction between *ccp1*Δ and *cnp1-1* (unpublished findings). Further research has also found that Ccp1 localises to centromeres[3].

Deleting *ccp1* has been reported to cause different effects - some researchers find that these deletion mutants have multiple or diffuse Cnp1^{CENP-A}-GFP foci[3]. Meanwhile others found that Cnp1^{CENP-A}-GFP remains as a single focus in the deletion mutant[4]. This is one of the questions this chapter aims to answer.

Furthermore, the work done previously in the Subramanian lab indicates that Cnp1^{CENP-A} levels decrease in the *ccp1*Δ single mutant, in contradiction with the study by Dong et al.[3]. For this reason this chapter aims to explore the role of Ccp1 further and establish its role in the context of Cnp1^{CENP-A} loading and maintenance.

4.2 Results

4.2.1 *ccp1* Δ shows increased de-silencing at the centromere

Temperature sensitivity assays were used to investigate the genetic interaction between Cnp1^{CENP-A} and Ccp1^{Vps75} and Rtt109, and the results are shown in Figure 4.1.

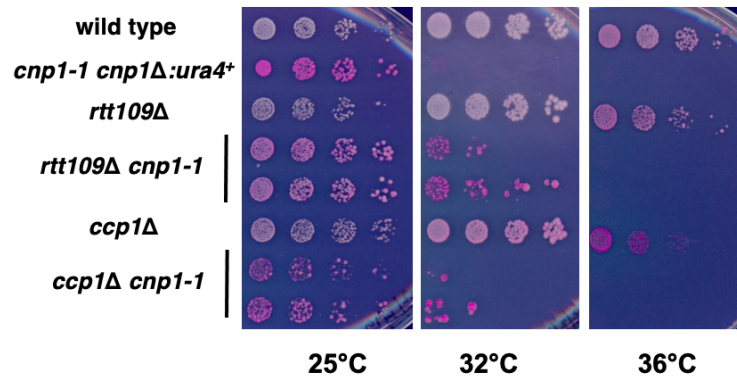


Figure 4.1: Temperature sensitivity assay comparing the viability of *ccp1* Δ and *rtt109* Δ mutants in either the *cnp1-1 cnp1* Δ :*ura4*⁺ or the wild type background. *ccp1* Δ and *rtt109* Δ cells survive at the restrictive temperature, however all cells containing the *cnp1-1* mutation do not survive at the restrictive temperature. Serial dilutions of cells of the indicated genotypes were plated on YES media supplemented with Phloxin B and incubated at indicated temperatures.

As shown in Figure 4.1 all cells with the *cnp1-1* mutation die at 36°C. At 32°C the *ccp1* Δ *cnp1-1* mutants are less viable than the *rtt109* Δ *cnp1-1* mutants, however the *cnp1-1* wild type strain is extremely temperature sensitive and not viable even at semi-restrictive temperature. Because of this it is not possible to confirm whether there is a genetic interaction between the *cnp1*, *ccp1* and *rtt109* genes. At 32°C the deletion of *rtt109* Δ appears to partially rescue the *cnp1-1* phenotype, however this was not consistently found in the repeats of the temperature sensitivity assays. For this reason it is not possible to conclude whether the absence of Rtt109 really does rescue the extreme temperature sensitivity exhibited by the strains harbouring the *cnp1-1* deletion.

As the temperature sensitivity assays could not have been used to determine whether

there is a genetic interaction between *cnp1*, *ccp1* and *rtt109*, the project aimed to establish whether Ccp1^{Vps75} and Rtt109 have a role to play in Cnp1^{CENP-A} deposition at the centromere.

To indirectly determine Cnp1^{CENP-A} levels at the centromere in *ccp1*Δ, *rtt109*Δ and *ccp1*Δ *rtt109*Δ compared to wild type cells, a centromere silencing assay was set up, and the results are shown in Figure 4.2. An illustration showing the position of the *arg3* gene in the central centromeric core in strains used in centromere silencing assays is shown in Figure 1.2.

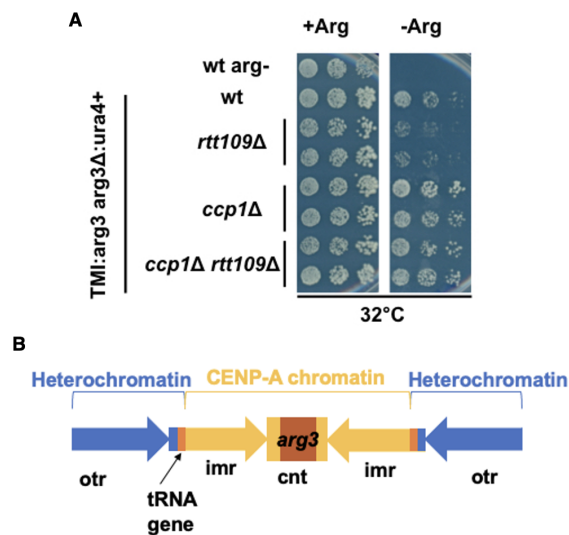


Figure 4.2: **(A)** *ccp1*Δ and *ccp1*Δ *rtt109*Δ show de-silencing, while *rtt109*Δ shows enhanced silencing at the centromere. Serial dilutions of cells of the indicated genotypes were plated on PMG media either supplemented with or without arginine and incubated at 32°C. **(B)** The position of the *arg3* gene in the central centromeric core. Imr = innermost repeats, otr = outermost repeats, cnt = central centromeric core.

*ccp1*Δ and *ccp1*Δ *rtt109*Δ mutants show higher levels of de-silencing at the centromere compared to wild type cells, indicating a decrease in Cnp1^{CENP-A} levels at centromeres. In contrast to this, the *rtt109*Δ mutant shows enhanced silencing at the centromere compared to the wild type cells.

The results therefore suggest that Ccp1^{Vps75} may play a role in Cnp1^{CENP-A} loading as in its absence the Cnp1^{CENP-A} levels decrease. In the absence of Rtt109, on the other hand, there is an increase in transcriptional silencing at the centromere. This

could be due to Rtt109 being involved in exchange of histone H3 with Cnp1^{CENP-A} during DNA replication.

4.2.2 In *ccp1* Δ mutant there is a decrease of GFP-Cnp1^{CENP-A} foci at the centromere

To further investigate the effect of deleting *ccp1* and *rtt109* on Cnp1^{CENP-A}, strains expressing Cnp1^{CENP-A} which has been N-terminally tagged with GFP in wild type, *ccp1* Δ and *rtt109* Δ backgrounds were imaged using a fluorescence microscope as described in Chapter 2, and the representative images have been shown in Figure 4.3.

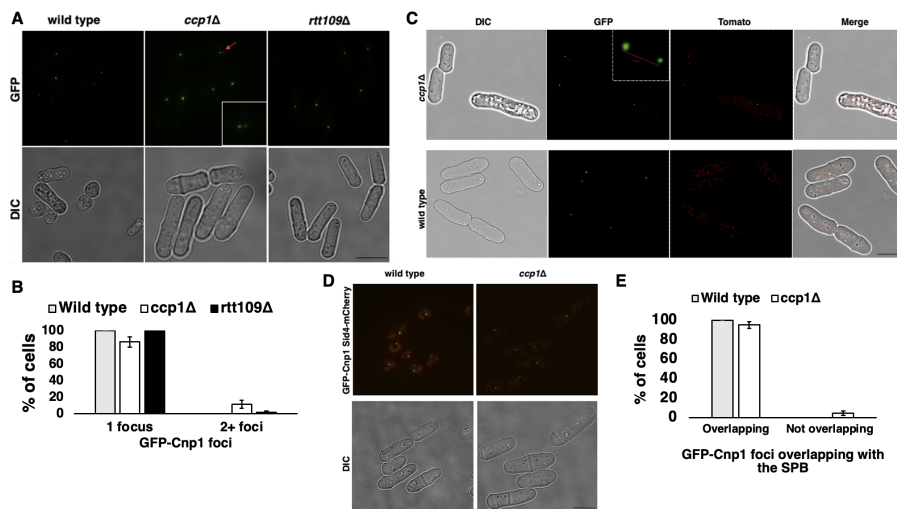


Figure 4.3: **(A)** Live images of wild type, *rtt109* Δ , and *ccp1* Δ cells expressing GFP-Cnp1^{CENP-A}. Scale bar = 5 μ m. Red arrow points to declustered centromeres, the magnified image of which is shown in the insert. **(B)** A bar chart comparing the number of GFP-Cnp1^{CENP-A} foci in the imaged strains. N = 3. Error bars represent the standard deviation. **(C)** Live images of wild type and *ccp1* Δ cells expressing GFP-Cnp1^{CENP-A} and Sid4-Tomato. Scale bar = 5 μ m. The distance between the two GFP-Cnp1^{CENP-A} foci was measured as 1.70 μ m, and the magnified image of these foci is shown in the insert. **(D)** Live images of wild type and *ccp1* Δ cells expressing GFP-Cnp1^{CENP-A} and Sid4-mCherry. Scale bar = 5 μ m. **(E)** A bar chart comparing the number of cells in which the GFP-Cnp1^{CENP-A} foci and the Sid4-mCherry foci overlap in the imaged strains. N = 3. Error bars represent the standard deviation.

Wild type cells have a single GFP-Cnp1^{CENP-A} focus due to the clustered centromeres of non-mitotic cells. The most significant effect on the number of GFP-Cnp1^{CENP-A} foci was observed in the *ccp1* Δ mutant. Microscopy also suggests that there is a decrease in the number of cells with a single GFP-Cnp1^{CENP-A} focus, as well as an increase in the number of cells with more than one GFP-Cnp1^{CENP-A} focus

in the *ccp1*Δ mutant. These cells are also larger than the wild type and *rtt109*Δ cells - it is possible that these cells are diploid and therefore elongated and larger. No additional experiments were done to check if *ccp1*Δ mutants' cell cycle is modified.

To gain a deeper understanding of the imaging data, the number of cells which did and did not show a single GFP-Cnp1^{CENP-A} focus was quantified and is presented in Figure 4.3.

The quantification of the imaging experiments suggests that the *rtt109*Δ mutant exhibits the smallest effect on the GFP-Cnp1^{CENP-A} foci. This suggests that Rtt109 is not required for the deposition of Cnp1^{CENP-A} at the centromere, while Ccp1^{Vps75} likely plays a role in this process.

As indicated in Figure 4.3, in *ccp1*Δ cells it is possible to see more than one GFP-Cnp1^{CENP-A} focus. It is possible that this mutation may cause defective centromeric clustering as a single GFP-Cnp1^{CENP-A} focus is expected due to the clustering of the three centromeres.

To look into this further, strains previously used in imaging experiments where the multiple Cnp1^{CENP-A} foci were first observed were crossed with a strain with a spindle pole body (SPB) marker, Sid4[297, 298] labelled with the Tomato fluorescent protein, in the wild type background.

Through this strains expressing GFP-Cnp1^{CENP-A} Sid4-Tomato in the wild type and *ccp1*Δ background were acquired. These strains were imaged on the Deltavision Elite, and on the Leica Stellaris super-resolution systems, however the Sid4-Tomato signal has been found to be very faint.

This was especially problematic on the Deltavision microscope, so the same strains were re-made using mCherry as the fluorescent marker. However, using the strains expressing GFP-Cnp1^{CENP-A} and Sid4-Tomato it was still possible to capture the declustered centromeres in the *ccp1*Δ mutant on the Leica STED super-resolution microscope that was being tested by Prof. Draviam's group, and the distance between two GFP-Cnp1^{CENP-A} foci was measured at 1.70 μm.

Live cell imaging was also repeated on the Deltavision Elite microscope using the strains expressing GFP-Cnp1^{CENP-A} and Sid4-mCherry. The images are presented in Figure 4.3

A single GFP-Cnp1^{CENP-A} focus is expected in cells as the three centromeres cluster together at the SPB. As centromeres cluster at the SPB, the distance between the fluorescent signals can be used as an indicator of whether the centromeres are clustering as expected.

As indicated in Figure 4.3, in the *ccp1*Δ mutant the centromere clustering appears to be defective as more than one GFP-Cnp1^{CENP-A} focus can be observed. In addition, the GFP-Cnp1^{CENP-A} signals do not always overlap with the Sid4-Tomato or Sid4-mCherry signals, suggesting that in the *ccp1*Δ mutant the centromeres may not always cluster at the SPB as expected. However, it is important to note that this experiment does not show that the GFP-Cnp1^{CENP-A} foci observed not clustering at the SPB are centromeres. Further experiments, e.g. using fluorescence in situ hybridisation (FISH), are needed to check if the observed multiple foci of GFP-Cnp1^{CENP-A} are due to ectopic GFP-Cnp1^{CENP-A} or if they are indeed centromeres.

To validate the results obtained with fluorescence microscopy and centromere silencing assays, as well as to measure the effects of *ccp1* and *rtt109* deletion on Cnp1^{CENP-A} more directly, ChIP was used to determine the Cnp1^{CENP-A} levels at the centromere.

In this experiment, non-tagged Cnp1^{CENP-A} strains were used, in wild type, *ccp1*Δ and *rtt109*Δ backgrounds. The results are shown in Figure 4.4 below.

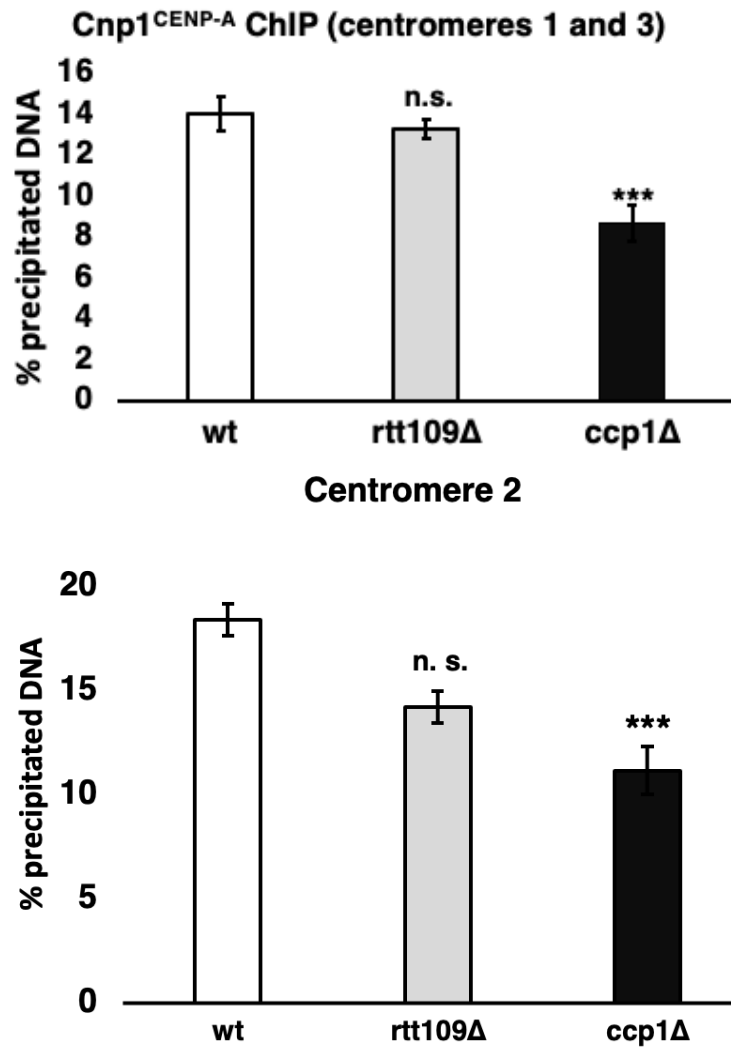


Figure 4.4: ChIP comparing Cnp1^{CENP-A} levels at *S. pombe* centromeres in the wild type, *ccp1*Δ and *rtt109*Δ cells. Error bars represent the standard error of the mean. The drop in the Cnp1^{CENP-A} abundance in the *ccp1*Δ mutant was found to be significant at *p* values less than 0.001 using Student's t-test.

As shown in Figure 4.4, ChIP experiments show that there is a significant decrease in Cnp1^{CENP-A} levels in the *ccp1*Δ mutant, whereas the changes in Cnp1^{CENP-A} levels in the *rtt109*Δ mutant were not significant. These results further suggest that Ccp1^{Vps75} aids Cnp1^{CENP-A} deposition at the centromere, and that Rtt109 is not required for this process.

ChIP was also used to measure the centromeric histone H3 levels to validate the results obtained by previous ChIP experiments which measured centromeric Cnp1^{CENP-A} levels. If levels of Cnp1^{CENP-A} decrease, the corresponding levels of histone H3 increase, so these experiments were performed to compliment the Cnp1^{CENP-A} ChIPs. The same strains that were used in the Cnp1^{CENP-A} ChIP were used for these experiments. Results are shown in Figure 4.5 below.

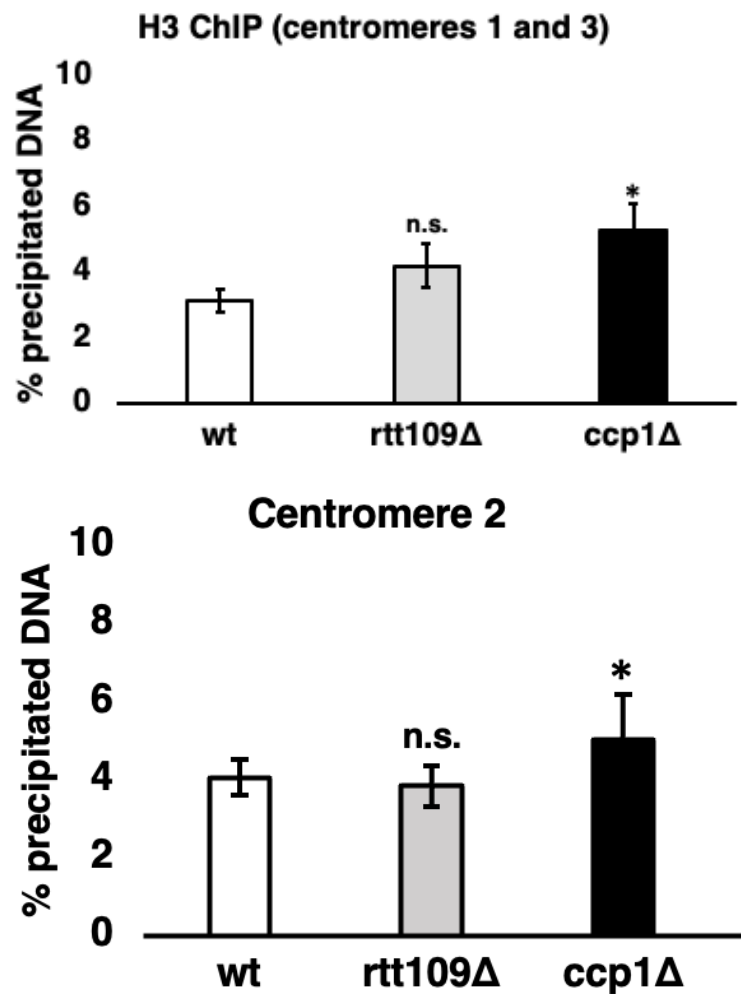


Figure 4.5: ChIP comparing histone H3 levels at *S. pombe* centromeres in the wild type, *ccp1*Δ and *rtt109*Δ cells. Error bars represent the standard error of the mean. The increase in the histone H3 levels in the *ccp1*Δ mutant was found to be significant at *p* values less than 0.05 using Student's t-test.

As shown in Figure 4.5, histone H3 levels in the *ccp1*Δ mutant increase compared to wild type levels.

This provides further support for the results obtained from the centromere si-

lencing assays and the Cnp1^{CENP-A} ChIP, which indicate that in the absence of Ccp1^{Vps75} the levels of Cnp1^{CENP-A} at the centromere decrease. Furthermore, the results presented in Figures and 4.4 and 4.5 suggest that Rtt109 is not involved in Cnp1^{CENP-A} deposition at the centromere.

4.3 Discussion

Previous studies in fission yeast have found Ccp1^{Vps75} to localise to central core of the centromere. Furthermore, it has been established that Ccp1^{Vps75}'s localisation to the centromere is cell-cycle dependent, with Ccp1^{Vps75}-GFP forming a single focus in interphase (but not in mitosis) at the edge of the nucleus[3, 4].

It has also been found that the Ccp1^{Vps75}-GFP signal co-localises with the SPB signal, which shows that Ccp1^{Vps75} is enriched at centromeres. This is supported by the findings from experiments using ChIP-Seq which show that Ccp1^{Vps75} associates exclusively to the central centromeric core region[4].

As shown in Figure 4.3, in wild type cells the GFP-Cnp1^{CENP-A} signal does co-localise with the SPB signal, however in the *ccp1*Δ mutant it can be observed that the two signals do not overlap in a portion of cells, indicating that the centromere clustering in the absence of Ccp1^{Vps75} is defective and that Ccp1^{Vps75} may therefore be involved in this process, whether it is through a direct interaction with Cnp1^{CENP-A} (as the two proteins have been found physically associate in yeast two-hybrid, co-immunoprecipitation and mass spectrometry experiments as well as in *in vitro* binding assays[3]) or through a different mechanism altogether.

To delve deeper into the relationship between Ccp1^{Vps75}, Rtt109 and Cnp1^{CENP-A} this study used temperature sensitive mutant of Cnp1^{CENP-A}, *cnp1-1*, the *ccp1*Δ, *rtt109*Δ and the double mutants *cnp1-1 rtt109*Δ and *cnp1-1 ccp1*Δ.

Both the single *cnp1-1* and the double *cnp1-1 rtt109*Δ and *cnp1-1 ccp1*Δ mutants have been found to be unviable at the restrictive temperature of 36°C (Figure 4.1). Indeed, as the single *cnp1-1* is unviable even at the semi-restrictive temperature it was not possible to make any conclusions on the potential genetic interactions between *cnp1*, *rtt109* and *ccp1*.

Previous assays of *cnp1-1 ccp1*Δ mutants have revealed that this mutant is severely

impaired at the semi-restrictive temperature (32°C) and unviable at the restrictive temperature (36°C), suggesting a synthetic interaction between *ccp1* and *cnp1* [3].

While the results from this study show that the double mutant is inviable at both the semi-restrictive and restrictive temperatures, due to the issues with the single *cnp1-1* mutant it was not possible to draw any conclusions from the temperature sensitivity assays.

The role of Ccp1^{Vps75} in centromeric Cnp1^{CENP-A} loading is still somewhat opaque, with some researchers reporting that it is an anti-Cnp1^{CENP-A} loading factor as they observe multiple or diffuse foci of Cnp1^{CENP-A}-GFP in *ccp1*Δ mutants [3]. On the other hand, some researchers find that Cnp1^{CENP-A}-GFP remains as a single focus in *ccp1*Δ mutants [4].

The data presented in this chapter suggests that deletion of Ccp1^{Vps75} affects Cnp1^{CENP-A} levels at centromeres (Figures 4.2, 4.3, 4.4).

Interestingly, a small increase in the number of cells exhibiting multiple GFP-Cnp1^{CENP-A} foci in the *ccp1*Δ mutant was also observed. This is in agreement with what has previously been observed for GFP-Cnp1^{CENP-A} in the *ccp1*Δ mutant [3], which could be due to centromere clustering defects in the *ccp1*Δ mutant.

Normally, centromeres cluster at the spindle pole body giving a single GFP-Cnp1^{CENP-A} focus. However, Ccp1^{Vps75} may be involved in regulating this process, so the mutants lacking Ccp1^{Vps75} could have defective centromere clustering.

In contrast to this, the authors of a previous study hypothesise that the occurrence of multiple Cnp1^{CENP-A}-GFP foci in the *ccp1*Δ mutant is not due to defective centromere clustering but rather due to the role of Ccp1^{Vps75} at the centromere. The authors of this study believe that Ccp1^{Vps75} is a Cnp1^{CENP-A} anti-loading factor and that therefore in its absence GFP-Cnp1^{CENP-A} localises to non-centromeric regions causing several GFP-Cnp1^{CENP-A} foci to be observed [3].

The authors further suggest Cnp1^{CENP-A}-GFP levels at the centromere remain unchanged[3], which is in stark contrast to the results presented in this study. It is possible that the use of C-terminally tagged Cnp1^{CENP-A} has affected the results as it is well established that the addition of tags on the C-terminus of Cnp1^{CENP-A} impairs the protein in fission yeast, as well as other organisms[89, 138, 209, 299, 300].

Furthermore, the author of this study has found that even the use of N-terminally Cnp1^{CENP-A}, which is preferable, in ChIP experiments is problematic and produces unreliable results. However, Dong et al. used gel images to quantify the ChIP results, rather than qPCR, so it is possible that this method of quantification was not sensitive enough to detect any change in Cnp1^{CENP-A} levels.

As suggested by the centromere silencing assay results shown in Figure 4.2 which are supported by results from anti-Cnp1^{CENP-A} and anti-H3 ChIPs shown in Figures 4.4 and 4.5, the levels of centromeric Cnp1^{CENP-A} decrease in the absence of Ccp1^{CENP-A}. This leads to the conclusion that Ccp1^{Vps75} is in fact a Cnp1^{CENP-A} *loading* factor, rather than working to remove Cnp1^{CENP-A} from the centromere.

Interestingly, when using epistasis mapping to study the function of Ccp1^{Vps75} it has been found that Ccp1^{Vps75} is associated with the DASH complex. Indeed, double mutants *ccp1* Δ *ask1* Δ and *ccp1* Δ *dad2* Δ have been shown to be hypersensitive to TBZ.

Mutants of Ccp1^{Vps75} and kinetochore components, such as Mis6^{CENP-I}, also exhibit hypersensitivity to TBZ and Ccp1^{Vps75} and Mis6^{CENP-I} have also been found to depend on one another to localise correctly[3, 4]. These findings support the hypothesis that Ccp1^{Vps75} is needed for proper centromere and kinetochore function.

These findings could also offer insight into the missing link between the recruitment of HJURP^{Scm3} by the Mis18 complex and the loading of Cnp1^{CENP-A} at the centromere.

In a somewhat different vein, *ccp1*Δ mutants have been found to have a small presence of heterochromatin in the central centromeric core and has been implicated in the regulation of H3K9me2 levels at small heterochromatin islands[4]. Therefore, a role for Ccp1^{Vps75} in maintaining the boundary between the pericentromeric heterochromatin and the centromere core has also been implied.

There is also data indicating that Ccp1^{Vps75} aids the incorporation of the proteins of the inner kinetochore, Mis6^{CENP-I} and Sim4^{CENP-K}. However, in a temperature sensitive mutant of Mis6^{CENP-I}, *mis6-302* the recruitment of Ccp1^{Vps75} is impaired, suggesting that there is interdependence between the inner kinetochore and Ccp1^{Vps75}. It is, however, important to keep in mind that Ccp1^{Vps75} is not localised at the centromere during mitosis, and therefore is not a constitutive kinetochore element.

TBZ sensitivity assays presented in Chapter 3 indicate that there are chromosome segregation defects in the *ccp1*Δ mutant, which could be due to a decrease in Cnp1^{CENP-A} levels at the centromere. These results therefore reinforce the idea that Ccp1^{Vps75} is a Cnp1^{CENP-A} loading factor, rather than a factor that antagonises Cnp1^{CENP-A} loading, as suggested by Dong et al.[3].

However, due to the fact that it is possible to delete *ccp1*, it is expected that Ccp1^{Vps75}, while it is a Cnp1^{CENP-A} loading factor, is not crucial for Cnp1^{CENP-A} deposition at the centromere; otherwise its deletion would be lethal.

The *rtt109*Δ mutant exhibits the smallest effect on the GFP-Cnp1^{CENP-A} levels - there is a very small decrease in the number of cells with GFP-Cnp1^{CENP-A} foci. This result suggests that Rtt109 is not crucial for the deposition of Cnp1^{CENP-A} at the centromere.

It has been found that post-translational modifications of histone H3 have an important role to play in the assembly of Cnp1^{CENP-A} and Rtt109 is a histone acetyltransferase[142, 301]. With the above in mind, it is quite interesting that in all of

the experiments conducted in the course of this project Rtt109 does not appear to have a role to play in Cnp1^{CENP-A} deposition at the centromere, as indicated by results presented in Figures 4.3, ??, 4.4, 4.5 as well as Chapter 3.

Another interesting finding on the potential role of Rtt109 in the dynamics of Cnp1^{CENP-A} is the fact that *rtt109*Δ mutants show enhanced silencing at the centromere as presented in Figure 4.2. A possible explanation for this observation is that Rtt109 could be involved in exchange of histone H3 with Cnp1^{CENP-A} during DNA replication. This has already been suggested by previous studies in *S. cerevisiae* so it is possible that a similar process takes place in *S. pombe*[302].

When the findings presented in this thesis are considered with the findings from previous studies of the role of Ccp1^{Vps75} it appears that Ccp1^{Vps75} has multiple roles - it maintains the boundary between pericentromeric heterochromatin and the central centromeric core, aids kinetochore assembly, and aids the Cnp1^{CENP-A} deposition - although this remains a somewhat open question.

As noted above, there is a study arguing that Ccp1^{Vps75} is an anti-Cnp1^{CENP-A} loading factor[3] while other authors[4], including the author of this thesis, put forward the idea that its role is to aid the exact opposite. Additionally, Ccp1^{Vps75} may also be involved in modulating the epigenetic stability at non-centromeric loci.

Chapter 5

Investigation of the interaction between Ccp1^{Vps75} and Cnp20^{CENP-T} in the context of Cnp1^{CENP-A} loading

5.1 Introduction

An interacting partner of Ccp1^{Vps75}, identified by Dr Subramanian in an immunoprecipitation experiment followed by LC-MS/MS, is Cnp20^{CENP-T}, a CCAN protein (unpublished data).

Cnp20^{CENP-T} is part of the CENP-TWSX tetramer, in which all subunits have histone fold domains. It is thought that the CENP-TWSX complex forms a nucleosome-like structure which flanks CENP-A nucleosomes at the centromere[65].

Cnp20^{CENP-T} has been found to be important in promoting epigenetic stability of centromeres in fission yeast and that cooperation of Cnp20^{CENP-T} and Cnp1^{CENP-A} is important for stable centromere inheritance[10], as the N-terminus of Cnp1^{CENP-A} recruits Cnp20^{CENP-T}.

A recently published study has shown that Ccp1^{Vps75} needs Cnp20^{CENP-T} to be correctly localised to the centromere. The same study also proposes that Ccp1^{Vps75} binds Cnp20^{CENP-T}'s N terminus through what the authors dub the Ccp1 interaction motif (CIM). CIM was found to be proximal to the motif binding Ndc80 in this study[66].

Furthermore, deletion of the CIM domain of Cnp20^{CENP-T} produces the same phenotype as deleting Ccp1^{Vps75} itself. and that phosphorylation of the CIM domain by CDK1 leads to a weaker interaction with Cnp20^{CENP-T}. Interestingly, the authors also suggest a competition between Ccp1^{Vps75} and Ndc80 for binding of the N terminus of Cnp20^{CENP-T}[66].

While previous studies have explored Cnp20^{CENP-T}'s role at the centromere, the nature of its interaction with Ccp1 remains somewhat unknown - even though there are studies showing that Cnp20^{CENP-T} is required for Ccp1^{Vps75}'s localisation at the centromere, this has not been replicated by any other research group and it is not known which part(s) of Ccp1^{Vps75}'s structure mediate the interaction with Cnp20^{CENP-T}.

5.2 Results

5.2.1 Deleting *ccp1* affects Cnp20^{CENP-T} levels at the centromere

To investigate the interaction between Ccp1^{Vps75} and Cnp20^{CENP-T}, Cnp20^{CENP-T}-GFP levels at centromeres in wild type and *ccp1*Δ backgrounds were investigated by fluorescence microscopy and the results are shown in Figure 5.1.

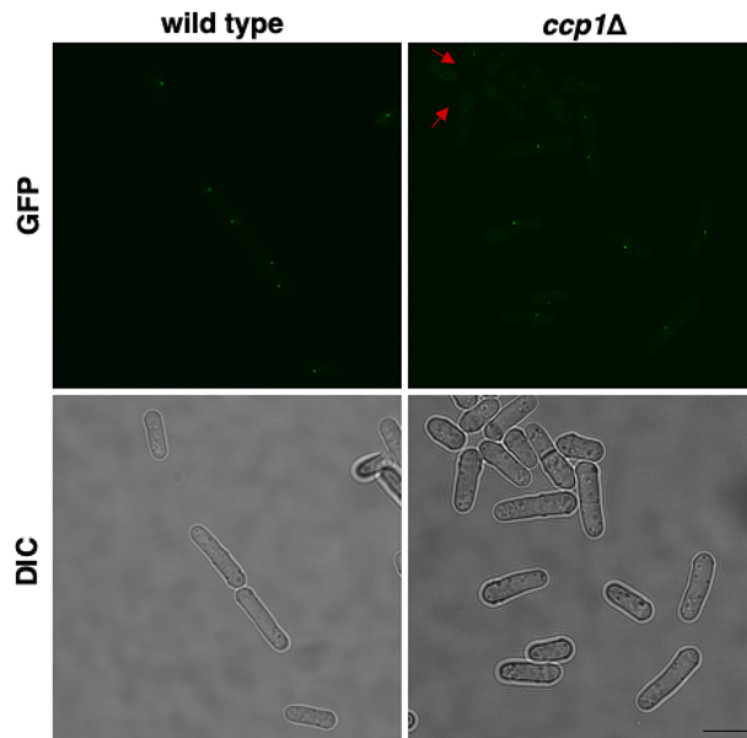


Figure 5.1: Live images of wild type and *ccp1*Δ cells expressing Cnp20^{CENP-T}-GFP. *ccp1*Δ show a decrease in the intensity of the Cnp20^{CENP-T} focus. Scale bar = 5 μm. Some of the cells where this can be observed are noted with a red arrow.

As shown in the Figure 5.1 above, in the *ccp1*Δ mutant, Cnp20^{CENP-T}-GFP foci show a decrease in intensity. As Cnp1^{CENP-A} ChIP results suggest that there is a decrease in the Cnp1^{CENP-A} levels in the *ccp1*Δ mutant, the decrease in Cnp20^{CENP-T}-GFP levels detected by ChIP could be due to the loss of Cnp1^{CENP-A} from the centromere and the effect that this has on the kinetochore proteins, rather than a direct interaction with Ccp1^{Vps75}.

In the previous chapter results suggesting that the centromere clustering may be

defective in the *ccp1*Δ cells (Figure 4.3). If the centromeres are declustered in this mutant, then the signal from declustered Cnp20^{CENP-T}-GFP may be more difficult to detect, leading to the signal appearing fainter.

To validate this finding and quantify the Cnp20^{CENP-T}-GFP levels at the centromere, ChIPs were performed. The same strains which were used for fluorescence microscopy in addition to an untagged wild type strain were also used for ChIPs and the results are shown in the Figure 5.2 below.

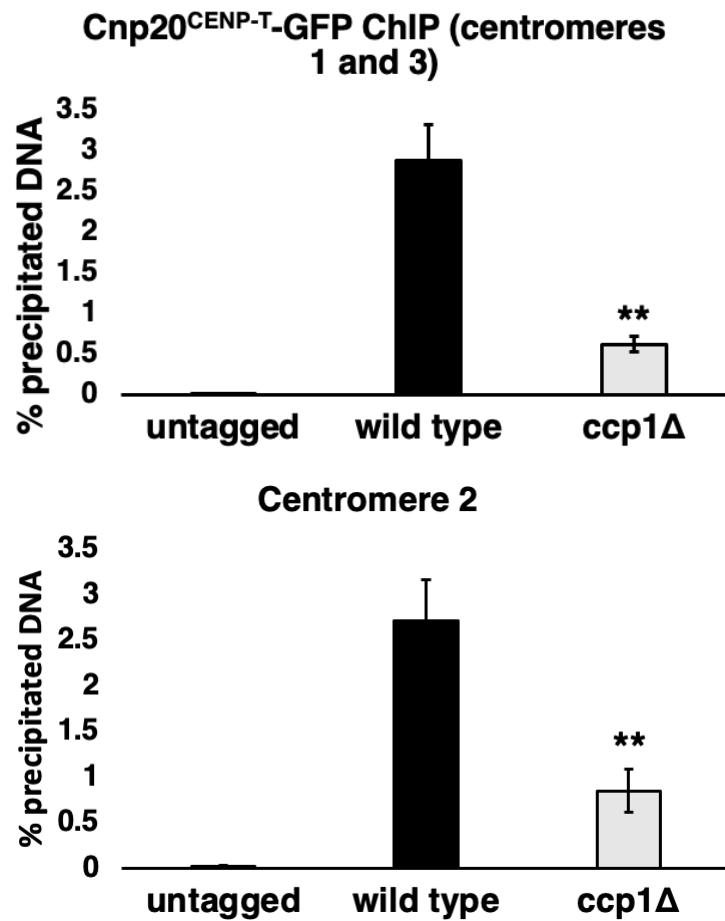


Figure 5.2: Deletion of Ccp1^{Vps75} results in a decrease in Cnp20^{CENP-T} levels at centromeres. ChIP comparing Cnp20^{CENP-T}-GFP levels at *S. pombe* centromeres in the wild type and *ccp1*Δ cells expressing Cnp20^{CENP-T}-GFP. Error bars represent standard error of the mean. The decrease in the Cnp20^{CENP-T}-GFP levels in the *ccp1*Δ mutant was found to be significant at *p* values less than 0.01 using Student's *t*-test.

Consistent with the findings from the microscopy experiment, there is a decrease in Cnp20^{CENP-T}-GFP levels at all centromeres in the *ccp1*Δ mutant.

5.2.2 The physical interaction between Ccp1^{Vps75} and Cnp20^{CENP-T}

To establish whether there is a direct physical interaction between Ccp1^{Vps75} and Cnp20^{CENP-T} immunoprecipitation followed by liquid chromatography and mass spectrometry (IP-LC/MS-MS) was used. The strains used for these experiments were the Ccp1^{Vps75}-GFP strain used in previous experiments in Chapter 3 and the untagged wild type fission yeast strain, also used previously for other experiments in Chapters 3 and 4.

When the experiment was first attempted, results presented in Table 5.1 below were obtained.

Table 5.1: Results obtained in an IP-LC/MS-MS experiment using the wild type fission yeast and Ccp1^{Vps75}-GFP strains. Accession numbers given in the table below refer to the UniProt database.

Identified protein	Accession number	Total spectrum count (wild type)	Total spectrum count (Ccp1 ^{Vps75} -GFP)
60S ribosomal protein L36-A	RL36A_SCHPO	1	1
Putative nucleosome assembly protein C36B7.08c (Ccp1)	YO48_SCHPO	0	3
40S ribosomal protein S18-B	RS18B_SCHPO	2	2
40S ribosomal protein S13	RS13_SCHPO	2	1
Coronin-like protein Crn1	CORO_SCHPO	0	1
60S ribosomal protein L23-B	RL23B_SCHPO	1	1
60S ribosomal protein L35	RL35_SCHPO	0	1
Glyceraldehyde-3-phosphate dehydrogenase 1	G3P1_SCHPO	0	1

The data obtained in the experiment shows an enrichment of Ccp1^{Vps75} in the

sample obtained from the immunoprecipitation of the Ccp1^{V_{ps75}}-GFP strain, which is expected, however, the rest of the identified proteins appear to be proteins that are simply abundant in the cell rather than specific interacting partners of Ccp1^{V_{ps75}}.

As the initial experiment was not successful, the mass spectrometry experiment was repeated and 287 proteins were identified. Of the 287 proteins, only twelve were from *S. pombe* (these are listed in the Table 5.2 below) and there were identified as histones (listed in the Table 5.3).

Table 5.2: Results obtained in an IP-LC/MS-MS experiment using the wild type fission yeast and Ccp1^{Vps75}-GFP strains. Accession numbers given in the table below refer to the UniProt database.

Identified protein	Accession number	Total spectrum count (wild type)	Total spectrum count (Ccp1 ^{Vps75} -GFP)
Putative nucleosome assembly protein C36B7.08c (Ccp1)	YO48.SCHPO	0	6
Glyceraldehyde-3-phosphate dehydrogenase 1	G3P1.SCHPO	9	4
Microtubule-associated protein Mug164	MU164.SCHPO	2	2
Phosphoglycerate kinase	PGK.SCHPO	2	2
40S ribosomal protein S18-B	RS18B.SCHPO	2	2
Pyruvate kinase	KPYK.SCHPO	1	4
60S ribosomal protein L31	RL31.SCHPO	1	0
60S ribosomal protein L36-A	RL36A.SCHPO	1	0
ADP-ribosylation factor 1	ARF1.SCHPO	3	0
60S ribosomal protein L12-A	RL12A.SCHPO	2	0
Cell division control protein 42 homolog	CDC42.SCHPO	2	0
Heat shock protein 90 homolog	HSP90.SCHPO	2	0

Table 5.3: Results obtained in an IP-LC/MS-MS experiment using the wild type fission yeast and Ccp1^{Vps75}-GFP strains. Accession numbers given in the table below refer to the UniProt database.

Identified protein	Accession number	Total spectrum count (wild type)	Total spectrum count (Ccp1 ^{Vps75} -GFP)
Histone H4 type VIII	H48_CHICK	6	2
Histone H2A type 1-C	H2A1C_RAT	8	3
Histone H2B type F-S	H2BFS_HUMAN	4	2

The results confirm enrichment of Ccp1^{Vps75} in the Ccp1^{Vps75}-GFP strain, which is expected. The rest of the proteins identified are largely the same proteins identified previously, which are not interacting partners of Ccp1^{Vps75}.

Three histones (H4, H2A, H2B) were identified as well, however these appear to be from different organisms and not *S. pombe*.

Because experiments using mass spectrometry did not prove successful, it was necessary to change the experimental approach to investigating the potential physical interaction between Ccp1^{Vps75} and Cnp20^{CENP-T}.

Co-immunoprecipitation followed by SDS-PAGE electrophoresis and Western blotting was performed using the strains expressing Ccp1^{Vps75}-GFP, Cnp20^{CENP-T}-FLAG or Ccp1^{Vps75}-GFP and Cnp20^{CENP-T}-FLAG. The α -FLAG M2 antibody and Dynabeads magnetic beads were used for immunoprecipitation followed by a Western blot using the Invitrogen α -GFP antibody. The results are shown in Figure 5.3 below.

As it can be seen in Figure 5.3, the resulting Western blot has a lot of background signal and that there appears to be interference from the IgG heavy chains. Therefore as it cannot be said with certainty that the detected bands are the proteins of interest, no conclusions about the potential physical interaction between Ccp1^{Vps75} and Cnp20^{CENP-T} could be made.

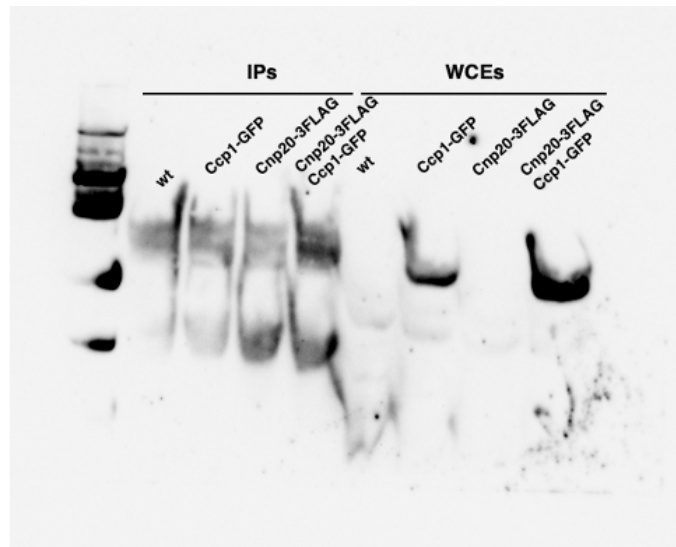


Figure 5.3: Co-IP of Ccp1^{Vps75}-GFP and Cnp20^{CENP-T}-FLAG. α -FLAG M2 antibody and Dynabeads were used for the immunoprecipitation, followed by a Western blot using the α -GFP antibody. The chemiluminescent signal was detected using BioRad Chemidocimaging system.

To attempt to fix this issue, in following experiments the antibody (either the Invitrogen α -GFP or the α -FLAG M2) was crosslinked to magnetic beads to minimise the interference from the IgG heavy chain and instead of using the conventional secondary antibodies Abcam VeriBlot was used as the secondary antibody, again to remove the IgG heavy chain interference as much as possible. The results are shown in Figures 5.4 and 5.5.

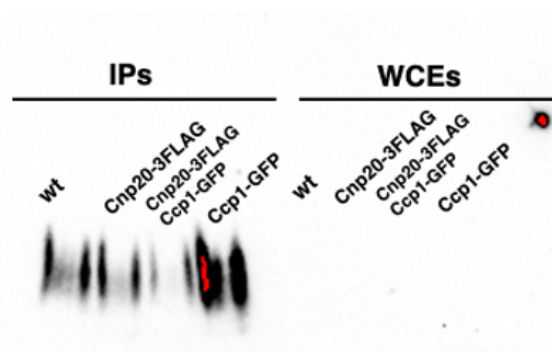


Figure 5.4: Co-IP of Ccp1^{Vps75}-GFP and Cnp20^{CENP-T}-FLAG. Invitrogen α -GFP antibody was crosslinked to Dynabeads and used for IP followed by a Western blot using α -FLAG M2 antibody and Abcam VeriBlot as the secondary antibody. The chemiluminescent signal was detected using Thermofisher iBright system.

While the Western blot shown in Figure 5.4 is much cleaner, it was still not possible to detect any specific bands - not just in the immunoprecipitates but also in the whole cell extracts. Using the α -GFP antibody for immunoprecipitation and the α -FLAG M2 antibody for the Western blot was abandoned as it has been found through such experiments that the detected bands are unspecific.

Finally, the co-IP was performed using α -FLAG M2 crosslinked to Dynabeads and α -GFP antibody for Western blotting. The results are shown in Figure 5.5 below.

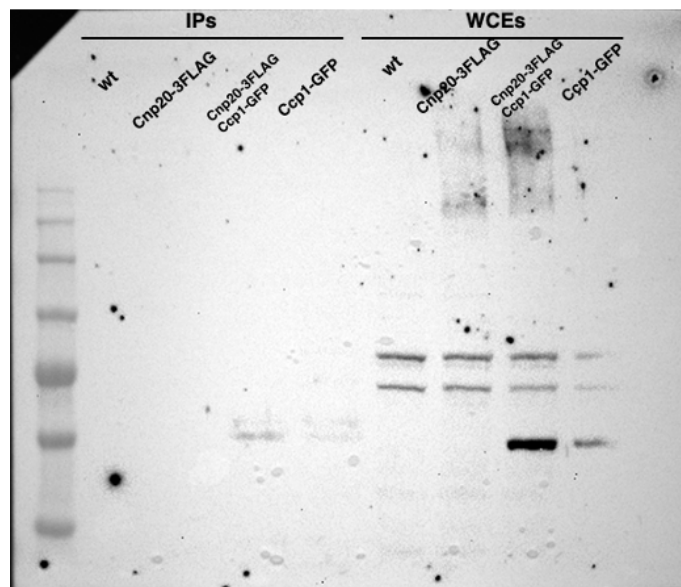


Figure 5.5: Co-IP of Ccp1^{Vps75}-GFP and Cnp20^{CENP-T}-FLAG. α -FLAG M2 antibody was crosslinked to Dynabeads and used for IP, followed by a Western blot using the Invitrogen α -GFP antibody and Abcam VeriBlot as the secondary antibody. The chemiluminescent signal was detected using Thermofisher iBright system.

In Figure 5.5 above a band corresponding to Ccp1^{Vps75}-GFP can be seen in the sample obtained by immunoprecipitation from the strain expressing Cnp20^{CENP-T}-FLAG Ccp1^{Vps75}-GFP, which may indicate that Ccp1^{Vps75} and Cnp20^{CENP-T} physically interact, possibly through the NAP domain of Ccp1^{Vps75}.

5.3 Discussion

CENP-T^{Cnp20} is an inner kinetochore protein and an essential part of the CCAN. It is essential for viability in higher eukaryotes as well as in fission yeast[303]. It has been found to serve as a platform for outer kinetochore assembly, namely as the platform upon which the Ndc80 complex is assembled during mitosis[65, 304–307]. The Ndc80 complex then mediates the microtubule attachments and acts as an interface between the kinetochore and microtubules[60, 308].

In addition, it has been found that CENP-T^{Cnp20} contains histone folds and interacts with CENP-W^{Wip1}, CENP-S^{Mhf1} and CENP-X^{Mhf2}, which all have histone folds too. The four proteins form the CENP-T-W-S-X complex *in vitro*, which is a heterotetrameric complex with a nucleosome-like structure[65, 309].

The CENP-T-W-S-X complex has also been shown to associate directly with the centromeric DNA. Indeed, the DNA binding of CENP-T-W-S-X has been shown to play a role in the formation of the kinetochore[65, 304]. The complex has also been shown to interact with histone H3 rather than CENP-A^{Cnp1}[304, 310].

Ccp1^{Vps75} is a NAP family protein and NAP proteins are known to be histone chaperones, and Ccp1^{Vps75} has been found to play a role in promoting Cnp1^{CENP-A} deposition at the centromere during the course of this study, as discussed in Chapter 4. Furthermore, Cnp20^{CENP-T} contains histone folds and forms a nucleosome-like structure. With the above in mind, it was hypothesised that the two proteins interact in the context of Cnp1^{CENP-A} deposition at the centromere. To test this hypothesis, Cnp20^{CENP-T}-GFP levels in wild type and *ccp1*Δ cells were assessed using fluorescence microscopy and results presented in Figure 5.1.

As shown in the Figure 5.1, in the *ccp1*Δ mutant, Cnp20^{CENP-T}-GFP foci show a decrease in intensity. However, this does not indicate a direct interaction with Ccp1^{Vps75} - the observed effect in the *ccp1*Δ cells could in fact be due to the declustering of Cnp20^{CENP-T}-GFP, possibly due to centromere declustering in the *ccp1*Δ

mutant as discussed in Chapter 4.

To validate and quantify the results obtained by microscopy, ChIPs using the same strains that were used in the microscopy experiments, as well as an untagged wild type strain, were performed. The results of the anti-Cnp20^{CENP-T}-GFP ChIPs are presented in the Figure 5.2.

The ChIP data shows that there is a significant decrease in the Cnp20^{CENP-T}-GFP levels at the centromere in the *ccp1*Δ mutant. This result could be due to the loss of Cnp1^{CENP-A} from the centromere in the *ccp1*Δ mutant as the loss of Cnp1^{CENP-A} has an effect on levels of multiple kinetochore proteins.

A recently published study has found that in fission yeast Cnp20^{CENP-T} is required for the centromere localisation of Ccp1^{Vps75}. The study analysed the localisation of GFP-Ccp1^{Vps75} in the temperature sensitive mutant of Cnp20^{CENP-T}, *cnp20-9*, and has found that GFP-Ccp1^{Vps75} does not localise to the centromere throughout the cell cycle in the *cnp20-9* mutant at the restrictive temperature[66], suggesting that Cnp20^{CENP-T} is needed to recruit Ccp1^{Vps75} to the centromere.

The authors also found that the centromere localisation of Cnp20^{CENP-T}-GFP and the focus intensity in the *ccp1*Δ mutant was unchanged when examined by fluorescence microscopy[66].

This finding is in stark contrast to what has been found in this study. As the authors of the study which found the centromeric Cnp20^{CENP-T}-GFP to be unaffected in the *ccp1*Δ mutant did not perform ChIPs to quantify the centromeric Cnp20^{CENP-T}-GFP levels in the mutant, it is not possible to make a comparison to the ChIP results obtained in this study, which clearly show a significant decrease in the Cnp20^{CENP-T}-GFP levels at the centromere in the *ccp1*Δ (Figure 5.2).

This is in agreement with the microscopy data (Figure 5.1) obtained in this study, which shows a decrease in the intensity of the Cnp20^{CENP-T}-GFP focus in the

*ccp1*Δ mutant. This would, therefore, suggest that Ccp1^{Vps75} is needed to recruit Cnp20^{CENP-T} to the centromere, rather than the other way around.

Because the findings obtained in this study have suggested that Ccp1^{Vps75} is needed to maintain Cnp20^{CENP-T} levels at the centromere, it was hypothesised that the two proteins physically interact through the NAP domain of Ccp1^{Vps75} which could recognise the histone folds in Cnp20^{CENP-T}.

The initial approach to testing this hypothesis has been to perform IP-LC/MS-MS to investigate this potential interaction, and to identify other interacting partners of Ccp1^{Vps75}. The results obtained by mass spectrometry have been presented in Tables 5.1, 5.2 and 5.3.

As it can be seen from the results obtained by mass spectrometry experiments, Cnp20^{CENP-T} has not been identified in these experiments. An enrichment of Ccp1^{Vps75} in the IP sample obtained from the strain expressing Ccp1^{Vps75}-GFP was shown, however other identified proteins appear to be proteins which are abundant in the cell and are not specific interacting partners of Ccp1^{Vps75}.

In subsequent modifications of the experiment it was still not possible to identify Cnp20^{CENP-T} as an interacting partner of Ccp1^{Vps75}, and the only proteins which were enriched in the IP sample from the Ccp1^{Vps75}-GFP strain were Ccp1^{Vps75} itself and pyruvate kinase, which again was an unspecific hit (Table 5.2).

Due to the fact that Ccp1^{Vps75} has been shown to interact with Cnp1^{CENP-A} and has a NAP domain, it would be expected to see Cnp1^{CENP-A} or other histones in an experiment like this. While three histones (H4, H2A and H2B) were identified (Table 5.3) in the mass spectrometry experiments, these appear to be from different organisms and not *S. pombe*.

However, as the core histones are highly conserved across eukaryotes in terms of both sequence and structure, it is possible that the histones identified in the MS

were incorrectly attributed to different species for this reason. Nonetheless, even with that in mind, an enrichment of histones in the IP sample from the Ccp1^{Vps75}-GFP strain was still not observed.

Given all of the problems that have been encountered with performing the IP-LC/MS-MS experiments, an alternative approach to investigating the potential physical interaction between Ccp1^{Vps75} and Cnp20^{CENP-T} had to be devised, and co-IP was performed using the wild type strain and strains expressing Ccp1^{Vps75}-GFP, Cnp20^{CENP-T}-FLAG and both. The results were presented in Figures 5.3, 5.4 and 5.5.

While not without teething issues of their own, these experiments have been able to confirm that in the IP sample obtained from the strain expressing Ccp1^{Vps75}-GFP Cnp20^{CENP-T} a band corresponding to Ccp1^{Vps75}-GFP can be observed in a Western blot using the α -GFP antibody performed after a pulldown using α -FLAG M2 antibody.

Therefore, this finding may indicate that Ccp1^{Vps75} and Cnp20^{CENP-T} do in fact physically interact, however further experiments are needed to validate this hypothesis. It may be that this interaction is required to recruit Cnp20^{CENP-T} to the centromere during interphase when Ccp1^{Vps75} localises to the centromere[3, 4].

Furthermore, it has been observed in this study that centromeric levels of Cnp20^{CENP-T}-GFP decrease in the *ccp1* Δ mutant(Figures 5.2, 5.1), so the loss of the direct physical interaction between Ccp1^{Vps75} and Cnp20^{CENP-T} in the *ccp1* Δ mutant could explain this observation. However, as discussed above, this is not the only feasible explanation for this observation.

In a recently published study, the interaction of Ccp1^{Vps75} and Cnp20^{CENP-T} has been confirmed in a yeast two hybrid system, as well as using tandem affinity purification of Ccp1^{Vps75}-TAP followed by mass spectrometry[66]. These results are in

agreement with what has been found in this study and provide further confirmation of the hypothesis that Ccp1^{Vps75} and Cnp20^{CENP-T} physically interact.

Furthermore, through yeast two hybrid screens it has been found that the Ccp1^{Vps75} homodimer mutant has been unable to interact with Cnp20^{CENP-T}, suggesting that the homodimeric structure of Ccp1^{Vps75} *in vivo* is crucial for establishing an interaction with Cnp20^{CENP-T}. The interaction may be facilitated by the N terminus of Cnp20^{CENP-T} as in the same yeast two hybrid screen it was found that the minimal interaction domain for the interaction between Ccp1^{Vps75} and Cnp20^{CENP-T} not to be abolished is the first 55 amino acids of Cnp20^{CENP-T}[66].

Similarly to NAP1 and Vps75, Ccp1 forms a homodimer with a central cleft that forms between two acidic earmuff domains. The central cleft of NAP1 and Vps75 has been shown to interact with the H3-H4 histone heterodimer[3, 311].

Keeping that in mind, as well as the findings outlined above, the author of this thesis hypothesises that the cleft formed in the Ccp1^{Vps75} homodimer by the two NAP domains mediates the interaction between Ccp1^{Vps75} and Cnp20^{CENP-T} as it is possible that the histone folds of Cnp20^{CENP-T} can be recognised by central cleft of Ccp1^{Vps75} just like canonical histones are recognised by the central cleft of NAP1 and Vps75.

The findings presented in this chapter suggest that the absence of Ccp1^{Vps75} has an effect on Cnp20^{CENP-T} levels at the centromere, and that the two proteins may associate in a complex.

As presented in Chapter 4, Ccp1^{Vps75} may promote the loading of Cnp1^{CENP-A} at the centromere. Ccp1^{Vps75} has been shown to interact with both Cnp20^{CENP-T}[66] and Cnp1^{CENP-A}[3], while the Cnp20^{CENP-T} and Cnp1^{CENP-A} do not interact, so it is possible that Ccp1^{Vps75} may act as an interface between the two proteins and bring Cnp20^{CENP-T} to the centromere.

The findings presented in this chapter suggest that Ccp1^{Vps75} may help to main-

tain not only the Cnp1^{CENP-A} levels at the centromere, but also the levels of Cnp20^{CENP-T} at the centromere (Figures 5.1, 5.2).

Chapter 6

Summary, conclusion and future perspectives

6.1 Summary of the results presented in the thesis

In Chapter 3 the potential interaction of Ccp1^{Vps75} and Rtt109 in the context of Cnp1^{CENP-A} deposition at the centromere was investigated. It has been shown in this study that *S. pombe* Ccp1 and *S. cerevisiae* Vps75 may not be true functional orthologs. It has been found that budding yeast Rtt109 and Vps75^{Ccp1} work together to bring about correct acetylation of histone H3 at K9, K27 and K56[5, 6]. However, in fission yeast Rtt109 does not appear to be essential for the function of Ccp1^{Vps75} and they may have separate functions. Alternatively, they could be a part of a larger pathway involved in the maintenance of Cnp1^{CENP-A}. This is supported by the hypersensitivity of the *ccp1*Δ *rtt109*Δ mutants to TBZ compared to the *ccp1*Δ and *rtt109*Δ single mutants (Figure 3.1).

Previous work has highlighted the role of Rtt109 in the cells' response to genotoxic agents[267], so it was investigated whether that Ccp1^{Vps75} and Rtt109 work together to regulate the resistance to genotoxic agents in *S. pombe*. The results presented

in this thesis suggest that *rtt109* Δ cells are hypersensitive to genotoxic agents, in agreement to what has previously been reported in both budding and fission yeast. However, *ccp1* Δ cells were found not to show sensitivity to genotoxic agents, and the observed sensitivity shown by *ccp1* Δ *rtt109* Δ mutants was likely attributable to the deletion of *rtt109* (Figure 3.2). This is in agreement with previous budding yeast studies that examined the sensitivity of *ups75* Δ cells to genotoxic agents. It also suggests that Ccp1^{Vps75} likely does not support the function of Rtt109 in regulating the resistance to genotoxic agents.

It is possible that Rtt109 may promote the function of Ccp1^{Vps75} in *S. pombe* even though it is not essential to its function. A decrease in Ccp1^{Vps75} levels in *rtt109* Δ mutants can be observed (as shown in Figures 3.3, 3.4, 3.5), however the observed decrease is not statistically significant. Therefore, fission yeast Rtt109 and Ccp1^{Vps75} most likely have separate functions and the budding yeast Vps75 and fission yeast Ccp1 may not be true functional orthologs. However, a possibility that both proteins are involved in a larger pathway that regulates chromosome segregation in *S. pombe* also remains to be considered.

In Chapter 4 the potential role of Ccp1^{Vps75} in the context of Cnp1^{CENP-A} loading was investigated. Previous studies have found that Ccp1^{Vps75} may act as a Cnp1^{CENP-A} anti-loading factor[3]. The results presented in this study show that *ccp1* Δ and *ccp1* Δ *rtt109* Δ mutants show higher levels of de-silencing at the centromere compared to wild type cells. This indicated that there is a decrease in the levels of Cnp1^{CENP-A} at centromeres (Figure 4.2). The *rtt109* Δ mutant, interestingly, shows enhanced silencing at the centromere compared to the wild type (Figure 4.2). It is possible that this happens due to Rtt109 being involved in exchange of histone H3 with Cnp1^{CENP-A} during DNA replication, which has been found to be the case in budding yeast[302].

In addition to this, in Chapter 3 it has been shown that the *ccp1* Δ mutant is hypersensitive to TBZ. This finding suggests that there are chromosome segregation defects in this mutant, which could be due to a decrease in Cnp1^{CENP-A} levels at the centromere, which is supported by the results from the centromere silencing assays (Figure 4.2). Put together, suggest that Ccp1^{Vps75} may in fact be a Cnp1^{CENP-A} loading factor, rather than a factor that antagonises Cnp1^{CENP-A} loading, as hypothesised by Dong et al.[3].

A significant effect on the number of GFP-Cnp1^{CENP-A} foci was observed in the *ccp1* Δ mutant in experiments using fluorescence microscopy on cells expressing GFP-Cnp1^{CENP-A} in the wild type, *ccp1* Δ and *rtt109* Δ backgrounds (Figure 4.3). Interestingly, the microscopy experiments have also shown that there is a decrease in the number of cells with a single GFP-Cnp1^{CENP-A} focus, as well as an increase in the number of cells with more than one GFP-Cnp1^{CENP-A} focus in the *ccp1* Δ mutant (Figure 4.3). The GFP-Cnp1^{CENP-A} levels are least affected by the *rtt109* Δ mutation (Figure 4.3), which suggests that Rtt109 may not required for the deposition of Cnp1^{CENP-A} at the centromere, as previously suggested in Chapter 3.

Fluorescence microscopy has also been used to investigate strains expressing GFP-Cnp1^{CENP-A} Sid4-Tomato or GFP-Cnp1^{CENP-A} Sid4-mCherry in the wild type and *ccp1* Δ background. In Figure 4.3, it can be seen that in the *ccp1* Δ mutant the centromere clustering may be defective as more than one GFP-Cnp1^{CENP-A} focus can be observed. Additionally, the GFP-Cnp1^{CENP-A} signals do not always overlap with the Sid4-Tomato or Sid4-mCherry signals, so the centromeres may not always cluster at the SPB as expected in the *ccp1* Δ mutant. This finding suggests the centromere clustering in the *ccp1* Δ mutant may be defective. It is possible that the observed defects are due to the chromosome missegregation in this mutant, as indicated by TBZ assays (Figure 3.1). However, further experiments are needed to determine whether the multiple GFP-Cnp1^{CENP-A} foci are all centromeres, or whether some

of these foci represent ectopic GFP-Cnp1^{CENP-A}. Further research also needs to be done to explore whether the *ccp1*Δ mutant is diploid as these cells appear to be larger in all microscopy experiments.

To determine the Cnp1^{CENP-A} levels at centromeres anti-Cnp1^{CENP-A} ChIPs were performed. In Figure 4.4, it can be seen that the ChIP data suggests that there is a significant decrease in Cnp1^{CENP-A} levels in the *ccp1*Δ mutant, whereas the changes in Cnp1^{CENP-A} levels in the *rtt109*Δ mutant were not significant. These results provide further support to the hypothesis that Ccp1^{Vps75} aids Cnp1^{CENP-A} deposition at the centromere, and that Rtt109 may not be required for this process. The data obtained by anti-Cnp1^{CENP-A} ChIP is supported by the findings from anti-H3 ChIPs (Figure 4.5). In the *ccp1*Δ mutant the centromeric histone H3 levels increase compared to wild type levels. This validates the results obtained from the centromere silencing assays and the anti-Cnp1^{CENP-A} ChIP, which both suggested that in the absence of Ccp1^{Vps75} the levels of Cnp1^{CENP-A} at the centromere decrease. As the centromeric Cnp1^{CENP-A} levels decrease, histone H3 levels are expected to increase, and the anti-H3 ChIP suggests that this is indeed what happens. Again, these results suggest that Rtt109 may not be involved in Cnp1^{CENP-A} deposition at the centromere, and that Ccp1^{Vps75} is likely a Cnp1^{CENP-A} loading factor in contrast to what has previously been reported[3].

Therefore, the results presented in this study indicate that Ccp1^{Vps75} is a Cnp1^{CENP-A} loading factor. Cnp1^{CENP-A} levels decrease in the absence of Ccp1^{Vps75}, as the *ccp1*Δ mutant shows transcriptional de-silencing at the centromere. Enhanced silencing is observed in the *rtt109*Δ mutant, which is possibly due to exchange of histone H3 with Cnp1^{CENP-A} during DNA replication. Anti-Cnp1^{CENP-A} ChIPs solidify the idea that Ccp1^{Vps75} aids Cnp1^{CENP-A} deposition at the centromere as there is a decrease in Cnp1^{CENP-A} levels at the centromere in the *ccp1*Δ mutant. The same can not be observed in the *rtt109*Δ mutant. In addition, there is also data to suggest that in the *ccp1*Δ mutant the centromere clustering is defective because a population of

cells with multiple GFP-Cnp1^{CENP-A} foci can be observed. In fact, in the *ccp1*Δ mutant there is a proportion of cells in which the GFP-Cnp1^{CENP-A} signal does not overlap with the SPB marker, so the centromeres may not cluster at the SPB in this mutant. However, as noted previously, further research needs to be done to ascertain if the multiple GFP-Cnp1^{CENP-A} foci observed are in fact centromeres or if they are ectopic GFP-Cnp1^{CENP-A}.

In Chapter 5 the potential interaction between Ccp1^{Vps75} and Cnp20^{CENP-T} was investigated. Previous studies have shown that Cnp20^{CENP-T} is essential for viability in higher eukaryotes as well as in fission yeast[303] and that it is a platform for outer kinetochore assembly[65, 304–307].

In addition, it has been found that CENP-T^{Cnp20} contains histone folds and interacts with CENP-W^{Wip1}, CENP-S^{Mhf1} and CENP-X^{Mhf2} to form the CENP-T-W-S-X complex *in vitro*, which is a heterotetrameric complex with a nucleosome-like structure[65, 309]. The CENP-T-W-S-X complex has also been shown to associate directly with the centromeric DNA, which plays a role in the kinetochore formation[65, 304]. The complex interacts with histone H3, but not CENP-A^{Cnp1}[304, 310].

Ccp1^{Vps75} has previously been found to be a NAP family protein and NAP proteins are known to be histone chaperones. Furthermore, in this study findings have been presented that suggest that Ccp1^{Vps75} promotes Cnp1^{CENP-A} deposition at the centromere (see Chapter 4). Because Cnp20^{CENP-T} contains histone folds and forms a nucleosome-like structure it was hypothesised that the two proteins interact in the context of Cnp1^{CENP-A} deposition at the centromere. Firstly, it was found that in the *ccp1*Δ mutant the intensity of the Cnp20^{CENP-T}-GFP foci decreases compared to the wild type cells (Figure 5.1). Therefore, Ccp1^{Vps75} may have a role in maintaining Cnp20^{CENP-T} levels at the centromere. Interestingly, this finding contrasts a recently

published study, which suggested that the focus intensity of the Cnp20^{CENP-T}-GFP remains unchanged in the *ccp1*Δ mutant[66].

ChIPs using the same strains that were used in the microscopy experiments, as well as an untagged wild type strain, were performed to investigate the effect of *ccp1* deletion on Cnp20^{CENP-T}-GFP levels. The ChIP data shows a significant decrease in the centromeric Cnp20^{CENP-T}-GFP levels in the *ccp1*Δ mutant (Figure 5.2). This supports what has been found using fluorescence microscopy and the hypothesis that Ccp1^{Vps75} may be involved in the maintenance of Cnp20^{CENP-T} at the centromere. ChIPs to quantify the centromeric Cnp20^{CENP-T}-GFP levels in the *ccp1*Δ mutant were not performed in the study arguing that Ccp1^{Vps75} does not contribute to the maintenance of centromeric Cnp20^{CENP-T} levels, so it is not possible to make a comparison to the ChIP results obtained in this study. However, the results presented in Chapter 5 clearly show a significant decrease in the Cnp20^{CENP-T}-GFP levels at the centromere in the *ccp1*Δ mutant as well as a decrease in the intensity of the Cnp20^{CENP-T}-GFP foci in the *ccp1*Δ mutant (Figures 5.1, 5.2).

As the findings from this study have suggested that Ccp1^{Vps75} is needed to maintain Cnp20^{CENP-T} levels at the centromere, it was hypothesised that the two proteins physically interact. The initial approach to testing this hypothesis by using IP-LC/MS-MS to investigate this potential interaction proved to be unsuccessful (Table 5.1, 5.2, 5.3). However, co-IP experiments have suggested that the two proteins do in fact physically interact (Figure 5.5). This is in agreement with recently published findings which show that Ccp1^{Vps75} interacts with Cnp20^{CENP-T} in experiments using tandem affinity purification followed by mass spectrometry as well as in yeast two hybrid screens[66]. The interaction is mediated by the N terminus of Cnp20^{CENP-T} on one end, however it is still unclear which structural elements mediate the interaction in Ccp1^{Vps75}.

Findings presented in this study suggest that Ccp1^{Vps75} may have a role not just in the loading of Cnp1^{CENP-A} at the centromere, but also in maintaining Cnp20^{CENP-T} levels at the centromere (Chapters 4, 5). The two proteins have been shown to directly interact, and it is possible that Ccp1^{Vps75} is the missing link between Cnp20^{CENP-T} and Cnp1^{CENP-A} which do not interact with one another, but both interact with Ccp1^{Vps75}. The author of this thesis hypothesises that the interaction between Ccp1^{Vps75} and Cnp20^{CENP-T} is mediated by the NAP domain of Ccp1^{Vps75}. The central cleft of human NAP1 and *S. cerevisiae* Vps75 has been shown to interact with histone H3-H4 heterodimer, therefore the central cleft of *S. pombe* Ccp1 may recognise the histone folds of Cnp20^{CENP-T} in a mechanism similar to that employed by other NAP family proteins.

6.2 Conclusion

This PhD project aimed to investigate the mechanisms, specifically those relating to the incorporation of Cnp1^{CENP-A} within centromeric chromatin, which regulate chromosome segregation in *S. pombe*. The project explored the interaction between Rtt109, Ccp1^{Vps75} and Cnp20^{CENP-T} in the context of Cnp1^{CENP-A} deposition regulation.

The results presented in this thesis suggest that in fission yeast Rtt109 and Ccp1^{Vps75} may have separate functions, while in budding yeast Rtt109 and Vps75^{Ccp1} work together to bring about correct acetylation of histone H3 at K9, K27 and K56. The results presented in Chapter 3 suggest that the *S. cerevisiae* Vps75 and *S. pombe* Ccp1 may not be true functional orthologs. However, the possibility these proteins are involved in a larger pathway that regulates chromosome segregation in *S. pombe* remains.

Furthermore, the results presented in Chapter 4 suggest that Ccp1^{Vps75} is a Cnp1^{CENP-A} loading factor, while Rtt109 may not be involved in the process of Cnp1^{CENP-A} deposition in fission yeast. In addition, the results suggest that there may be centromere clustering defects in the *ccp1* Δ mutant, and that the centromeres are not clustering at the SPB, however further research is needed for firm conclusions to be drawn about this.

Lastly, the findings presented in Chapter 5 suggest that Ccp1^{Vps75} helps to maintain the Cnp20^{CENP-T} levels at the centromere in addition to promoting centromeric Cnp1^{CENP-A} loading. Ccp1^{Vps75} and Cnp20^{CENP-T} may directly interact, and the author of this thesis hypothesises that Ccp1^{Vps75} may play the role of a link between Cnp20^{CENP-T} and Cnp1^{CENP-A} given that they do not interact with one another, but both interact with Ccp1^{Vps75}. It is possible that the interaction between Ccp1^{Vps75} and Cnp20^{CENP-T} is mediated by the NAP domain of Ccp1^{Vps75}. This speculation

is based on the fact that in human NAP1 and *S. cerevisiae* Vps75 the central cleft, a feature found in the Ccp1 homodimer as well, interacts with histone H3-H4 heterodimer. It is therefore not inconceivable that the central cleft of *S. pombe* Ccp1 recognises the histone folds of Cnp20^{CENP-T} in the same manner the other NAP family proteins recognise histones.

6.3 Future perspectives

Unfortunately, the scope of the experiments for this project was heavily impacted by the COVID-19 pandemic, so while this project offers some answers about the role of fission yeast Ccp1 and Rtt109, the deposition of Cnp1^{CENP-A} and the interaction of Cnp20^{CENP-T} with Ccp1^{Vps75}, it also raises interesting and exciting questions that still remain to be explored.

First of all, the results presented in this thesis suggest that in fission yeast Rtt109 and Ccp1^{Vps75} most likely have separate functions. Budding yeast research shows that Rtt109 and Vps75^{Ccp1} work together to bring about correct acetylation of histone H3 at K9, K27 and K56. So while the results presented in Chapter 3 suggest that in fission yeast these proteins may not work together, the possibility these proteins are involved in a larger pathway that regulates chromosome segregation in *S. pombe* remains. Therefore, establishing whether these two proteins interact in *S. pombe* by using co-IP could bring more clarity to that question.

Secondly, it would be interesting to explore the chromosome missegregation in the *ccp1*Δ, *rtt109*Δ and the *ccp1*Δ *rtt109*Δ mutants and the centromere clustering defects observed in the *ccp1*Δ mutant in more depth. In TBZ assays presented in this thesis both of the single mutants, and especially the double mutant, have been shown to be sensitive to TBZ, indicating that they may have chromosome segregation defects. Using fluorescence microscopy to image such defects using an antibody generated against *Trypanosoma brucei* TAT1 (tubulin) could provide more clarity on the exact nature of the chromosome segregation defects that seem to arise in the *ccp1*Δ, *rtt109*Δ and *ccp1*Δ *rtt109*Δ mutants.

To investigate centromere declustering, it could also be beneficial to synchronise cells. By synchronising cells and imaging the *ccp1*Δ mutants throughout the cell cycle, it may be possible to identify the phase(s) of the cell cycle when the declus-

tering takes place. To do this, strains with the *cdc25-22* mutation in the wild type and *ccp1*Δ backgrounds would need to be made. *cdc25-22* would allow for the cells to be arrested in the G₂/M stage of the cell cycle, and then released into the M phase while the GFP-Cnp1^{CENP-A} signal throughout the cell cycle is followed.

Another interesting avenue of research would be to explore the interaction between Ccp1^{Vps75} and Cnp20^{CENP-T} using temperature sensitive mutants of Cnp20^{CENP-T}. ChIP and fluorescence imaging experiments could be used to determine Ccp1^{Vps75} levels and centromere localisation in *cnp20⁺* and *cnp20^{ts}* mutants, as well as a wild type strain expressing Ccp1^{Vps75}-GFP. This would help answer the question of whether Cnp20^{CENP-T} is required for the centromere localisation of Ccp1^{Vps75}. The results presented in this thesis suggest that Ccp1^{Vps75} helps to maintain Cnp20^{CENP-T} levels at the centromere, however a recently published study argues that in fission yeast Cnp20^{CENP-T} is required for the centromere localisation of Ccp1^{Vps75} and that the centromere localisation of Cnp20^{CENP-T}-GFP and the focus intensity in the *ccp1*Δ mutant was unchanged when examined by fluorescence microscopy[66].

Therefore, there is space to explore this interaction further and to bring clarity to how kinetochores are assembled on centromere. Accurate chromosome segregation relies on correct kinetochore assembly; while this process is obviously crucial to the survival of the cell, it is still poorly understood and the author of this thesis firmly believes that the potential role of Ccp1^{Vps75} as the missing link between Cnp20^{CENP-T} and Cnp1^{CENP-A} is an avenue worth exploring further.

Furthermore, the results presented in Chapter 5 suggest that Cnp20^{CENP-T} and Ccp1^{Vps75} may physically interact. Indeed, the same has been found by other researchers in a recently published study which confirmed the interaction through yeast two hybrid screens and tandem affinity purification followed by mass spectrometry.

While the same study found that the interaction is mediated through the N terminus of Cnp20^{CENP-T} by the Ndc80 receptor-adjacent Ccp1 interacting motif (CIM)[66], it is still unclear which structural features of Ccp1^{Vps75} mediate this interaction. As discussed in Chapter 5 the author of this thesis believes that the NAP domain of Ccp1^{Vps75}, specifically the central cleft of the Ccp1^{Vps75} homodimer, mediates the interaction with Cnp20^{CENP-T}.

To investigate this hypothesis NAP domain mutants of Ccp1^{Vps75} could be made. This would allow for a study of whether point mutations of the conserved residues in the NAP domain of Ccp1^{Vps75} would cause the interaction between Ccp1^{Vps75} and Cnp20^{CENP-T} to be abolished. A multiple sequence alignment of NAP domain proteins from different species and conserved residues which could be mutated in such an experiment are shown in Figure 6.1 below.

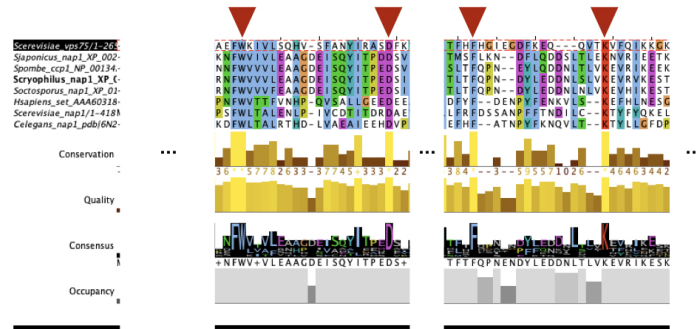


Figure 6.1: Multiple sequence alignment of NAP proteins from different organisms and the residues proposed for mutations. *S. pombe* Ccp1 sequence aligned with Nap1 from *S. japonicus*, *S. cryophilus*, *S. octosporus*, *S. cerevisiae*, *C. elegans*, Vps75 from *S. cerevisiae*, and SET from *H. sapiens*. The conserved residues within the NAP domain of *S. pombe* Ccp1 indicated with red arrows could be mutated to alanine to assess the impact of these mutations on the interaction between Ccp1^{Vps75} and Cnp20^{CENP-T}.

Finally, as Rtt109 is a HAT protein that has been shown to acetylate histone H3 at K9, K27 and K56 *in vivo* in budding yeast and Vps75^{Ccp1} aids this acetylation[6], another interesting avenue of research could be to investigate whether in fission yeast Ccp1^{Vps75}, Rtt109 or acetylation of K56, K27 and K9 are required to deposit Cnp1^{CENP-A} on a minichromosome. A ChIP could be used to determine Cnp1^{CENP-A} levels in *ccp1*Δ *rtt109*Δ and *ccp1*Δ *rtt109*Δ mutants compared to wild type cells which harbour a centromeric plasmid/minichromosome encoding central domain DNA and flanking DNA repeats, as well as *ade6-704* which enables for determination of minichromosome loss (red colonies on low-adenine media) or minichromosome retention (white/pink colonies on low-adenine media). If the minichromosome has been retained by the cell, centromere function has been established because in the absence of centromere establishment, minichromosomes are rapidly lost. This experiment may suggest which proteins are required for Cnp1^{CENP-A} establishment on naïve centromeric DNA.

In conclusion, the correct centromere, and subsequently kinetochore, establishment is a crucial process to cell survival. However, this process is still relatively poorly understood, and this project aimed to shed more light on factors that aid Cnp1^{CENP-A} deposition at the centromere. In this thesis Ccp1^{Vps75} has been identified as a factor aiding the centromere deposition of Cnp1^{CENP-A}, and Cnp20^{CENP-T}, an inner kinetochore protein, has been identified as its interacting partner. Therefore, the author of this thesis suggests and believes that further research into fission yeast Ccp1 could shed more light onto how Cnp1^{CENP-A} is deposited at the centromere, and how the CENP-T^{Cnp20} branch of the CCAN may be recruited to the centromere.

These findings could ultimately support basic and translational research into cancer as it has been well documented that chromosome missegregation can contribute not just to development of cancer, but also to chemotherapeutic resistance due to chromosomal instability.

Bibliography

1. Musacchio, A. & Desai, A. A Molecular View of Kinetochores Assembly and Function. *Biology* **6**, 5 (2017).
2. Schalch, T. & Steiner, F. A. Structure of centromere chromatin: from nucleosome to chromosomal architecture. *Chromosoma* **126**, 443–455 (2017).
3. Dong, Q. *et al.* Ccp1 homodimer mediates chromatin integrity by antagonizing CENP-A loading. *Molecular Cell* **263**, 219–227 (2016).
4. Lu, M. & He, X. Ccp1 modulates epigenetic stability at centromeres and affects heterochromatin distribution in *Schizosaccharomyces pombe*. *Journal of Biological Chemistry* **293**, 12068–12080 (2018).
5. Xhemalce, B. *et al.* Regulation of Histone H3 Lysine 56 Acetylation in *Schizosaccharomyces pombe*. *Journal of Biological Chemistry* **282**, 15040–15047 (2007).
6. Keck, K. M. & Pemberton, L. F. Interaction with the histone chaperone Vps75 promotes nuclear localization and HAT activity of Rtt109 in vivo. *Traffic* **12**, 826–39 (2011).
7. Van Hooser, A. A. *et al.* Specification of kinetochores-forming chromatin by the histone H3 variant CENP-A. *Journal of Cell Science* **114**, 3529–42 (2001).
8. Stellfox, M. E., Bailey, A. O. & Foltz, D. R. Putting CENP-A in its place. *Cellular and Molecular Life Sciences* **70**, 387–406 (2013).
9. Mitchell Smith, M. Centromeres and variant histones: what, where, when and why? *Current Opinion in Cell Biology* **14**, 279–285 (2002).

10. Folco, H. D. *et al.* The CENP-A N-tail confers epigenetic stability to centromeres via the CENP-T branch of the CCAN in fission yeast. *Current Biology* **25**, 348–356 (2015).
11. Potapova, T. & Gorbsky, G. The Consequences of Chromosome Segregation Errors in Mitosis and Meiosis. *Biology* **6**, 12 (2017).
12. Hoffman, C. S., Wood, V. & Fantes, P. A. An Ancient Yeast for Young Geneticists: A Primer on the *Schizosaccharomyces pombe* Model System. *Genetics* **201**, 403–423 (2015).
13. Vyas, A., Freitas, A. V., Ralston, Z. A. & Tang, Z. Fission Yeast *Schizosaccharomyces pombe*: A Unicellular “Micromammal” Model Organism. *Current Protocols* **1** (2021).
14. Glowczewski, L., Koshland, D. & Smith, M. M. Cse4p Is a Component of the Core Centromere of. *Cell* **94**, 607–613 (1998).
15. Henikoff, S. & Henikoff, J. G. ”Point” Centromeres of *Saccharomyces* Harbor Single Centromere-Specific Nucleosomes. *Genetics* **190**, 1575–1577 (2012).
16. Pluta, A. F., Mackay, A. M., Ainsztein, A. M., Goldberg, I. G. & Earnshaw, W. C. The centromere: hub of chromosomal activities. *Science* **270**, 1591–4 (1995).
17. Hayles, J. & Nurse, P. Introduction to Fission Yeast as a Model System. *Cold Spring Harbor Protocols* (2018).
18. Wood, V. *et al.* The genome sequence of *Schizosaccharomyces pombe*. *Nature* **415**, 871–880 (2002).
19. Niwa, O., Matsumoto, T., Chikashige, Y. & Yanagida, M. Characterization of *Schizosaccharomyces pombe* minichromosome deletion derivatives and a functional allocation of their centromere. *The EMBO Journal* **8**, 3045–52 (1989).

20. Allshire, R. C. & Ekwall, K. Epigenetic Regulation of Chromatin States in *Schizosaccharomyces pombe*. *Cold Spring Harbor Perspectives in Biology* **7**, a018770 (2015).
21. Allshire, R. C. & Karpen, G. H. Epigenetic regulation of centromeric chromatin: old dogs, new tricks? *Nature Reviews Genetics* **9**, 923–37 (2008).
22. Matsuda, A., Asakawa, H., Haraguchi, T. & Hiraoka, Y. Spatial organization of the *Schizosaccharomyces pombe* genome within the nucleus. *Yeast* **34**, 55–66 (2017).
23. French, B. T. & Straight, A. F. Swapping CENP-A at the centromere. *Nature Cell Biology* **15**, 1028–30 (2013).
24. Zofall, M. & Grewal, S. I. Swi6/HP1 Recruits a JmjC Domain Protein to Facilitate Transcription of Heterochromatic Repeats. *Molecular Cell* **22**, 681–692 (2006).
25. Grewal, S. I. RNAi-dependent formation of heterochromatin and its diverse functions. *Current Opinion in Genetics & Development* **20**, 134–41 (2010).
26. Luger, K., Mäder, A. W., Richmond, R. K., Sargent, D. F. & Richmond, T. J. Crystal structure of the nucleosome core particle at 2.8Å resolution. *Nature* **389**, 251–260 (1997).
27. Justin, N., De Marco, V., Aasland, R. & Gamblin, S. J. Reading, writing and editing methylated lysines on histone tails: new insights from recent structural studies. *Current Opinion in Structural Biology* **20**, 730–738 (2010).
28. Margueron, R. & Reinberg, D. Chromatin structure and the inheritance of epigenetic information. *Nature Reviews Genetics* **11**, 285–296 (2010).
29. Suzuki, M. M. & Bird, A. DNA methylation landscapes: provocative insights from epigenomics. *Nature Reviews Genetics* **9**, 465–476 (2008).
30. Zhou, V. W., Goren, A. & Bernstein, B. E. Charting histone modifications and the functional organization of mammalian genomes. *Nature Reviews Genetics* **12**, 7–18 (2011).

31. Avvakumov, N., Nourani, A. & Côté, J. Histone Chaperones: Modulators of Chromatin Marks. *Molecular Cell* **41**, 502–514 (2011).
32. Das, C., Tyler, J. K. & Churchill, M. E. The histone shuffle: histone chaperones in an energetic dance. *Trends in Biochemical Sciences* **35**, 476–489 (2010).
33. Takahashi, K., Chen, E. S. & Yanagida, M. Requirement of Mis6 Centromere Connector for Localizing a CENP-A-Like Protein in Fission Yeast. *Science* **288**, 2215–2219 (2000).
34. Coffman, V. C., Wu, P., Parthun, M. R. & Wu, J.-Q. CENP-A exceeds microtubule attachment sites in centromere clusters of both budding and fission yeast. *Journal of Cell Biology* **195**, 563–572 (2011).
35. Lando, D. *et al.* Quantitative single-molecule microscopy reveals that CENP-ACnp1 deposition occurs during G2 in fission yeast. *Open Biology* **2**, 120078–120078 (2012).
36. Scott, K. C., Merrett, S. L. & Willard, H. F. Article A Heterochromatin Barrier Partitions the Fission Yeast Centromere into Discrete Chromatin Domains. *Current Biology* **16**, 119–129 (2006).
37. Allshire, R. C., Javerzat, J. P., Redhead, N. J. & Cranston, G. Position effect variegation at fission yeast centromeres. *Cell* **76**, 157–69 (1994).
38. Pidoux, A. L., Richardson, W. & Allshire, R. C. Sim4: a novel fission yeast kinetochore protein required for centromeric silencing and chromosome segregation. *The Journal of Cell Biology* **161**, 295–307 (2003).
39. Allshire, R. C., Nimmo, E. R., Ekwall, K., Javerzat, J. P. & Cranston, G. Mutations derepressing silent centromeric domains in fission yeast disrupt chromosome segregation. *Genes & Development* **9**, 218–233 (1995).
40. Thon, G., Cohen, A. & Klar, A. J. Three additional linkage groups that repress transcription and meiotic recombination in the mating-type region of *Schizosaccharomyces pombe*. *Genetics* **138**, 29–38 (1994).

41. Thon, G. & Klar, A. J. The *clr1* locus regulates the expression of the cryptic mating-type loci of fission yeast. *Genetics* **131**, 287–296 (1992).
42. Ekwall, K. & Ruusala, T. Mutations in *rik1*, *clr2*, *clr3* and *clr4* genes asymmetrically derepress the silent mating-type loci in fission yeast. *Genetics* **136**, 53–64 (1994).
43. Grunstein, M. & Gasser, S. M. Epigenetics in *Saccharomyces cerevisiae*. *Cold Spring Harbor Perspectives in Biology* **5**, a017491–a017491 (2013).
44. Wilkinson, C. R. M., Bartlett, R., Nurse, P. & Bird, A. P. The fission yeast gene *pmt1* encodes a DNA methyltransferase homologue. *Nucleic Acids Research* **23**, 203–210 (1995).
45. Ekwall, K. *et al.* The Chromodomain Protein Swi6: A Key Component at Fission Yeast Centromeres. *Science* **269**, 1429–1431 (1995).
46. Van Der Horst, A. & Lens, S. M. Cell division: Control of the chromosomal passenger complex in time and space. *Chromosoma* **123**, 25–42 (2014).
47. *The Molecular Biology of Schizosaccharomyces pombe* (ed Egel, R.) ISBN: 978-3-642-05631-4 (Springer Berlin Heidelberg, Berlin, Heidelberg, 2004).
48. Nimmo, E., Cranston, G. & Allshire, R. Telomere-associated chromosome breakage in fission yeast results in variegated expression of adjacent genes. *The EMBO Journal* **13**, 3801–3811 (1994).
49. Nimmo, E. R., Pidoux, A. L., Perry, P. E. & Allshire, R. C. Defective meiosis in telomere-silencing mutants of *Schizosaccharomyces pombe*. *Nature* **392**, 825–828 (1998).
50. Kanoh, J., Sadaie, M., Urano, T. & Ishikawa, F. Telomere Binding Protein Taz1 Establishes Swi6 Heterochromatin Independently of RNAi at Telomeres. *Current Biology* **15**, 1808–1819 (2005).
51. Cam, H. P. *et al.* Comprehensive analysis of heterochromatin- and RNAi-mediated epigenetic control of the fission yeast genome. *Nature Genetics* **37**, 809–819 (2005).

52. Thon, G. & Verhein-Hansen, J. Four Chromo-domain Proteins of *Schizosaccharomyces pombe* Differentially Repress Transcription at Various Chromosomal Locations. *Genetics* **155**, 551–568 (2000).
53. McKinley, K. L. & Cheeseman, I. M. The molecular basis for centromere identity and function. *Nature Reviews Molecular Cell Biology* **17**, 16–29 (2016).
54. Steiner, N. C. & Clarke, L. A novel epigenetic effect can alter centromere function in fission yeast. *Cell* **79**, 865–74 (1994).
55. Sullivan, B. A. & Schwartz, S. Identification of centromeric antigens in dicentric Robertsonian translocations: CENP-C and CENP-E are necessary components of functional centromeres. *Human Molecular Genetics* **4**, 2189–97 (1995).
56. Murphy, T. D. & Karpen, G. H. Localization of Centromere Function in a *Drosophila* Minichromosome. *Cell* **82**, 599–609 (1995).
57. Emily A. Foley & Kapoor, T. M. Microtubule attachment and spindle assembly checkpoint signaling at the kinetochore. *Nature Reviews Molecular Cell Biology* **14**, 25–37 (2013).
58. Musacchio, A. The Molecular Biology of Spindle Assembly Checkpoint Signaling Dynamics. *Current Biology* **25**, R1002–R1018 (2015).
59. Hayashi, T. *et al.* Mis16 and Mis18 are required for CENP-A loading and histone deacetylation at centromeres. *Cell* **118**, 715–29 (2004).
60. Cheeseman, I. M., Chappie, J. S., Wilson-Kubalek, E. M. & Desai, A. The Conserved KMN Network Constitutes the Core Microtubule-Binding Site of the Kinetochore. *Cell* **127**, 983–997 (2006).
61. Weir, J. R. *et al.* Insights from biochemical reconstitution into the architecture of human kinetochores. *Nature* **537**, 249–253 (2016).
62. Kato, H. *et al.* A Conserved Mechanism for Centromeric Nucleosome Recognition by Centromere Protein CENP-C. *Science* **340**, 1110–1113 (2013).

63. Guse, A., Carroll, C. W., Moree, B., Fuller, C. J. & Straight, A. F. In vitro centromere and kinetochore assembly on defined chromatin templates. *Nature* **477**, 354–358 (2011).
64. Bailey, A. O. *et al.* Posttranslational modification of CENP-A influences the conformation of centromeric chromatin. *Proceedings of the National Academy of Sciences* **110**, 11827–11832 (2013).
65. Nishino, T. *et al.* CENP-T-W-S-X forms a unique centromeric chromatin structure with a histone-like fold. *Cell* **148**, 487–501 (2012).
66. Dong, Q. *et al.* Ccp1-Ndc80 switch at the N terminus of CENP-T regulates kinetochore assembly. *Proceedings of the National Academy of Sciences* **118** (2021).
67. Hyland, K. M., Kingsbury, J., Koshland, D. & Hieter, P. Ctf19p: A novel kinetochore protein in *Saccharomyces cerevisiae* and a potential link between the kinetochore and mitotic spindle. *The Journal of Cell Biology* **145**, 15–28 (1999).
68. Hornung, P. *et al.* A cooperative mechanism drives budding yeast kinetochore assembly downstream of CENP-A. *The Journal of Cell Biology* **206**, 509–524 (2014).
69. Masumoto, H., Masukata, H., Muro, Y., Nozaki, N. & Okazaki, T. A human centromere antigen (CENP-B) interacts with a short specific sequence in alphoid DNA, a human centromeric satellite. *The Journal of Cell Biology* **109**, 1963–73 (1989).
70. Fachinetti, D. *et al.* DNA Sequence-Specific Binding of CENP-B Enhances the Fidelity of Human Centromere Function. *Developmental Cell* **33**, 314–327 (2015).
71. Mendiburo, M. J., Padeken, J., Fulop, S., Schepers, A. & Heun, P. *Drosophila* CENH3 Is Sufficient for Centromere Formation. *Science* **334**, 686–690 (2011).

72. Harrington, J. J., Bokkelen, G. V., Mays, R. W., Gustashaw, K. & Willard, H. F. Formation of de novo centromeres and construction of first-generation human artificial microchromosomes. *Nature Genetics* **15**, 345–355 (1997).
73. Catania, S., Pidoux, A. L. & Allshire, R. C. Sequence Features and Transcriptional Stalling within Centromere DNA Promote Establishment of CENP-A Chromatin. *PLOS Genetics* — DOI (2015).
74. Iwata-Otsubo, A. *et al.* Expanded Satellite Repeats Amplify a Discrete CENP-A Nucleosome Assembly Site on Chromosomes that Drive in Female Meiosis. *Current Biology* **27**, 2365–2373 (2017).
75. Kasinathan, S. & Henikoff, S. Non-B-Form DNA Is Enriched at Centromeres. *Molecular Biology and Evolution* **35**, 949–962 (2018).
76. Shukla, M. *et al.* Centromere DNA Destabilizes H3 Nucleosomes to Promote CENP-A Deposition during the Cell Cycle. *Current Biology* **28**, 3924–3936 (2018).
77. Logsdon, G. A. *et al.* Human Artificial Chromosomes that Bypass Centromeric DNA. *Cell* **178**, 624–639 (2019).
78. Murillo-Pineda, M. & Jansen, L. E. Genetics, epigenetics and back again: Lessons learned from neocentromeres. *Experimental Cell Research* **389**, 111909 (2020).
79. Wieland, G., Orthaus, S., Ohndorf, S., Diekmann, S. & Hemmerich, P. Functional Complementation of Human Centromere Protein A (CENP-A) by Cse4p from *Saccharomyces cerevisiae*. *Molecular and Cellular Biology* **24**, 6620–6630 (2004).
80. Black, B. E. *et al.* Structural determinants for generating centromeric chromatin. *Nature* **430**, 578–582 (2004).
81. Black, B. E., Brock, M. A., Bédard, S., Woods, V. L. & Cleveland, D. W. An epigenetic mark generated by the incorporation of CENP-A into centromeric

- nucleosomes. *Proceedings of the National Academy of Sciences* **104**, 5008–5013 (2007).
82. Black, B. E. *et al.* Centromere Identity Maintained by Nucleosomes Assembled with Histone H3 Containing the CENP-A Targeting Domain. *Molecular Cell* **25**, 309–322 (2007).
 83. Carroll, C. W., Silva, M. C., Godek, K. M., Jansen, L. E. & Straight, A. F. Centromere assembly requires the direct recognition of CENP-A nucleosomes by CENP-N. *Nature Cell Biology* **11**, 896–902 (2009).
 84. Carroll, C. W., Milks, K. J. & Straight, A. F. Dual recognition of CENP-A nucleosomes is required for centromere assembly. *Journal of Cell Biology* **189**, 1143–1155 (2010).
 85. Hu, H. *et al.* Structure of a CENP-A–histone H4 heterodimer in complex with chaperone HJURP. *Genes & Development* **25**, 901–906 (2011).
 86. Logsdon, G. A. *et al.* Both tails and the centromere targeting domain of CENP-A are required for centromere establishment. *Journal of Cell Biology* **208**, 521–531 (2015).
 87. Dunleavy, E. M., Almouzni, G. & Karpen, G. H. H3.3 is deposited at centromeres in S phase as a placeholder for newly assembled CENP-A in G1 phase. *Nucleus* **2**, 146–157 (2011).
 88. Jansen, L. E., Black, B. E., Foltz, D. R. & Cleveland, D. W. Propagation of centromeric chromatin requires exit from mitosis. *Journal of Cell Biology* **176**, 795–805 (2007).
 89. Schuh, M., Lehner, C. F. & Heidmann, S. Incorporation of *Drosophila* CID/CENP-A and CENP-C into Centromeres during Early Embryonic Anaphase. *Current Biology* **17**, 237–243 (2007).
 90. Mellone, B. G. *et al.* Assembly of *Drosophila* Centromeric Chromatin Proteins during Mitosis. *PLoS Genetics* **7**, e1002068 (2011).

91. Dunleavy, E. M. *et al.* The Cell Cycle Timing of Centromeric Chromatin Assembly in *Drosophila* Meiosis Is Distinct from Mitosis Yet Requires CAL1 and CENP-C. *PLoS Biology* **10**, e1001460 (2012).
92. Lidsky, P. V., Sprenger, F. & Lehner, C. F. Distinct modes of centromere protein dynamics during cell cycle progression in *Drosophila* S2R+ cells. *Journal of Cell Science* (2013).
93. Lermontova, I. *et al.* Loading of Arabidopsis Centromeric Histone CENH3 Occurs Mainly during G2 and Requires the Presence of the Histone Fold Domain. *The Plant Cell* **18**, 2443–2451 (2006).
94. Foltz, D. R. *et al.* Centromere-specific assembly of CENP-a nucleosomes is mediated by HJURP. *Cell* **137**, 472–84 (2009).
95. Cho, U.-S. & Harrison, S. C. Recognition of the centromere-specific histone Cse4 by the chaperone Scm3. *Proceedings of the National Academy of Sciences of the United States of America* **108**, 9367–71 (2011).
96. Williams, J. S., Hayashi, T., Yanagida, M. & Russell, P. Fission yeast Scm3 mediates stable assembly of Cnp1/CENP-A into centromeric chromatin. *Molecular Cell* **33**, 287–98 (2009).
97. Pidoux, A. L. *et al.* Fission Yeast Scm3: A CENP-A Receptor Required for Integrity of Subkinetochore Chromatin. *Molecular Cell* **33**, 299–311 (2009).
98. Chen, C.-C. *et al.* CAL1 is the *Drosophila* CENP-A assembly factor. *Journal of Cell Biology* **204**, 313–329 (2014).
99. Stoler, S. *et al.* Scm3, an essential *Saccharomyces cerevisiae* centromere protein required for G2/M progression and Cse4 localization. *Proceedings of the National Academy of Sciences* **104**, 10571–10576 (2007).
100. Medina-Pritchard, B. *et al.* Molecular basis for Cdk1-regulated timing of Mis18 complex assembly and CENP-A deposition. *EMBO reports* **18**, 894–905 (2017).

101. Fujita, Y. *et al.* Priming of centromere for CENP-A recruitment by human hMis18alpha, hMis18beta, and M18BP1. *Developmental Cell* **12**, 17–30 (2007).
102. Moree, B., Meyer, C. B., Fuller, C. J. & Straight, A. F. CENP-C recruits M18BP1 to centromeres to promote CENP-A chromatin assembly. *The Journal of Cell Biology* **194**, 855–71 (2011).
103. Westhorpe, F. G., Fuller, C. J. & Straight, A. F. A cell-free CENP-A assembly system defines the chromatin requirements for centromere maintenance. *Journal of Cell Biology* **209**, 789–801 (2015).
104. Wang, J. *et al.* Mitotic Regulator Mis18 β Interacts with and Specifies the Centromeric Assembly of Molecular Chaperone Holliday Junction Recognition Protein (HJURP). *Journal of Biological Chemistry* **289**, 8326–8336 (2014).
105. French, B. T., Westhorpe, F. G., Limouse, C. & Straight, A. F. *Xenopus laevis* M18BP1 Directly Binds Existing CENP-A Nucleosomes to Promote Centromeric Chromatin Assembly. *Developmental Cell* **42**, 190–199 (2017).
106. Stankovic, A. *et al.* A Dual Inhibitory Mechanism Sufficient to Maintain Cell-Cycle-Restricted CENP-A Assembly. *Molecular Cell* **65**, 231–246 (2017).
107. Silva, M. C. *et al.* Cdk Activity Couples Epigenetic Centromere Inheritance to Cell Cycle Progression. *Developmental Cell* **22**, 52–63 (2012).
108. Spiller, F. *et al.* Molecular basis for Cdk1-regulated timing of Mis18 complex assembly and CENP-A deposition. *EMBO reports* **18**, 894–905 (2017).
109. McKinley, K. L. & Cheeseman, I. M. Polo-like kinase 1 licenses CENP-A deposition at centromeres. *Cell* **158**, 397–411 (2014).
110. Fu, H. *et al.* SENP6-mediated M18BP1 deSUMOylation regulates CENP-A centromeric localization. *Cell Research* **29**, 254–257 (2019).
111. Yilmaz, D. *et al.* Activation of homologous recombination in G1 preserves centromeric integrity. *Nature* **600**, 748–753 (2021).

112. Dunleavy, E. M. *et al.* A NASP (N1/N2)-related protein, Sim3, binds CENP-A and is required for its deposition at fission yeast centromeres. *Molecular Cell* **28**, 1029–44 (2007).
113. Fachinetti, D. *et al.* CENP-A Modifications on Ser68 and Lys124 Are Dispensable for Establishment, Maintenance, and Long-Term Function of Human Centromeres. *Developmental Cell* **40**, 104–113 (2017).
114. Yu, Z. *et al.* Dynamic Phosphorylation of CENP-A at Ser68 Orchestrates Its Cell-Cycle-Dependent Deposition at Centromeres. *Developmental Cell* **32**, 68–81 (2015).
115. Wang, K., Yu, Z., Liu, Y. & Li, G. Ser68 Phosphorylation Ensures Accurate Cell-Cycle-Dependent CENP-A Deposition at Centromeres. *Developmental Cell* **40**, 5–6 (2017).
116. Wang, K. *et al.* Phosphorylation at Ser68 facilitates DCAF11-mediated ubiquitination and degradation of CENP-A during the cell cycle. *Cell Reports* **37**, 109987 (2021).
117. Bailey, A. O. *et al.* Identification of the Post-translational Modifications Present in Centromeric Chromatin. *Molecular & Cellular Proteomics* **15**, 918–931 (2016).
118. Takada, M. *et al.* FBW7 Loss Promotes Chromosomal Instability and Tumorigenesis via Cyclin E1/CDK2-Mediated Phosphorylation of CENP-A. *Cancer Research* **77**, 4881–4893 (2017).
119. Suzuki, N. *et al.* CENP-B Interacts with CENP-C Domains Containing Mif2 Regions Responsible for Centromere Localization. *Journal of Biological Chemistry* **279**, 5934–5946 (2004).
120. Hudson, D. F. *et al.* Centromere Protein B Null Mice are Mitotically and Meiotically Normal but Have Lower Body and Testis Weights. *Journal of Cell Biology* **141**, 309–319 (1998).

121. Kapoor, M. *et al.* The cenpB gene is not essential in mice. *Chromosoma* **107**, 570–576 (1998).
122. Perez-Castro, A. V. *et al.* Centromeric Protein B Null Mice Are Viable with No Apparent Abnormalities. *Developmental Biology* **201**, 135–143 (1998).
123. Roure, V. *et al.* Reconstituting Drosophila Centromere Identity in Human Cells. *Cell Reports* **29**, 464–479 (2019).
124. Phansalkar, R., Lapierre, P. & Mellone, B. G. Evolutionary insights into the role of the essential centromere protein CAL1 in Drosophila. *Chromosome Research* **20**, 493–504 (2012).
125. Schittenhelm, R. B., Althoff, F., Heidmann, S. & Lehner, C. F. Detrimental incorporation of excess Cenp-A/Cid and Cenp-C into Drosophila centromeres is prevented by limiting amounts of the bridging factor Cal1. *Journal of Cell Science* **123**, 3768–3779 (2010).
126. Chen, C.-C. *et al.* Establishment of Centromeric Chromatin by the CENP-A Assembly Factor CAL1 Requires FACT-Mediated Transcription. *Developmental Cell* **34**, 73–84 (2015).
127. Furuyama, T., Dalal, Y. & Henikoff, S. Chaperone-mediated assembly of centromeric chromatin in vitro. *Proceedings of the National Academy of Sciences* **103**, 6172–6177 (2006).
128. Boltengagen, M. *et al.* A novel role for the histone acetyltransferase Hat1 in the CENP-A/CID assembly pathway in Drosophila melanogaster. *Nucleic Acids Research* **44**, 2145–2159 (2016).
129. Gassmann, R. *et al.* An inverse relationship to germline transcription defines centromeric chromatin in *C. elegans*. *Nature* **484**, 534–537 (2012).
130. Steiner, F. A. & Henikoff, S. Holocentromeres are dispersed point centromeres localized at transcription factor hotspots. *eLife* **3** (2014).

131. Maddox, P. S., Hyndman, F., Monen, J., Oegema, K. & Desai, A. Functional genomics identifies a Myb domain-containing protein family required for assembly of CENP-A chromatin. *The Journal of Cell Biology* **176**, 757–763 (2007).
132. De Groot, C. *et al.* The N-terminal tail of *C. elegans* CENP-A interacts with KNL-2 and is essential for centromeric chromatin assembly. *Molecular Biology of the Cell* **32**, 1193–1201 (2021).
133. Prosée, R. F. *et al.* Transgenerational inheritance of centromere identity requires the CENP-A N-terminal tail in the *C. elegans* maternal germ line. *PLoS Biology* **19**, e3000968 (2021).
134. Lee, B. C. H., Lin, Z. & Yuen, K. W. Y. RbAp46/48LIN-53 Is Required for Holocentromere Assembly in *Caenorhabditis elegans*. *Cell Reports* **14**, 1819–1828 (2016).
135. Lin, Z. & Yuen, K. W. Y. RbAp46/48LIN-53 and HAT-1 are required for initial CENP-AHCP-3 deposition and de novo holocentromere formation on artificial chromosomes in *Caenorhabditis elegans* embryos. *Nucleic Acids Research* **49**, 9154–9173 (2021).
136. Subramanian, L., Toda, N. R., Rappsilber, J. & Allshire, R. C. Eic1 links Mis18 with the CCAN/Mis6/Ctf19 complex to promote CENP-A assembly. *Open Biology* **4** (2014).
137. Takahashi, K., Takayama, Y., Masuda, F., Kobayashi, Y. & Saitoh, S. Two distinct pathways responsible for the loading of CENP-A to centromeres in the fission yeast cell cycle. *Philosophical Transactions of the Royal Society B: Biological Sciences* **360**, 595–607 (2005).
138. Takayama, Y. *et al.* Biphasic Incorporation of Centromeric Histone CENP-A in Fission Yeast. *Molecular Biology of the Cell* **19** (ed Bloom, K.) 682–690 (2008).

139. Camahort, R. *et al.* Scm3 Is Essential to Recruit the Histone H3 Variant Cse4 to Centromeres and to Maintain a Functional Kinetochore. *Molecular Cell* **26**, 853–865 (2007).
140. Pearson, C. G. *et al.* Stable Kinetochore-Microtubule Attachment Constrains Centromere Positioning in Metaphase. *Current Biology* **14**, 1962–1967 (2004).
141. Barnhart, M. C. *et al.* HJURP is a CENP-A chromatin assembly factor sufficient to form a functional de novo kinetochore. *The Journal of Cell Biology* **194**, 229–43 (2011).
142. Bergmann, J. H. *et al.* Epigenetic engineering: histone H3K9 acetylation is compatible with kinetochore structure and function. *Journal of Cell Science* **125**, 411–421 (2012).
143. Singh, P. *et al.* CDK-regulated dimerization of M18BP1 on a Mis18 hexamer is necessary for CENP-A loading. *eLife* **6**, 1–25 (2017).
144. Carlsten, J. O. *et al.* Mediator Promotes CENP-A Incorporation at Fission Yeast Centromeres. *Molecular and Cellular Biology* **32**, 4035–4043 (2012).
145. Cardinale, S. *et al.* Hierarchical Inactivation of a Synthetic Human Kinetochore by a Chromatin Modifier. *Molecular Biology of the Cell* **20**, 4194–4204 (2009).
146. Choi, E. S. *et al.* Identification of Noncoding Transcripts from within CENP-A Chromatin at Fission Yeast Centromeres. *Journal of Biological Chemistry* **286**, 23600–23607 (2011).
147. Nakano, M. *et al.* Inactivation of a Human Kinetochore by Specific Targeting of Chromatin Modifiers. *Developmental Cell* **14**, 507–522 (2008).
148. Zhu, J., Cheng, K. C. L. & Yuen, K. W. Y. Histone H3K9 and H4 Acetylations and Transcription Facilitate the Initial CENP-AHCP3 Deposition and De Novo Centromere Establishment in *Caenorhabditis elegans* Artificial Chromosomes. *Epigenetics & Chromatin* **11**, 16 (2018).

149. Bobkov, G. O., Gilbert, N. & Heun, P. Centromere transcription allows CENP-A to transit from chromatin association to stable incorporation. *Journal of Cell Biology* **217**, 1957–1972 (2018).
150. Kristjuhan, A. & Svejstrup, J. Q. Evidence for distinct mechanisms facilitating transcript elongation through chromatin in vivo. *The EMBO Journal* **23**, 4243–4252 (2004).
151. Kulaeva, O. I., Hsieh, F.-K. & Studitsky, V. M. RNA polymerase complexes cooperate to relieve the nucleosomal barrier and evict histones. *Proceedings of the National Academy of Sciences* **107**, 11325–11330 (2010).
152. Lee, C.-K., Shibata, Y., Rao, B., Strahl, B. D. & Lieb, J. D. Evidence for nucleosome depletion at active regulatory regions genome-wide. *Nature Genetics* **36**, 900–905 (2004).
153. Schwabish, M. A. & Struhl, K. Evidence for Eviction and Rapid Deposition of Histones upon Transcriptional Elongation by RNA Polymerase II. *Molecular and Cellular Biology* **24**, 10111–10117 (2004).
154. Prasad, P. & Ekwall, K. New insights into how chromatin remodellers direct CENP-A to centromeres. *The EMBO Journal* **30**, 1875–1876 (2011).
155. Choi, E. S., Cheon, Y., Kang, K. & Lee, D. The Ino80 complex mediates epigenetic centromere propagation via active removal of histone H3. *Nature Communications* **8**, 529 (2017).
156. Bobkov, G. O. M. *et al.* Spt6 is a maintenance factor for centromeric CENP-A. *Nature Communications* **11**, 2919 (2020).
157. Bergmann, J. H., Martins, N. M. C., Larionov, V., Masumoto, H. & Earnshaw, W. C. HACKing the centromere chromatin code: insights from human artificial chromosomes. *Chromosome Research* **20**, 505–519 (2012).
158. Ohkuni, K. & Kitagawa, K. Endogenous Transcription at the Centromere Facilitates Centromere Activity in Budding Yeast. *Current Biology* **21**, 1695–1703 (2011).

159. Ling, Y. H. & Yuen, K. W. Y. Point centromere activity requires an optimal level of centromeric noncoding RNA. *Proceedings of the National Academy of Sciences* **116**, 6270–6279 (2019).
160. Blower, M. D. Centromeric Transcription Regulates Aurora-B Localization and Activation. *Cell Reports* **15**, 1624–1633 (2016).
161. Chan, F. L. *et al.* Active transcription and essential role of RNA polymerase II at the centromere during mitosis. *Proceedings of the National Academy of Sciences* **109**, 1979–1984 (2012).
162. Du, Y., Topp, C. N. & Dawe, R. K. DNA Binding of Centromere Protein C (CENPC) Is Stabilized by Single-Stranded RNA. *PLoS Genetics* **6**, e1000835 (2010).
163. Ferri, F., Bouzinba-Segard, H., Velasco, G., Hubé, F. & Francastel, C. Non-coding murine centromeric transcripts associate with and potentiate Aurora B kinase. *Nucleic Acids Research* **37**, 5071–5080 (2009).
164. Jambhekar, A., Emerman, A. B., Schweidenback, C. T. H. & Blower, M. D. RNA Stimulates Aurora B Kinase Activity during Mitosis. *PLoS ONE* **9**, e100748 (2014).
165. McNulty, S. M., Sullivan, L. L. & Sullivan, B. A. Human Centromeres Produce Chromosome-Specific and Array-Specific Alpha Satellite Transcripts that Are Complexed with CENP-A and CENP-C. *Developmental Cell* **42**, 226–240 (2017).
166. Quénet, D. & Dalal, Y. A long non-coding RNA is required for targeting centromeric protein A to the human centromere. *eLife* **3** (2014).
167. Rošić, S., Köhler, F. & Erhardt, S. Repetitive centromeric satellite RNA is essential for kinetochore formation and cell division. *Journal of Cell Biology* **207**, 335–349 (2014).

168. Topp, C. N., Zhong, C. X. & Dawe, R. K. Centromere-encoded RNAs are integral components of the maize kinetochore. *Proceedings of the National Academy of Sciences* **101**, 15986–15991 (2004).
169. Wong, L. H. *et al.* Centromere RNA is a key component for the assembly of nucleoproteins at the nucleolus and centromere. *Genome Research* **17**, 1146–1160 (2007).
170. Walfridsson, J. The CHD remodeling factor Hrp1 stimulates CENP-A loading to centromeres. *Nucleic Acids Research* **33**, 2868–2879 (2005).
171. Choi, E. S. *et al.* Factors That Promote H3 Chromatin Integrity during Transcription Prevent Promiscuous Deposition of CENP-ACnp1 in Fission Yeast. *PLoS Genetics* **8**, e1002985 (2012).
172. Ngan, V. K. & Clarke, L. The centromere enhancer mediates centromere activation in *Schizosaccharomyces pombe*. *Molecular and Cellular Biology* **17**, 3305–3314 (1997).
173. Pidoux, A. L. & Allshire, R. C. The role of heterochromatin in centromere function. *Philosophical Transactions of the Royal Society B: Biological Sciences* **360**, 569–579 (2005).
174. Folco, H. D., Pidoux, A. L., Urano, T. & Allshire, R. C. Heterochromatin and RNAi Are Required to Establish CENP-A Chromatin at Centromeres. *Science* **319**, 94–97 (2008).
175. Castillo, A. G. *et al.* Telomeric Repeats Facilitate CENP-ACnp1 Incorporation via Telomere Binding Proteins. *PLoS ONE* **8**, e69673 (2013).
176. Ishii, K. *et al.* Heterochromatin Integrity Affects Chromosome Reorganization After Centromere Dysfunction. *Science* **321**, 1088–1091 (2008).
177. Sato, H., Masuda, F., Takayama, Y., Takahashi, K. & Saitoh, S. Epigenetic Inactivation and Subsequent Heterochromatinization of a Centromere Stabilize Dicentric Chromosomes. *Current Biology* **22**, 658–667 (2012).

178. Park, K. C. *et al.* Roles of Mis18 α in Epigenetic Regulation of Centromeric Chromatin and CENP-A Loading. *Molecular Cell* **46**, 260–273 (2012).
179. Subramanian, L. *et al.* Centromere localization and function of Mis 18 requires Yippee-like domain-mediated oligomerization. *EMBO reports* **17**, 496–507 (2016).
180. Pan, D. *et al.* CDK-regulated dimerization of M18BP1 on a Mis18 hexamer is necessary for CENP-A loading. *eLife* **6** (2017).
181. Nardi, I. K., Zasadzińska, E., Stellfox, M. E., Knippler, C. M. & Foltz, D. R. Licensing of Centromeric Chromatin Assembly through the Mis18 α -Mis18 β Heterotetramer. *Molecular Cell* **61**, 774–787 (2016).
182. Fujita, R. *et al.* Association of M18BP1/KNL2 with CENP-A Nucleosome Is Essential for Centromere Formation in Non-mammalian Vertebrates. *Developmental Cell* **42**, 181–189 (2017).
183. An, S., Koldewey, P., Chik, J., Subramanian, L. & Cho, U. S. Mis16 Switches Function from a Histone H4 Chaperone to a CENP-ACnp1-Specific Assembly Factor through Eic1 Interaction. *Structure* **26**, 960–971 (2018).
184. An, S., Kim, H. & Cho, U.-S. Mis16 Independently Recognizes Histone H4 and the CENP-ACnp1-Specific Chaperone Scm3sp. *Journal of Molecular Biology* **427**, 3230–3240 (2015).
185. Hayashi, T. *et al.* Schizosaccharomyces pombe centromere protein Mis19 links Mis16 and Mis18 to recruit CENP-A through interacting with NMD factors and the SWI/SNF complex. *Genes to Cells* **19**, 541–554 (2014).
186. Swartz, S. Z. *et al.* Quiescent Cells Actively Replenish CENP-A Nucleosomes to Maintain Centromere Identity and Proliferative Potential. *Developmental Cell* **51**, 35–48 (2019).
187. Novais-Cruz, M. *et al.* Mitotic progression, arrest, exit or death relies on centromere structural integrity, rather than de novo transcription. *eLife* **7** (2018).

188. Jeronimo, C., Poitras, C. & Robert, F. Histone Recycling by FACT and Spt6 during Transcription Prevents the Scrambling of Histone Modifications. *Cell Reports* **28**, 1206–1218 (2019).
189. Kato, H. *et al.* Spt6 prevents transcription-coupled loss of posttranslationally modified histone H3. *Scientific Reports* **3**, 2186 (2013).
190. Bortvin, A. & Winston, F. Evidence That Spt6p Controls Chromatin Structure by a Direct Interaction with Histones. *Science* **272**, 1473–1476 (1996).
191. Sdano, M. A. *et al.* A novel SH2 recognition mechanism recruits Spt6 to the doubly phosphorylated RNA polymerase II linker at sites of transcription. *eLife* **6** (2017).
192. Yoh, S. M., Cho, H., Pickle, L., Evans, R. M. & Jones, K. A. The Spt6 SH2 domain binds Ser2-P RNAPII to direct Iws1-dependent mRNA splicing and export. *Genes & Development* **21**, 160–174 (2007).
193. Hédouin, S., Grillo, G., Ivkovic, I., Velasco, G. & Francastel, C. CENP-A chromatin disassembly in stressed and senescent murine cells. *Scientific Reports* **7**, 42520 (2017).
194. Mertins, P. *et al.* Integrated proteomic analysis of post-translational modifications by serial enrichment. *Nature Methods* **10**, 634–637 (2013).
195. Zasadzińska, E. *et al.* Inheritance of CENP-A Nucleosomes during DNA Replication Requires HJURP. *Developmental Cell* **47**, 348–362 (2018).
196. Richet, N. *et al.* Structural insight into how the human helicase subunit MCM2 may act as a histone chaperone together with ASF1 at the replication fork. *Nucleic Acids Research* **43**, 1905–1917 (2015).
197. Clément, C. & Almouzni, G. MCM2 binding to histones H3–H4 and ASF1 supports a tetramer-to-dimer model for histone inheritance at the replication fork. *Nature Structural & Molecular Biology* **22**, 587–589 (2015).

198. Huang, H. *et al.* A unique binding mode enables MCM2 to chaperone histones H3–H4 at replication forks. *Nature Structural & Molecular Biology* **22**, 618–626 (2015).
199. Zasadzińska, E., Barnhart-Dailey, M. C., Kuich, P. H. J. L. & Foltz, D. R. Dimerization of the CENP-A assembly factor HJURP is required for centromeric nucleosome deposition. *The EMBO Journal* **32**, 2113–2124 (2013).
200. Bodor, D. L. *et al.* The quantitative architecture of centromeric chromatin. *eLife* **3** (2014).
201. Nechemia-Arbely, Y. *et al.* DNA replication acts as an error correction mechanism to maintain centromere identity by restricting CENP-A to centromeres. *Nature Cell Biology* **21**, 743–754 (2019).
202. Shrestha, R. L. *et al.* Mislocalization of centromeric histone H3 variant CENP-A contributes to chromosomal instability (CIN) in human cells. *Oncotarget* **8**, 46781–46800 (2017).
203. Moreno-Moreno, O., Torras-Llort, M. & Azorin, F. The E3-ligases SCFPpa and APC/CCdh1 co-operate to regulate CENP-ACID expression across the cell cycle. *Nucleic Acids Research* **47**, 3395–3406 (2019).
204. Gascoigne, K. E. *et al.* Induced Ectopic Kinetochores Bypasses the Requirement for CENP-A Nucleosomes. *Cell* **145**, 410–422 (2011).
205. Heun, P. *et al.* Mislocalization of the Drosophila Centromere-Specific Histone CID Promotes Formation of Functional Ectopic Kinetochores. *Developmental Cell* **10**, 303–315 (2006).
206. Au, W.-C., Crisp, M. J., DeLuca, S. Z., Rando, O. J. & Basrai, M. A. Altered Dosage and Mislocalization of Histone H3 and Cse4p Lead to Chromosome Loss in *Saccharomyces cerevisiae*. *Genetics* **179**, 263–275 (2008).
207. Olszak, A. M. *et al.* Heterochromatin boundaries are hotspots for de novo kinetochore formation. *Nature Cell Biology* **13**, 799–808 (2011).

208. McGovern, S. L., Qi, Y., Pusztai, L., Symmans, W. F. & Buchholz, T. A. Centromere protein-A, an essential centromere protein, is a prognostic marker for relapse in estrogen receptor-positive breast cancer. *Breast Cancer Research* **14**, R72 (2012).
209. Gonzalez, M., He, H., Dong, Q., Sun, S. & Li, F. Ectopic Centromere Nucleation by CENP-A in Fission Yeast. *Genetics* **198**, 1433–1446 (2014).
210. Athwal, R. K. *et al.* CENP-A nucleosomes localize to transcription factor hotspots and subtelomeric sites in human cancer cells. *Epigenetics & Chromatin* **8**, 2 (2015).
211. Shelby, R. D., Vafa, O. & Sullivan, K. F. Assembly of CENP-A into Centromeric Chromatin Requires a Cooperative Array of Nucleosomal DNA Contact Sites. *Journal of Cell Biology* **136**, 501–513 (1997).
212. Aristizabal-Corrales, D., Yang, J. & Li, F. Cell Cycle-Regulated Transcription of CENP-A by the MBF Complex Ensures Optimal Level of CENP-A for Centromere Formation. *Genetics* **211**, 861–875 (2019).
213. Wang, X., Rosales, J. L., Gao, X. & Lee, K.-Y. Centromeric chromatin integrity is compromised by loss of Cdk5rap2, a transcriptional activator of CENP-A. *Biomedicine & Pharmacotherapy* **138**, 111463 (2021).
214. Bade, D., Pauleau, A.-L., Wendler, A. & Erhardt, S. The E3 Ligase CUL3/RDX Controls Centromere Maintenance by Ubiquitylating and Stabilizing CENP-A in a CAL1-Dependent Manner. *Developmental Cell* **28**, 508–519 (2014).
215. Huang, A. *et al.* Phosphorylation of Drosophila CENP-A on serine 20 regulates protein turn-over and centromere-specific loading. *Nucleic Acids Research* **47**, 10754–10770 (2019).
216. Maehara, K., Takahashi, K. & Saitoh, S. CENP-A Reduction Induces a p53-Dependent Cellular Senescence Response To Protect Cells from Executing Defective Mitoses. *Molecular and Cellular Biology* **30**, 2090–2104 (2010).

217. Lomonte, P., Sullivan, K. F. & Everett, R. D. Degradation of Nucleosome-associated Centromeric Histone H3-like Protein CENP-A Induced by Herpes Simplex Virus Type 1 Protein ICP0. *Journal of Biological Chemistry* **276**, 5829–5835 (2001).
218. Falk, S. J. *et al.* CENP-C reshapes and stabilizes CENP-A nucleosomes at the centromere. *Science* **348**, 699–703 (2015).
219. Guo, L. Y. *et al.* Centromeres are maintained by fastening CENP-A to DNA and directing an arginine anchor-dependent nucleosome transition. *Nature Communications* **8**, 15775 (2017).
220. Ranjitkar, P. *et al.* An E3 Ubiquitin Ligase Prevents Ectopic Localization of the Centromeric Histone H3 Variant via the Centromere Targeting Domain. *Molecular Cell* **40**, 455–464 (2010).
221. Au, W. C. *et al.* A Novel Role of the N Terminus of Budding Yeast Histone H3 Variant Cse4 in Ubiquitin-Mediated Proteolysis. *Genetics* **194**, 513–518 (2013).
222. Mishra, M., Huang, J. & Balasubramanian, M. K. The yeast actin cytoskeleton. *FEMS Microbiology Reviews* **38**, 213–27 (2014).
223. Zhou, N., Shi, L., Shan, S. & Zhou, Z. Molecular basis for the selective recognition and ubiquitination of centromeric histone H3 by yeast E3 ligase Psh1. *Journal of Genetics and Genomics* **48**, 463–472 (2021).
224. Canzonetta, C. *et al.* SAGA DUB-Ubp8 Deubiquitylates Centromeric Histone Variant Cse4. *G3 Genes—Genomes—Genetics* **6**, 287–298 (2016).
225. Hildebrand, E. M. & Biggins, S. Regulation of Budding Yeast CENP-A levels Prevents Misincorporation at Promoter Nucleosomes and Transcriptional Defects. *PLOS Genetics* **12**, e1005930 (2016).
226. Cheng, H., Bao, X. & Rao, H. The F-box Protein Rcy1 Is Involved in the Degradation of Histone H3 Variant Cse4 and Genome Maintenance. *Journal of Biological Chemistry* **291**, 10372–10377 (2016).

227. Au, W.-C. *et al.* Skp, Cullin, F-box (SCF)-Met30 and SCF-Cdc4-Mediated Proteolysis of CENP-A Prevents Mislocalization of CENP-A for Chromosomal Stability in Budding Yeast. *PLoS Genetics* **16**, e1008597 (2020).
228. Ohkuni, K. *et al.* SUMO-targeted ubiquitin ligase (STUbL) Slx5 regulates proteolysis of centromeric histone H3 variant Cse4 and prevents its mislocalization to euchromatin. *Molecular Biology of the Cell* **27**, 1500–1510 (2016).
229. Ogiyama, Y., Ohno, Y., Kubota, Y. & Ishii, K. Epigenetically induced paucity of histone H2A.Z stabilizes fission-yeast ectopic centromeres. *Nature Structural & Molecular Biology* **20**, 1397–1406 (2013).
230. Mathew, V. *et al.* The Histone-Fold Protein CHRAC14 Influences Chromatin Composition in Response to DNA Damage. *Cell Reports* **7**, 321–330 (2014).
231. Gkikopoulos, T. *et al.* The SWI/SNF complex acts to constrain distribution of the centromeric histone variant Cse4. *The EMBO Journal* **30**, 1919–1927 (2011).
232. Deyter, G. M. & Biggins, S. The FACT complex interacts with the E3 ubiquitin ligase Psh1 to prevent ectopic localization of CENP-A. *Genes & Development* **28**, 1815–1826 (2014).
233. Helfricht, A. *et al.* Remodeling and spacing factor 1 (RSF1) deposits centromere proteins at DNA double-strand breaks to promote non-homologous end-joining. *Cell Cycle* **12**, 3070–3082 (2013).
234. Pessina, F. *et al.* Functional transcription promoters at DNA double-strand breaks mediate RNA-driven phase separation of damage-response factors. *Nature Cell Biology* **21**, 1286–1299 (2019).
235. Zeitlin, S. G. *et al.* Double-strand DNA breaks recruit the centromeric histone CENP-A. *Proceedings of the National Academy of Sciences* **106**, 15762–15767 (2009).

236. Juhász, S., Elbakry, A., Mathes, A. & Löbrich, M. ATRX Promotes DNA Repair Synthesis and Sister Chromatid Exchange during Homologous Recombination. *Molecular Cell* **71**, 11–24 (2018).
237. Koschmann, C. *et al.* ATRX loss promotes tumor growth and impairs nonhomologous end joining DNA repair in glioma. *Science Translational Medicine* **8** (2016).
238. Lacoste, N. *et al.* Mislocalization of the Centromeric Histone Variant CenH3/CENP-A in Human Cells Depends on the Chaperone DAXX. *Molecular Cell* **53**, 631–644 (2014).
239. Clapier, C. R. Sophisticated Conversations between Chromatin and Chromatin Remodelers, and Dissonances in Cancer. *International Journal of Molecular Sciences* **22**, 5578 (2021).
240. Mitra, S. *et al.* Genetic screening identifies a SUMO protease dynamically maintaining centromeric chromatin. *Nature Communications* **11**, 501 (2020).
241. Taneja, N. *et al.* SNF2 Family Protein Fft3 Suppresses Nucleosome Turnover to Promote Epigenetic Inheritance and Proper Replication. *Molecular Cell* **66**, 50–62 (2017).
242. Jahn, L. J. *et al.* Dependency of Heterochromatin Domains on Replication Factors. *G3 Genes—Genomes—Genetics* **8**, 477–489 (2018).
243. Lee, J. *et al.* Chromatin remodeller Fun30 Fft3 induces nucleosome disassembly to facilitate RNA polymerase II elongation. *Nature Communications* (2017).
244. Strålfors, A., Walfridsson, J., Bhuiyan, H. & Ekwall, K. The FUN30 Chromatin Remodeler, Fft3, Protects Centromeric and Subtelomeric Domains from Euchromatin Formation. *PLoS Genetics* **7**, e1001334 (2011).
245. Durand-Dubief, M. *et al.* SWI/SNF-Like Chromatin Remodeling Factor Fun30 Supports Point Centromere Function in *S. cerevisiae*. *PLoS Genetics* **8**, e1002974 (2012).

246. Obuse, C. *et al.* Proteomics analysis of the centromere complex from HeLa interphase cells: UV-damaged DNA binding protein 1 (DDB-1) is a component of the CEN-complex, while BMI-1 is transiently co-localized with the centromeric region in interphase. *Genes to Cells* **9**, 105–120 (2004).
247. Perpelescu, M., Nozaki, N., Obuse, C., Yang, H. & Yoda, K. Active establishment of centromeric CENP-A chromatin by RSF complex. *Journal of Cell Biology* **185**, 397–407 (2009).
248. Pessina, F. & Lowndes, N. F. The RSF1 Histone-Remodelling Factor Facilitates DNA Double-Strand Break Repair by Recruiting Centromeric and Fanconi Anaemia Proteins. *PLoS Biology* **12**, e1001856 (2014).
249. Chambers, A. L. *et al.* The INO80 chromatin remodeling complex prevents polyploidy and maintains normal chromatin structure at centromeres. *Genes & Development* **26**, 2590–2603 (2012).
250. Singh, P. P. *et al.* Hap2–Ino80-facilitated transcription promotes de novo establishment of CENP-A chromatin. *Genes & Development* **34**, 226–238 (2020).
251. Okada, M., Okawa, K., Isobe, T. & Fukagawa, T. CENP-H-containing Complex Facilitates Centromere Deposition of CENP-A in Cooperation with FACT and CHD1. *Molecular Biology of the Cell* **20**, 3986–3995 (2009).
252. Podhraski, V. *et al.* CenH3/CID Incorporation Is Not Dependent on the Chromatin Assembly Factor CHD1 in *Drosophila*. *PLoS ONE* **5**, e10120 (2010).
253. Sullivan, B. A. & Karpen, G. H. Centromeric chromatin exhibits a histone modification pattern that is distinct from both euchromatin and heterochromatin. *Nature Structural & Molecular Biology* **11**, 1076–1083 (2004).
254. Fischle, W., Wang, Y. & Allis, C. D. Binary switches and modification cassettes in histone biology and beyond. *Nature* **425**, 475–9 (2003).
255. Jenuwein, T. & Allis, C. D. Translating the histone code. *Science* **293**, 1074–80 (2001).

256. Yamada, T., Fischle, W., Sugiyama, T., Allis, C. D. & Grewal, S. I. The Nucleation and Maintenance of Heterochromatin by a Histone Deacetylase in Fission Yeast. *Molecular Cell* **20**, 173–185 (2005).
257. Nakayama, J.-i., Rice, J. C., Strahl, B. D., Allis, C. D. & Grewal, S. I. S. Role of Histone H3 Lysine 9 Methylation in Epigenetic Control of Heterochromatin Assembly. *Science* **292**, 110–113 (2001).
258. Schneider, R. *et al.* Histone H3 lysine 4 methylation patterns in higher eukaryotic genes. *Nature Cell Biology* **6**, 73–7 (2004).
259. Wirén, M. *et al.* Genomewide analysis of nucleosome density histone acetylation and HDAC function in fission yeast. *The EMBO Journal* **24**, 2906–2918 (2005).
260. Shankaranarayana, G. D., Motamedi, M. R., Moazed, D. & Grewal, S. I. Sir2 Regulates Histone H3 Lysine 9 Methylation and Heterochromatin Assembly in Fission Yeast. *Current Biology* **13**, 1240–1246 (2003).
261. Seto, E. & Yoshida, M. Erasers of Histone Acetylation: The Histone Deacetylase Enzymes. *Cold Spring Harbor Perspectives in Biology* **6**, a018713–a018713 (2014).
262. Sugiyama, T. *et al.* SHREC, an Effector Complex for Heterochromatic Transcriptional Silencing. *Cell* **128**, 491–504 (2007).
263. Zhang, K., Mosch, K., Fischle, W. & Grewal, S. I. S. Roles of the Clr4 methyltransferase complex in nucleation, spreading and maintenance of heterochromatin. *Nature Structural & Molecular Biology* **15**, 381–388 (2008).
264. Cowieson, N. P., Partridge, J. F., Allshire, R. C. & McLaughlin, P. J. Dimerisation of a chromo shadow domain and distinctions from the chromodomain as revealed by structural analysis. *Current Biology* **10**, 517–525 (2000).
265. Canzio, D. *et al.* Chromodomain-Mediated Oligomerization of HP1 Suggests a Nucleosome-Bridging Mechanism for Heterochromatin Assembly. *Molecular Cell* **41**, 67–81 (2011).

266. Lantermann, A. B. *et al.* Schizosaccharomyces pombe genome-wide nucleosome mapping reveals positioning mechanisms distinct from those of Saccharomyces cerevisiae. *Nature Structural & Molecular Biology* **17**, 251–257 (2010).
267. Xhemalce, B. & Kouzarides, T. A chromodomain switch mediated by histone H3 Lys 4 acetylation regulates heterochromatin assembly. *Genes & Development* **24**, 647–652 (2010).
268. Keller, C. *et al.* HP1Swi6 Mediates the Recognition and Destruction of Heterochromatic RNA Transcripts. *Molecular Cell* **47**, 215–227 (2012).
269. Srivastava, S. & Foltz, D. R. Posttranslational modifications of CENP-A: marks of distinction. *Chromosoma* **127**, 279–290 (2018).
270. Goutte-Gattat, D. *et al.* Phosphorylation of the CENP-A amino-terminus in mitotic centromeric chromatin is required for kinetochore function. *Proceedings of the National Academy of Sciences* **110**, 8579–8584 (2013).
271. Samel, A., Cuomo, A., Bonaldi, T. & Ehrenhofer-Murray, A. E. Methylation of CenH3 arginine 37 regulates kinetochore integrity and chromosome segregation. *Proceedings of the National Academy of Sciences* **109**, 9029–9034 (2012).
272. Hammond, C. M. *et al.* The histone chaperone Vps75 forms multiple oligomeric assemblies capable of mediating exchange between histone H3–H4 tetramers and Asf1–H3–H4 complexes. *Nucleic Acids Research* **44**, 6157–6172 (2016).
273. Bowman, A. *et al.* The histone chaperones Vps75 and Nap1 form ring-like, tetrameric structures in solution. *Nucleic Acids Research* **42**, 6038–6051 (2014).
274. D’Arcy, S. & Luger, K. Understanding histone acetyltransferase Rtt109 structure and function: how many chaperones does it take? *Current Opinion in Structural Biology* **21**, 728–734 (2011).

275. Marmorstein, R. & Trievel, R. C. Histone modifying enzymes: structures, mechanisms, and specificities. *Biochimica et Biophysica Acta* **1789**, 58–68 (2009).
276. Lin, C. & Yuan, Y. A. Structural Insights into Histone H3 Lysine 56 Acetylation by Rtt109. *Structure* **16**, 1503–1510 (2008).
277. Tang, Y. *et al.* Structure of the Rtt109-AcCoA/Vps75 complex and implications for chaperone-mediated histone acetylation. *Structure* **19**, 221–231 (2011).
278. Li, Q. *et al.* Acetylation of Histone H3 Lysine 56 Regulates Replication-Coupled Nucleosome Assembly. *Cell* **134**, 244–255 (2008).
279. Driscoll, R., Hudson, A. & Jackson, S. P. Yeast Rtt109 Promotes Genome Stability by Acetylating Histone H3 on Lysine 56. *Science* **315**, 649–652 (2007).
280. Jonas, F., Yaakov, G. & Barkai, N. Rtt109 promotes nucleosome replacement ahead of the replication fork. *Genome Research* **32**, 1089–1098 (2022).
281. Eng, J. K., McCormack, A. L. & Yates, J. R. An approach to correlate tandem mass spectral data of peptides with amino acid sequences in a protein database. *Journal of the American Society for Mass Spectrometry* **5**, 976–989 (1994).
282. Sievers, F. *et al.* Fast, scalable generation of high-quality protein multiple sequence alignments using Clustal Omega. *Molecular Systems Biology* **7**, 539 (2011).
283. Goujon, M. *et al.* A new bioinformatics analysis tools framework at EMBL-EBI. *Nucleic Acids Research* **38**, W695–W699 (2010).
284. Harris, M. A. *et al.* Fission stories: using PomBase to understand *Schizosaccharomyces pombe* biology. *Genetics* **220** (2022).
285. Clark, K., Karsch-Mizrachi, I., Lipman, D. J., Ostell, J. & Sayers, E. W. GenBank. *Nucleic acids research* **44**, 67–72 (2016).

286. Hou, H. *et al.* Csi1 links centromeres to the nuclear envelope for centromere clustering. *The Journal of Cell Biology* **199**, 735–744 (2012).
287. Hiraga, S.-i., Botsios, S. & Donaldson, A. D. Histone H3 lysine 56 acetylation by Rtt109 is crucial for chromosome positioning. *The Journal of Cell Biology* **183**, 641–651 (2008).
288. Tsubota, T. *et al.* Histone H3-K56 acetylation is catalyzed by histone chaperone-dependent complexes. *Molecular cell* **25**, 703–12 (2007).
289. Han, J. *et al.* Rtt109 acetylates histone H3 lysine 56 and functions in DNA replication. *Science* **315**, 653–5 (2007).
290. Schneider, J., Bajwa, P., Johnson, F. C., Bhaumik, S. R. & Shilatifard, A. Rtt109 is required for proper H3K56 acetylation: a chromatin mark associated with the elongating RNA polymerase II. *The Journal of Biological Chemistry* **281**, 37270–4 (2006).
291. Collins, S. R. *et al.* Functional dissection of protein complexes involved in yeast chromosome biology using a genetic interaction map. *Nature* **446**, 806–10 (2007).
292. Hyland, E. M. *et al.* Insights into the role of histone H3 and histone H4 core modifiable residues in *Saccharomyces cerevisiae*. *Molecular and Cellular Biology* **25**, 10060–70 (2005).
293. Masumoto, H., Hawke, D., Kobayashi, R. & Verreault, A. A role for cell-cycle-regulated histone H3 lysine 56 acetylation in the DNA damage response. *Nature* **436**, 294–8 (2005).
294. Ozdemir, A. *et al.* Characterization of lysine 56 of histone H3 as an acetylation site in *Saccharomyces cerevisiae*. *The Journal of Biological Chemistry* **280**, 25949–52 (2005).
295. Fillingham, J. *et al.* Chaperone control of the activity and specificity of the histone H3 acetyltransferase Rtt109. *Molecular and Cellular Biology* **28**, 4342–53 (2008).

296. Burgess, R. J., Zhou, H., Han, J. & Zhang, Z. A role for Gen5 in replication-coupled nucleosome assembly. *Molecular Cell* **37**, 469–80 (2010).
297. Chang, L. & Gould, K. L. Sid4p is required to localize components of the septation initiation pathway to the spindle pole body in fission yeast. *Proceedings of the National Academy of Sciences of the United States of America* **97**, 5249–54 (2000).
298. Morrell, J. L. *et al.* Sid4p-Cdc11p assembles the septation initiation network and its regulators at the *S. pombe* SPB. *Current Biology* **14**, 579–84 (2004).
299. Kalitsis, P. *et al.* Partially functional Cenpa-GFP fusion protein causes increased chromosome missegregation and apoptosis during mouse embryogenesis. *Chromosome research* **11**, 345–57 (2003).
300. Wisniewski, J. *et al.* Imaging the fate of histone Cse4 reveals de novo replacement in S phase and subsequent stable residence at centromeres. *eLife* **3**, e02203 (2014).
301. Bergmann, J. H. *et al.* Epigenetic engineering shows H3K4me2 is required for HJURP targeting and CENP-A assembly on a synthetic human kinetochore. *The EMBO Journal* **30**, 328–340 (2011).
302. Hammond, C. M., Strømme, C. B., Huang, H., Patel, D. J. & Groth, A. Histone chaperone networks shaping chromatin function. *Nature Reviews Molecular Cell Biology* **18**, 141–158 (2017).
303. Tanaka, K., Li Chang, H., Kagami, A. & Watanabe, Y. CENP-C Functions as a Scaffold for Effectors with Essential Kinetochore Functions in Mitosis and Meiosis. *Developmental Cell* **17**, 334–343 (2009).
304. Hori, T. *et al.* CCAN Makes Multiple Contacts with Centromeric DNA to Provide Distinct Pathways to the Outer Kinetochore. *Cell* **135**, 1039–1052 (2008).
305. Schleiffer, A. *et al.* CENP-T proteins are conserved centromere receptors of the Ndc80 complex. *Nature Cell Biology* **14**, 604–613 (2012).

306. Lang, J., Barber, A. & Biggins, S. An assay for de novo kinetochore assembly reveals a key role for the CENP-T pathway in budding yeast. *eLife* **7** (2018).
307. Rago, F., Gascoigne, K. E. & Cheeseman, I. M. Distinct Organization and Regulation of the Outer Kinetochore KMN Network Downstream of CENP-C and CENP-T. *Current Biology* **25**, 671–677 (2015).
308. Maure, J.-F. *et al.* The Ndc80 Loop Region Facilitates Formation of Kinetochore Attachment to the Dynamic Microtubule Plus End. *Current Biology* **21**, 207–213 (2011).
309. Takeuchi, K. *et al.* The centromeric nucleosome-like CENP–T–W–S–X complex induces positive supercoils into DNA. *Nucleic Acids Research* **42**, 1644–1655 (2014).
310. Tschernyschkow, S. *et al.* Rule-based modeling and simulations of the inner kinetochore structure. *Progress in Biophysics and Molecular Biology* **113**, 33–45 (2013).
311. Bowman, A. *et al.* The histone chaperones Nap1 and Vps75 bind histones H3 and H4 in a tetrameric conformation. *Molecular Cell* **41**, 398–408 (2011).